Inducing cellular senescence in cancer

by

Ian J. Restall

Graduate Program
in
Biochemistry

Submitted in partial fulfillment
of the requirements for the degree of
Doctor of Philosophy in Biochemistry
with specialization in Human and Molecular Genetics

Submitted September, 2012
Degree granted March, 2013

Faculty of Medicine
University of Ottawa
Ottawa, Ontario
Canada

Abstract

Cellular senescence is a permanent cell cycle arrest that is induced as a response to cellular stress. Replicative senescence is a well-described mechanism that limits the replicative capacity of cells and must be overcome by cancer cells. Oncogene-induced senescence (OIS) is a form of premature senescence and a potent tumor suppressor mechanism. OIS is induced in normal cells as a result of deregulated oncogene or tumor suppressor gene expression. An exciting area of research is the identification of novel targets that induce senescence in cancer cells as a therapeutic approach. In this study, a novel mechanism is described where the inhibition of Hsp90 in small cell lung cancer (SCLC) cells induced premature senescence rather than cell death. The senescence induced following Hsp90 inhibition was p21-dependent and the loss of p21 allowed SCLC cells to bypass the induction of senescence. Additionally, we identified a novel mechanism where the depletion of PKCι induced senescence in glioblastoma multiforme (GBM) cells. PKCι depletion-induced senescence did not activate the DNA-damage response pathway and was p21-dependent. Further perturbations of mitosis, using an aurora kinase inhibitor, increased the number of senescent cells when combined with PKCι depletion. This suggests that PKCι depletion-induced senescence involves defects in mitotic progression. Senescent glioblastoma cells at a basal level of senescence in culture, induced by p21 overexpression, and induced after PKCι depletion had aberrant centrosomes. Mitotic slippage is an early exit from mitosis without cell division that occurs when the spindle assembly checkpoint (SAC) is not satisfied. Senescent glioblastoma cells had multiple markers of mitotic slippage. Therefore, PKCι depletion-induced senescence involves mitotic slippage and results in

aberrant centrosomes. A U87MG cell line with a doxycycline-inducible shRNA targeting PKCι was developed to deplete PKCι in established xenografts. PKCι was depleted in established glioblastoma xenografts in mice and resulted in decreased cell proliferation, delayed tumor growth and improved survival. This study has demonstrated that both Hsp90 and PKCι are novel targets to induce senescence in cancer cells as a potential therapeutic approach.

Acknowledgements

First and foremost I would like to thank Dr. Ian Lorimer. Thank you Ian for taking me in as a fourth year honours student when you already had a full lab and weren't planning on hiring any more students. I will always remember my excitement after my interview with you and when you sent your email response before I even made it home. Needless to say, I called my parents to tell them I'd be able to accomplish my life goal of performing cancer research. More than simply the opportunity to work in your lab, you provided me with the necessary guidance and independence to be able to make progress on lab work while still dreaming up new ideas. Importantly, when some ideas got a bit off track you taught me to train my focus on what's important. I'll always look back on these projects fondly. It was truly interesting and exciting science. Thanks again for your wonderful and ongoing mentorship.

The entire Lorimer lab, current and past members, have cultivated a fun and enriching environment to do lab work. Every day has been a positive one with you all around, even when cells didn't grow or westerns didn't transfer. Thank you Mitch for the constant humor and for eventually tempting me onto the iota team. Thank you Doris for all the help with the centrosome project and immunofluorescence, we were quite a well-synchronized team. Sylvie, thank you for the training starting on day one and the fun times for the following six years, even if it meant less country music for you. Manijeh, your inexhaustible kindness and selflessness is something I'll have to try hard to emulate in the future, and I'll always be looking forward to your crispy rice. Jenn and Tang, thanks for all the coffee breaks, dinners, news articles and conversation. I'll always be fond of the time we spent together even if it was mostly in the lab. To the after hours club, you know who you are. I want to especially thank Jude for her unrelenting support, for not letting me take myself too seriously in the lab and for feeding me more than her fair share of lunches. The chance to co-first author a paper with you was a truly unforgettable experience.

I would like to thank my friends and family outside of the lab. Your constant support and love was so important while being far from home for so many years. Finally, a special thank you to my parents. Not just for the constant support and making sure I was staying healthy but also for fueling my inquisitive nature from a young age.

Table of Contents

List of Abbreviations

17-AAG	17-allylamino-17-demethoxygeldanamycin
Akt	Protein Kinase B (PKB)
ALT	Alternative lengthening of telomeres
APC/C	Anaphase-Promoting Complex/Cyclosome
aPKC	Atypical protein kinase C
ATM	Ataxia telangiectasia mutated
ATP	Adenosine-5'-triphosphate
ATR	ATM and Rad3-related
BrdU	5-bromo-2'-deoxyuridine
Cdc20	Cell-division cycle protein 20
Cdc42	Cell division control protein 42 homolog
Cdk	Cyclin dependent kinase
Cdki	Cyclin-dependent kinase inhibitor
DAPI	4',6-diamidino-2-phenylindole
DNA	Deoxyribonucleic acid
EGFR	Epidermal growth factor receptor
GA	Geldanamycin
GBM	Glioblastoma multiforme
GLB1	Galactosidase, beta 1
Grp94	Heat shock protein 90kDa beta member 1
H3K9me3	Histone H3 tri-methylated on Lysine 9
Her2	Human Epidermal Growth Factor Receptor 2
Hsf1	Heat shock factor 1
Hsp27	Heat shock protein 27
Hsp70	Heat shock protein 70
Hsp90	Heat shock protein 90
IF	Immunofluorescence
IHC	Immunohistochemistry
MTOC	Microtubule-organizing center
NSCLC	Non-small cell lung cancer
OIS	Oncogene-induced senescence
p16	p16INK4A
p21	p21CIP1/WAF1
PanIN	Pancreatic intraepithelial neoplasia
PB1	Phox Bem 1
PDAC	Pancreatic ductal adenocarcinoma
PDK1	Phosphatidylinositol-3 dependent kinase
PI3K	Phosphatidylinositol 3-kinase
PIN	Prostate intraepithelial neoplasia
PKC	Protein kinase C

PKCζ	Protein Kinase C zeta
PKCι	Protein Kinase C iota
PTEN	Phosphatase and tensin homolog
RA	Radicicol
Ras	Rat sarcoma
Rb	Retinoblastoma protein
RNA	Ribonucleic acid
SAC	Spindle Assembly Checkpoint
SAHF	Senescence-associated heterochromatic foci
SAβGal	Senescence-associated beta-galactosidase
SCLC	Small cell lung cancer
shRNA	Short hairpin RNA
siRNA	Small interfering RNA
SNP	Single-nucleotide polymorphism
Trap1	Heat shock protein 75 kDa, mitochondrial
v-Src	Viral sarcoma
X-gal	5-bromo-4-chloro-3-indoyl β-D-galactopyranoside

List of Figures

List of Tables

1. Introduction

1.1 Replicative senescence

Hayflick and Moorhead first described replicative senescence in 1961 when they described the replicative limit of fetal human diploid fibroblasts grown in cell culture (Hayflick and Moorhead, 1961). At that time, it was thought that human cells grown outside of the body had a limitless potential to replicate. Hayflick and Moorhead described human cell strains entering Phase III, the terminal phase, as becoming senescent at the cellular level. Furthermore, within this initial description of replicative senescence, Hayflick and Moorhead concluded: "a consideration of the cause of the eventual degeneration of these strains leads to the hypothesis that non-cumulative external factors are excluded and that the phenomenon is attributable to intrinsic factors which are expressed as senescence at the cellular level." This hypothesis has two important points regarding the mechanism of replicative senescence, both of which have been observed to be true with the benefit of time and continued experimentation. The first is that external factors are excluded; this was a long-standing criticism and for decades it was argued that replicative senescence was merely an artifact of tissue culture. The second is the asserted importance of intrinsic factors within the cell, which can now be viewed as an allusion to the observation that the shortening of telomeres leads to the crisis that is expressed as replicative senescence, described in the following section. This initial description of the limited replicative lifespan, replicative senescence, had a very important impact on how researchers thought about human cells in culture.

1.2 Mechanism of replicative senescence

The end-replication problem of DNA polymerase, where incomplete replication occurs at the ends of chromosomes, was first independently described in the early 1970s by Olovnikov in 1971 and Watson in 1972 (Olovnikov, 1971, 1973; Watson, 1972). The original paper published by Olovnikov in 1971 was published in Russian and he then published a similar work in English in 1973, which has often been referenced instead of his original Russian paper (Olovnikov, 1973, 1996). Importantly, Olovnikov described the gradual shortening of telomeres as a cellular means of counting mitoses and proposed that it could be the mechanism, or intrinsic factor, behind the Hayflick limit and the description of replicative senescence in 1961 (Olovnikov, 1971, 1973). Almost two decades after Olovnikov's original hypotheses were published, it was experimentally confirmed that the telomeres of ageing cultured human fibroblasts shortened with population doublings (Harley et al., 1990). The elongation of shortened telomere ends is carried out by the telomere terminal transferase enzyme, or telomerase. Telomerase was first described in the ciliate *Tetrahymena*, as a ribonucleoprotein complex that is able to synthesize the repeated telomeric sequence TTGGGG, elongating shortened telomeres (Greider and Blackburn, 1985, 1987). Subsequently, the identification of the human telomerase enzyme that is able to synthesize the repeated telomeric sequence TTAGGG was described (Morin, 1989). Elongation of the telomeres by expressing the human telomerase catalytic subunit both increased the cellular lifespan and decreased senescent markers of cultured normal human cells (Bodnar et al., 1998). Shortened telomeres can no longer protect the ends of chromosomes and the uncapped telomere ends of senescent cells

activate a DNA damage checkpoint response (d'Adda di Fagagna et al., 2003; Takai et al., 2003). As a whole, these experiments provided the link between the shortening of telomeres and the induction of replicative senescence.

1.3 Senescence and cancer

Senescence has long been implicated in the development of cancer at the cellular level. Replicative senescence must be bypassed for malignant transformation to occur. Earlier work has shown that replicative senescence is bypassed in most malignancies (~85-90% of primary cancers) by the expression of telomerase (Shay and Bacchetti, 1997). The majority of the remaining 10-15% of cancers extend the ends of telomeres by a mechanism called the alternative lengthening of telomeres (ALT) (Cesare and Reddel, 2010). Extending the telomeres of malignant cells is essential for the constant and seemingly endless growth of cancer cells. The role of senescence in cancer is not limited to the role of replicative senescence on cell proliferation; senescence is also induced as an outcome following the treatment of human cancers. The induction of senescence has been observed in patient samples following treatment with chemotherapeutics and ionizing radiation (Gewirtz et al., 2008; Zhang and Yang, 2011). Senescence that is not primarily driven by telomere attrition is referred to as premature senescence (also referred to as accelerated senescence or stress-induced premature senescence) and is induced as a response to a variety of cellular stresses. Tissue from breast cancer patients treated neo-adjuvantly with a chemotherapy combination (cyclophosphamide, doxorubicin, 5-fluorouracil) showed an increase in senescence-associated beta-galactosidase SAβGal staining when compared to untreated

tumors and especially to normal tissue (te Poele et al., 2002). Although few samples were tested, Roberson *et al* were also able to show that of two tumor samples taken from patients with non-small cell lung cancer (NSCLC) both stained positively for SAβGal, when compared to normal lung tissue, after treatment with carboplatin and taxol. Three untreated patient tumors did not show strong SAβGal staining compared to normal lung, demonstrating that senescence was induced as a result of the chemotherapeutic regimen (Roberson et al., 2005). The induction of senescence in tumors following treatment demonstrates that senescence is not limited to the prevention of transformation; it is an important treatment outcome in established tumors.

A form of premature senescence called oncogene-induced senescence (OIS) prevents malignancy by arresting normal cells following the overexpression of an oncogene or the loss of a tumor suppressor. Almost 30 years ago, it was first observed that overexpressing oncogenic Ras in fibroblasts does not result in cellular transformation (Land et al., 1983). In order to transform normal fibroblast with oncogenic Ras, a second oncogene had to be introduced, such as Myc or the adenoviral E1A protein (Franza et al., 1986; Land et al., 1983). At the time, the mechanism with which the E1A protein aided in cellular transformation was not known. Shortly thereafter, it was determined that the E1A protein binds to the retinoblastoma protein (Rb) and this suggested for the first time that the role of E1A is to inhibit the tumor suppressor function of Rb (Whyte et al., 1988). Fibroblasts overexpressing activated Ras alone entered a cellular crisis and lost the ability to divide (Land et al., 1983). The cellular mechanism responsible for the failure of oncogenic Ras to transform

fibroblasts had to wait 14 years for an explanation. A novel method of tumor suppression was described when Seranno *et al* were able to show that a form of premature senescence, with a phenotype identical to replicative senescence, was induced upon expression of the Ras oncogene (Serrano et al., 1997). This was later termed oncogene-induced senescence (OIS) and the cellular crisis and inability to divide is now seen as the morphology and permanent arrest characteristic of OIS. More recently, the overexpression of many different oncogenes or the silencing of many individual tumor suppressors have been shown to activate oncogene-induced senescence *in vitro* and *in vivo* (Gorgoulis and Halazonetis, 2010). Senescent cells are highly detectable in premalignant tissue but are no longer prevalent in the malignant form. This has been observed by using a variety of mouse models including lung cancer, pancreatic ductal adenocarcinoma (PDAC), melanoma, and breast cancer (Collado et al., 2005; Dankort et al., 2007; Dhomen et al., 2009; Guerra et al., 2011; Sarkisian et al., 2007). Furthermore, senescence has been observed in premalignant human biopsies of pancreatic intraepithelial neoplasia (PanIN), melanocytic nevi, dermal neurofibroma, prostate intraepithelial neoplasia (PIN), and colon adenomas (Bartkova et al., 2006; Chen et al., 2005; Courtois-Cox et al., 2006; Guerra et al., 2011; Michaloglou et al., 2005). This demonstrates that oncogene-induced senescence is an important form of senescence that has to be bypassed for malignant transformation. Since the activation of oncogenes drives OIS, secondary mutations have to occur to bypass the irreversible cell cycle arrest defined by senescence. The most commonly mutated proteins to bypass OIS are in the p16-Rb and p53-p21 pathways, although others have also been described. When looked at together, the tumor suppressors Rb and p53 represent one

of the most commonly lost functions in human cancer (Sherr, 1996). Together, this suggests that similarly to replicative senescence, OIS has to be bypassed for the establishment and maintenance of cancer cells.

1.4 In vivo evidence of the reactivation of senescence

In addition to the activation of OIS in normal human diploid cells, the induction of senescence in malignant cells, which have bypassed OIS, is a very exciting opportunity for the treatment of cancer. Two separate groups have shown that restoring p53 expression in mouse tumors lacking p53 results in tumor regression following the induction of senescence (Ventura et al., 2007; Xue et al., 2007). Sarcomas that developed in mice lacking p53 regressed after restoring p53 expression and the primary outcome after restoring p53 is the induction of senescence in the absence of apoptosis (Ventura et al., 2007). Furthermore, reactivation of p53 in nude mice with established invasive hepatocarcinomas, expressing HRasV12, triggered OIS and resulted in tumor clearance by the innate immune response (Xue et al., 2007). An elegant study by Kang and Yevsa *et al* provided a mechanism for the clearance of senescent hepatocytes from the liver, after undergoing OIS driven by NRasG1V (Kang et al., 2011). They describe the process of senescence surveillance, where the clearance of senescent hepatocytes by antigen-specific $CD4^+$ T-cells limits the development of hepatocellular carcinomas. CD4-/- mice, which could not clear senescent cells from the liver, showed a significant growth of tumors with reduced expression of the cell cycle regulator $p19^{arf}$ (Kang et al., 2011). Collectively, these studies demonstrate that

restoring the ability of established tumors to undergo senescence is a potential therapeutic strategy.

1.5 Markers of senescence

Multiple markers of senescence are used to confirm the senescent phenotype. Examples of these include an enlarged cell morphology (nucleus and cytoplasm), an increase in senescence-associated beta-galactosidase (SAβGal) staining, formation of senescence-associated heterochromatin foci (SAHF), increased expression of the cyclin-dependent kinase inhibitors (Cdki) p21 or p16, and a decrease in Ki-67 positivity (Lawless et al., 2010; Serrano et al., 1997). The enlarged cell morphology was one of the earliest described changes in senescent fibroblasts. Hayflick and Moorehead described Phase III, the terminal (senescent) phase, of cultured human fibroblasts where "in addition to the loss of mitotic activity and accumulation of debris, the cells become much less polarized, more spread out, and lose contact inhibition" (Hayflick and Moorhead, 1961). Hayflick also described senescent cells as more frequently having abnormally large interphase nuclei. He described the bizarre shapes as being reminiscent of irradiated cultures (Hayflick, 1965; Hayflick and Moorhead, 1961). The enlarged and spread out morphology of both the cytoplasm and the nucleus is still one of the hallmarks of senescent cells in culture.

The most commonly used method of staining senescent cells both *in vitro* and *in vivo* is SAβGal staining. In 1995 it was shown by Dimri *et al* that there was a senescence-associated increase in β-galactosidase activity when used at pH 6 (Dimri et al., 1995). Staining cells with the β-galactosidase substrate 5-bromo-4-chloro-3-indoyl

β-D-galactopyranoside (X-gal) results in the formation of an insoluble blue substrate. Most mammalian cells stain blue using an X-gal based stain when performed at pH 4. When stained at pH 6, senescent cells stain positive for β-galactosidase activity, whereas pre-senescent, terminally differentiated, quiescent, and immortalized cells do not. Furthermore, SAβGal staining allowed this group to show an age-dependent accumulation of senescent cells in the skin of donors of various ages (Dimri et al., 1995). At the time it was not known if the presence of SAβGal staining at pH 6 was due to an altered form of the β-galactosidase enzyme or an increase in its expression. It has been known for more than forty years that there is an accumulation in the number and size of lysosomes in senescent cells (Robbins et al., 1970). In 2000, Kurz *et al* were able to demonstrate that SAβGal stain increased with a buildup of β-galactosidase protein and an increase in lysosomal content (Kurz et al., 2000). Knowing that levels of β-galactosidase protein accumulate in senescent cells, it was then shown that the GLB1 gene, which encodes lysosomal β-D-galactosidase, was responsible for SAβGal activity. This confirmed the mechanism and location of SAβGal stain in senescent cells (Lee et al., 2006). The chromogenic method for SAβGal staining has been further validated as a major marker of senescent cells and other methods involving a fluorescent substrate for β-galactosidase activity have begun to be used in a handful of studies (Debacq-Chainiaux et al., 2009).

The defining characteristic of senescent cells is the loss of proliferation potential following the induction of senescence. The absence of proliferative markers, such as Ki-67 and BrdU incorporation, is commonly used to depict the long-term cell cycle arrest of senescent cells. The Ki-67 antigen was first identified and described in 1983 by

Gerdes *et al* as a nuclear antigen that is specific to proliferating cells (Gerdes et al., 1983). During interphase Ki-67 is associated with the nucleolus, likely due to its involvement in the early stages of ribosomal RNA synthesis (Bullwinkel et al., 2006; Rahmanzadeh et al., 2007; Verheijen et al., 1989a). Levels of Ki-67 are highest during mitosis where it associates with condensed chromosomes (Lopez et al., 1991; Verheijen et al., 1989b). Bromodeoxyuridine (BrdU) is also used as a proliferative marker both *in vitro* and *in vivo*. BrdU is either added to media *in vitro* or injected into mice *in vivo* where it is incorporated into DNA while it is synthesized during S-phase. Following its incorporation into cells BrdU is detected using an antibody specific to the BrdU molecule; this labels cells that have entered S-phase while BrdU was present. These two markers are two commonly used methods to demonstrate that senescent cells are not proliferating or cycling through the cell cycle.

Another marker of senescent cells was first described in 2003 and is termed senescence-associated heterochromatin formation (SAHF). Narita *et al* first described the formation of condensed heterochromatin structures in senescent fibroblasts that are enriched for the heterochromatin marker histone H3 tri-methylated on Lysine 9 (H3K9me3) (Narita et al., 2003). The formation of SAHF was shown to be dependent on the p16-Rb pathway and shRNA targeting p16 or Rb circumvented the establishment of SAHF (Narita et al., 2003). SAHF formation is suggested as a possible mechanism for the stable cell cycle arrest that is observed in senescence, as compared to quiescence. The large foci of the SAHF phenotype have been shown to be individual compacted chromosomes, highlighting the high degree of heterochromatin formation (Zhang et al., 2007). More recently, it has been shown that senescence can be established without the

formation of SAHF (Kosar et al., 2011). This group went further to show that the induction of SAHF was cell-type dependent and was associated with p16 expression. Even though SAHF formation is an important consequence and marker of senescence, the induction of this large-scale heterochromatin formation is not essential to all instances of premature senescence.

The predominant molecular pathways of senescence induction are the p53-p21 or p16-Rb pathways (Figure 1). This is a simplified overview of the pathways as there is not only many other proteins involved but there is also crosstalk and some convergence between the two pathways themselves. This representation of the senescence pathways also centers on the G1/S phase cell cycle arrest as the predominant cell cycle arrest observed in senescent cells. In senescence the p53-p21 pathway has two predominant mechanisms of increasing p53 protein levels. One is through the DNA damage response pathway via ATM/ATR, resulting in the disruption of the E3 ubiquitin ligase Mdm2 binding to and degrading p53 (Chehab et al., 1999). The other mechanism is through the inactivation of Mdm2 by Arf (Sherr, 2001). The *CDKN1A* gene, encoding p21, is a p53 responsive gene and the original importance of p21 was attributed to its role as the mediator of p53-dependent G1 cell cycle arrest (Deng et al., 1995). The primary effector of the G1 arrest observed in senescence is through inhibition of the E2F transcription factors, which regulate genes that promote entry into S-phase, by Rb. Non-phosphorylated (hypophosphorylated) Rb binds to and represses the function of E2F proteins. When Rb is phosphorylated by cyclin E-Cdk2, cyclin D-Cdk4, or cyclin D-Cdk6, Rb is released from and no longer inhibits E2F activity. The main function of p21 during G1 cell cycle arrest is its inhibition of cyclin E-Cdk2

Figure 1.1. Molecular pathways of senescence induction

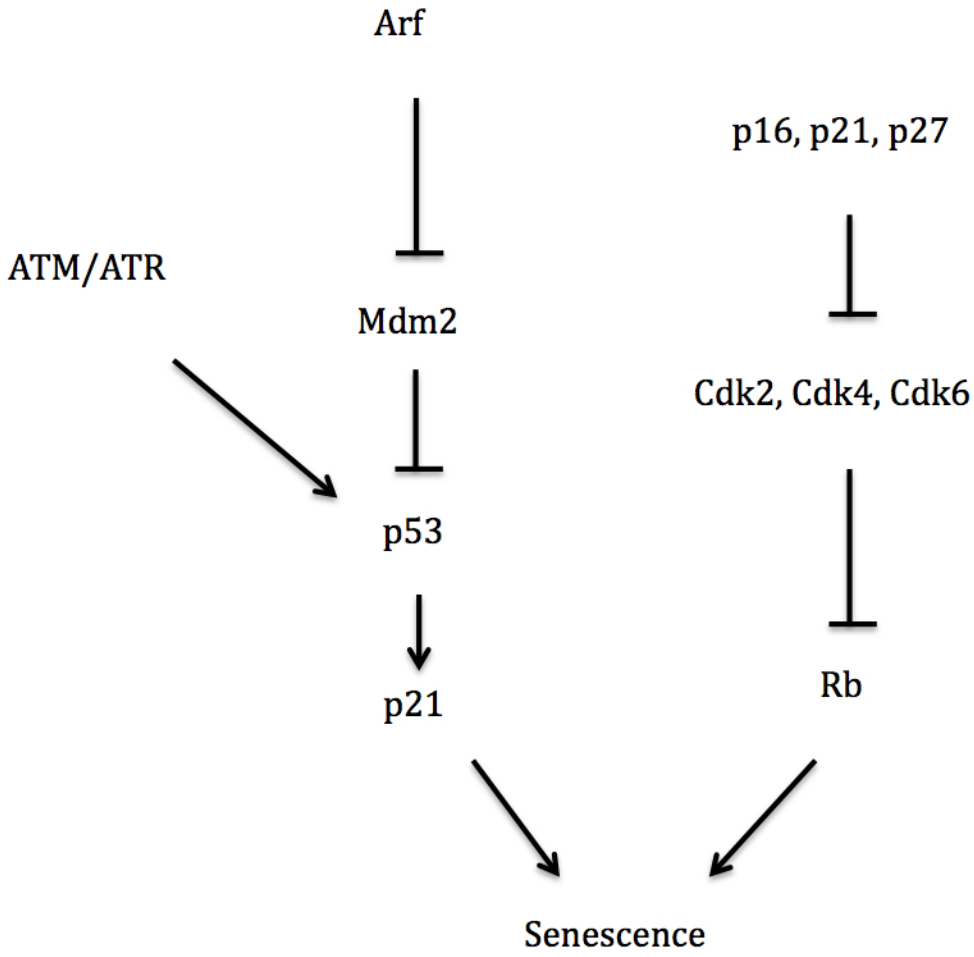
Arf
p16, p21, p27
ATM/ATR
Mdm2
Cdk2, Cdk4, Cdk6
p53
p21
Rb
Senescence

activity (Abbas and Dutta, 2009). The principal mechanism of the p16-Rb pathway is the inhibition of cyclin D-Cdk4/6 activity by p16 (Lowe and Sherr, 2003). The inhibition of these cyclin-Cdk complexes results in the hypophosphorylation of Rb, repression of E2F activity and an inability to progress into S phase. The increased expression or dependence on the proteins involved in these pathways are often used as markers of senescence induction.

To date there is no senescence-specific marker that can, on its own, specifically and reproducibly determine that a cell is senescent, therefore it is important to assess multiple markers of senescence to be confident in its description. The use of a senescence-associated marker such as SAβGal or SAHF, morphological changes of cells, a lack of proliferation markers, and observed molecular changes that provide details of the mechanism are often used in combination to be confident in the description of cellular senescence.

1.6 Heat shock protein 90

Heat shock proteins are molecular chaperone proteins that maintain cellular proteostasis by aiding the proper folding, preventing aggregation, assisting in intracellular trafficking, or promoting degradation of cellular proteins (Taipale et al., 2010). The heat shock response was first described in *Drosophila* larvae by Ritossa in 1962 where it was shown that variations in chromosome activity and an increase in RNA synthesis occurred after larvae were subjected to an increase in temperature from 25°C to 30°C (De Maio et al., 2012; Ritossa, 1962). This initial observation lead to the initial description of heat shock proteins in 1974 and their diverse and ubiquitous

molecular functions continue to be discovered and examined (De Maio et al., 2012; Tissieres et al., 1974). Heat shock protein 70 (Hsp70) is one of the most frequently used chaperones in the cell and has been shown to bind a large variety of proteins to allow proper folding and prevent aggregation (Beckmann et al., 1990; Wegele et al., 2004). Unlike Hsp70, Hsp90 is not directly required for the folding of most proteins but has been shown to be necessary for a specific set of proteins referred to as client proteins. Although client proteins are a specific set of proteins, the number of Hsp90 clients is now in the hundreds and they encompass many diverse cellular functions (Taipale et al., 2010). An updated list of Hsp90 client proteins is available in a database maintained by the Picard Laboratory (Echeverria et al., 2011). Hsp90 is essential for eukaryotic survival, is one of the most conserved heat shock proteins and is found in all branches of the Eukarya domain (Wegele et al., 2004). In unstressed cells Hsp90 is one of the most abundant proteins, comprising 1-2% of total cytosolic protein levels (Wegele et al., 2004). Expression levels of Hsp90 are induced not only after heat shock but also following a variety of proteotoxic stresses such as oxidative stress, exposure to heavy metals, acidosis, toxins, bacterial infections, and some viral infections (Leppa and Sistonen, 1997; Whitesell and Lindquist, 2005). There are two isoforms of Hsp90, termed Hsp90α and Hsp90β. Hsp90α is more inducible than Hsp90β, which is more constitutive, therefore when Hsp90 is written without specifying the isoform it generally refers to Hsp90α (Csermely et al., 1998). Cytosolic Hsp90 also has two paralogs; Grp94 is found in the endoplasmic reticulum where it mainly helps in the maturation of nascent proteins and protein quality control, and Trap1 is found in the mitochondria where it protects against oxidative stress and prevents cell death (Eletto

et al., 2010; Kang, 2012). Hsp90 has been shown to have a role in the pathology of multiple human diseases such as neurodegenerative diseases, cystic fibrosis, ischemia, various infections and cancer (Csermely et al., 1998; Smith et al., 1998; Whitesell and Lindquist, 2005).

1.7 Hsp90 and Cancer

The identification of both Hsp90 client proteins and the role of Hsp90 in cancer cell maintenance were made possible by the use of specific inhibitors to Hsp90. In 1994 Whitesell *et al* showed for the first time that the benzoquinone ansamycin antibiotic geldanamycin (GA) could revert v-Src transformed cells by inhibiting the v-Src-Hsp90 complex (Whitesell et al., 1994). This was the first evidence that the pharmacological inhibition of Hsp90 and disruption of its ability to chaperone an oncoprotein had therapeutic potential against cancer cells. The inhibition of Hsp90 also helped to explain the already established ability of benzoquinone ansamycins to have antitumor activity (Whitesell et al., 1992). Geldanamycin was then shown to inhibit the Hsp90 chaperone function by binding the ATP binding pocket and inhibiting the ATP dependent function of Hsp90 (Prodromou et al., 1997). Inhibition of Hsp90 dependent refolding of heat-denatured proteins by benzoquinone ansamycins results in degradation by the ubiquitin proteasome system (Schneider et al., 1996). Since the mechanism of inhibition by geldanamycin, and another natural product radicicol (RA), has been elucidated, many new compounds have been designed. Due to chemical instability and side effects observed *in vivo* using geldanamycin, a modified version called 17-allylamino-17-demethoxygeldanamycin (17-AAG, or tanespimycin) was

shown to have improved pharmacological properties (Neckers and Workman, 2012). Currently, 20 different compounds have entered clinical trials as a cancer therapeutic and more compounds are in preclinical development (Travers et al., 2012). To date, two clinical trials have shown the benefit and potential of using Hsp90 inhibitors in cancer patients. In a Phase II trial, the 17-AAG analog IPI504 had a clinical benefit in all non-small cell lung cancer (NSCLC) patients with an ALK rearrangement (two partial responses, one prolonged stable disease). However, only 3 of the 76 patients entered in the trial had ALK rearrangements and the overall objective response rate of all 76 patients was only 7% (Sequist et al., 2010). More convincing data was obtained from a Phase II study in patients with trastuzumab-resistant Her2-positive metastatic breast cancer where 17-AAG was given in combination with trastuzumab. This study used Response Evaluation Criteria in Solid Tumors (RECIST) criteria to show a clinical benefit (complete response, partial response, or stable disease) in 59% of patients (Modi et al., 2011). Apart from these results, data from other clinical trials has been underwhelming. There is however optimism that the second generation of Hsp90 inhibitors about to enter or currently beginning clinical trials will improve dose-limiting toxicity, degradation of client proteins during treatment, timing of drug administration, and maintenance Hsp90 inhibition in tumors (Travers et al., 2012).

In 2003 an important study by Kamal *et al* shed light on the molecular mechanism for the therapeutic index observed when using Hsp90 inhibitors on cancer cells compared to normal cells (Kamal et al., 2003). They were able to demonstrate that Hsp90 in cancer cells was predominantly found in an active form (high ATPase activity) as a complex with cochaperones, whereas Hsp90 in normal cells was predominantly

found in a less active and uncomplexed form. Furthermore, using Hsp90 obtained from human clinical tumor or normal tissue samples, they showed that tumor Hsp90 had a 100-fold higher binding affinity for 17-AAG (Kamal et al., 2003). More recently, Moulick *et al* showed that the Hsp90 inhibitor PU-H71, structurally distinct from 17-AAG, preferably bound to Hsp90 isolated from tumor cells. They were also able to show that PU-H71 preferably bound to Hsp90 complexed with co-chaperones and the oncoprotein Bcr-Abl as compared to the uncomplexed fraction bound to the normal Abl protein (Moulick et al., 2011). Many client proteins of Hsp90 have known roles in the development or maintenance of cancer, such as: Raf-1, Akt, Her2, cdk4, telomerase, and Hif-1α (Basso et al., 2002; Holt et al., 1999; Sato et al., 2000; Schulte et al., 1995; Stepanova et al., 1996). Importantly, Hsp90 has been shown to preferentially chaperone and stabilize mutant oncogenic proteins in comparison to the normal wild-type forms. Examples of this preference for oncogenic proteins include mutant V600E BRaf, Bcr-Abl, v-Src, and mutant p53 (Brugge et al., 1983; Grbovic et al., 2006; Moulick et al., 2011; Oppermann et al., 1981). Higher expression of Hsp90 is: associated with decreased survival in breast cancer; a marker of progression in melanoma; a marker of recurrence in gastrointestinal stromal tumors; and a marker of poor response to neoadjuvant chemoradiotherapy in rectal cancer (Kang et al., 2010; McCarthy et al., 2008; Pick et al., 2007).

1.8 Protein Kinase C iota

The protein kinase C (PKC) family of kinases is a set of serine/threonine kinases that are structurally related. The PKC family is divided into three categories based on

the presence of particular domains: four conventional PKCs (cPKC; α, βI, βII, γ); four novel PKCs (nPKC; δ, ε, η, θ); and two atypical PKCs (aPKC; ζ, ι). In contrast to the conventional and novel PKC groups, the aPKCs are not dependent on calcium or diacylglycerol (DAG) for their activation (Nishizuka, 1995; Ono et al., 1989). Instead of the binding motifs that bind calcium or DAG, the distinct N-terminus of the aPKCs has a Phox-Bem1 (PB1) domain that mediates protein-protein interactions (Lamark et al., 2003). The activation of aPKCs is modulated by these protein-protein interactions, as is the case in the PKCι-Par6-cdc42 polarity complex where Cdc42 activates PKCι via Par6, which interact through its PB1 domain (Lamark et al., 2003; Yamanaka et al., 2001). Downstream of the phosphoinositide 3-kinase (PI3K) pathway, 3-phosphoinositide dependent protein kinase-1 (PDK1) activates aPKCs by directly phosphorylating a threonine residue in its activation loop (Balendran et al., 2000; Chou et al., 1998; Le Good et al., 1998). Protein kinase C iota (PKCι), or PKCλ in mice, is the more ubiquitously expressed of the two atypical PKCs during mouse embryogenesis (Kovac et al., 2007). There are differences in the functionality of the two aPKCs: PKCι knockout mice are embryonic lethal, whereas PKCζ knockout mice are grossly normal with some alterations in lymphoid tissue (Bandyopadhyay et al., 2004; Leitges et al., 2001). However, despite some differences in functionality the amino acid sequences of PKCι and PKCζ share 72% similarity (Akimoto et al., 1994).

1.9 PKCι and Cancer

The role of PKCι in cancer has been well established and is continuing to be expanded upon. PKCι was the first PKC isozyme that was shown to be an oncogene

(Regala et al., 2005b). PKCι is required for Ras-mediated transformation of rat intestinal epithelium and tumor growth in mouse NSCLC xenografts (Murray et al., 2004; Regala et al., 2005a). Previous work from our lab has demonstrated that PKCι represses cisplatin-induced apoptosis, promotes invasion and motility, and is necessary for glioblastoma cell proliferation (Baldwin et al., 2010; Baldwin et al., 2006; Baldwin et al., 2008). PKCι is overexpressed in multiple human tumor types including but not limited to brain, breast, ovarian, and NSCLC (Eder et al., 2005; Kojima et al., 2008; Murray et al., 2011; Patel et al., 2008; Regala et al., 2005b). Furthermore, elevated expression of PKCι predicts poor survival in NSCLC, PDAC, cholangiocarcinoma, and ovarian cancer (Eder et al., 2005; Li et al., 2008; Regala et al., 2005b; Scotti et al., 2010). The higher expression of PKCι in many cancers is attributed to amplification of the *PRKCI* gene, which is located on chromosome 3q26, an area that is frequently amplified in human cancers (Murray et al., 2011). Amplification of 3q26 correlates with the *PRKCI* copy number and PKCι RNA expression in serous epithelial ovarian cancer and PKCι protein expression in esophageal squamous cell carcinoma (Eder et al., 2005; Yang et al., 2008). However, there is also evidence of high PKCι expression in cancers that do not frequently have chromosome 3q26 amplification, such as PDAC and colon cancer (Murray et al., 2004; Murray et al., 2011; Scotti et al., 2010). Therefore, other mechanisms of increasing PKCι expression occur in some tumor types. Together, these observations provide strong evidence for the pharmacological targeting of PKCι as a therapeutic for human cancers.

1.10 Centrosomes

Centrosome integrity and number are essential to the progression through the cell cycle, especially for the establishment of the spindle assembly in mitosis. The single centrosome present in the G1 phase is duplicated during S phase and these two centrosomes separate when the nuclear envelope breaks down during M phase to establish the microtubule organizing centers (MTOCs). Centrosome abnormalities such as an increase in number, or supernumerary centrosomes, have been observed in the majority of tumors throughout the human body (Nigg, 2002). Centrosomal abnormalities have been described as an early event in tumor progression (Kayser et al., 2005; Lingle et al., 2002; Pihan et al., 2003). Furthermore, centrosomal aberrations have been shown to increase with tumor progression in ovarian, non-Hodgkin's lymphoma, breast, prostate, head and neck, and bladder cancers. (Hsu et al., 2005; Kramer et al., 2003; Lingle et al., 2002; Pihan et al., 2001; Reiter et al., 2009; Yamamoto et al., 2004). In non-transformed cells, depletion of 14 out of 15 centrosomal proteins using small interfering RNA (siRNA) was shown to cause a G1 cell cycle arrest in human diploid cell lines. This arrest was accompanied by a reduction of Cdk2-cyclin A activity and the further loss of the Cdk inhibitor p21 bypassed the G1 arrest. This was characterized to show that centrosome defects trigger a p38-p53-p21 dependent checkpoint that induces a G1/S cell cycle arrest (Mikule et al., 2007). This study did not assess if senescence was being induced following the depletion of these proteins. Nevertheless, other studies have shown that depletion of centrosomal proteins such as TACC3, PCM1 and pericentrin induces senescence (Schmidt et al., 2010; Srsen et al., 2006). Disruption of proper centrosomal function can trigger senescence in normal

cells. Importantly, if dysfunctional centrosomes are left unchecked, they have the potential to promote the initiation and progression of cancer.

1.11 Hypothesis

Cellular senescence must be bypassed for the proliferation of cancer cells; therefore, inhibition or depletion of proteins that suppress senescence in human cancer cells will result in the induction of premature senescence.

Aim of thesis

The main objective of this thesis is to identify and characterize the induction of premature senescence in human cancer cells by:

1. Characterizing the inhibition of Hsp90 as a novel mechanism to induce premature senescence in small cell lung cancer cells.
2. Characterizing the depletion of PKCι as a novel mechanism to induce premature senescence in glioblastoma cells.
3. Identifying the mechanism of PKCι depletion-induced senescence in glioblastoma cells.

2. Induction of Premature Senescence by Hsp90 Inhibition in Small Cell Lung Cancer

Ian J Restall[1,2] and Ian A J Lorimer[1,2,3]

[1]Ottawa Hospital Research Institute and the [2]Department of Biochemistry, Microbiology and Immunology, [3]Department of Medicine, University of Ottawa, Ottawa, Ontario, Canada

Running Title: Induction of premature senescence by Hsp90 inhibition

Keywords: Hsp90, senescence, small cell lung cancer, geldanamycin, radicicol

Address correspondence to: Ian A. J. Lorimer, The Ottawa Hospital Cancer Centre, Centre for Cancer Therapeutics

Contribution of Authors
The content of this manuscript was written by I.J. Restall with the help of Dr. I.A.J. Lorimer. All of the experiments presented in this manuscript are the work of I.J. Restall.

Published: PLoS ONE. 2010; 5(6): art. no. e11076

SUMMARY

Background: The molecular chaperone Hsp90 is a promising new target in cancer therapy and selective Hsp90 inhibitors are currently in clinical trials. Previously these inhibitors have been reported to induce either cell cycle arrest or cell death in cancer cells. Whether the cell cycle arrest is reversible or irreversible has not generally been assessed. Here we have examined in detail the cell cycle arrest and cell death responses of human small cell lung cancer cell lines to Hsp90 inhibition.

Methodology/ Principal Findings: In MTT assays, small cell lung cancer cells showed a biphasic response to the Hsp90 inhibitors geldanamycin and radicicol, with low concentrations causing proliferation arrest and high concentrations causing cell death. Assessment of Hsp90 intracellular activity using loss of client protein expression showed that geldanamycin concentrations that inhibited Hsp90 correlated closely with those causing proliferation arrest but not cell death. The proliferation arrest induced by low concentrations of geldanamycin was not reversed for a period of over thirty days following drug removal and showed features of senescence. Rare populations of variant small cell lung cancer cells could be isolated that had additional genetic alterations and no longer underwent irreversible proliferation arrest in response to Hsp90 inhibitors.

Conclusions/ Significance: We conclude that: (1) Hsp90 inhibition primarily induces premature senescence, rather than cell death, in small cell lung cancer cells; (2) small cell lung cancer cells can bypass this senescence through further genetic alterations; (3) Hsp90 inhibitor-induced cell death in small cell lung cancer cells is due to inhibition of a target other than cytosolic Hsp90. These results have implications with regard to

how these inhibitors will behave in clinical trials and for the design of future inhibitors in this class.

INTRODUCTION

Hsp90 functions as a chaperone in normal cells, promoting the correct folding of both newly synthesized proteins and proteins that have been partially denatured due to stress (1). It appears to be primarily involved in late stages of folding, probably by recognizing exposed hydrophobic surfaces on partially folded proteins. The basic mechanism of Hsp90-induced protein folding involves conformational switching between open and closed conformations that is regulated by ATP hydrolysis (2). Rates of Hsp90 ATP hydrolysis are controlled in turn by its association with various cochaperones.

Although the number of proteins known to require Hsp90 for correct folding continues to increase, Hsp90 is clearly selective for a subset of cellular proteins. These include a number of proteins with known oncogenic activity, including Her2, Raf1 and Cdk4 (3). In some cases Hsp90 shows preferential association with the mutant, oncogenic forms of proteins; this has been shown for both Src kinase and the EGF receptor (4-6). Hsp90 also shows an increased association with cochaperones and higher ATPase activity in cancer cells, both *in vitro* and *in vivo* (7). For these reasons there is considerable interest in Hsp90 as a target for cancer therapy.

Geldanamycin and radicicol are two structurally unrelated natural products that bind to the ATP binding site of Hsp90, blocking the conformational cycling that is necessary for its chaperone activity. These compounds show good selectivity for Hsp90, although they also bind to the Hsp90 endoplasmic reticulum paralog Grp94 and the Hsp90 mitochondrial paralog Trap1 at higher concentrations (8-10). While these compounds establish in principle that Hsp90 is a "druggable" target from a

pharmacology perspective, poor solubility and non-specific toxicities make them unsuitable for use in humans. Derivatized versions of geldanamycin have been produced that have improved pharmacological properties, although they still have some of the limitations of the parent compound (11). In spite of this, there is evidence from some trials that Hsp90 inhibition is achievable, based on biomarker analysis in patient lymphocytes (12,13) and tumour samples (14). There is also some evidence for anticancer activity (15). Recently novel Hsp90 inhibitors have been developed that do not have the limitations of previous compounds, and these are now entering clinical trials (11). With these advances in the pharmacology of Hsp90 inhibition, a critical new area of investigation will be the identification of subsets of cancer patients that are most likely to benefit from Hsp90 inhibition.

Lung cancer is the largest cause of cancer deaths worldwide. About 15 % of lung cancers are of a subtype known as small cell lung cancer. This cancer usually presents as metastatic disease and is usually not treated with surgery. Small cell lung cancer generally responds very well to radiation and chemotherapy initially, but the majority of patients relapse with resistant disease and die within two years (16). The majority of small cell lung cancers have neuroendocrine properties and actively secrete polypeptide hormones (17). These secreted hormones cause a range of paraneoplastic syndromes that are common complications of small cell lung cancer.

Here we have investigated the response of small cell lung cancer cells to Hsp90 inhibition. A previous study had shown that Hsp90 inhibitors induce cell death in small cell lung cancer cells via activation of the intrinsic pathway for apoptosis (18). Our findings are consistent with this, but we observed that cell death only occurs at

concentrations far higher than those required for inhibition of cytosolic Hsp90. We observe that treatment of small cell lung cancer cells with Hsp90 inhibitors at concentrations that are sufficient to inhibit cytosolic Hsp90 induces premature senescence rather than cell death.

RESULTS

Response of human small cell lung cancer cell lines to Hsp90 inhibition: The human small cell lung cancer cell line H69 showed a biphasic response to treatment with a range of geldanamycin concentrations (Figure 1A). In a MTT assay, a 48 h exposure of cells to 0.1 μM geldanamycin decreased viable cell numbers by approximately 40 %. Increasing the concentration of geldanamycin to up to 3 μM did not cause a further decrease in viable cell numbers. With concentrations of geldanamycin > 4 μM, numbers of viable H69 cells decreased to essentially zero. Radicicol, a second Hsp90 inhibitor that is structurally unrelated to geldanamycin, also gave a biphasic dose response curve with H69 cells, although with a less distinct plateau phase (Figure 1B). Two other small cell lung cancer cell lines (H187 and H889) also show a biphasic response to geldanamycin (Figure 1 C and D); however the U87MG glioblastoma cell line showed only the first phase of this response (*i.e*. the phase seen at low geldanamycin concentrations) (Figure 1E).

As the first phase could be potentially due to either inhibition of cell proliferation or selective killing of a subset of SCLC cells, further assays were performed to distinguish between these possibilities. The response of H69 cells to treatment with a range of geldanamycin concentrations was assayed by cell counts, using trypan blue exclusion to distinguish live cells from dead cells (Figure 1F). The live cell counts also showed a biphasic response when assayed by this method. Total cell counts were similar to live cell counts in the first phase of the biphasic response curve but diverged in the second phase. These data show that geldanamycin primarily

Figure 1. Response of small cell lung cancer cells to Hsp90 inhibition. A, MTT assay of H69 cells treated with geldanamycin for 48 h; B, MTT assay of H69 cells treated with radicicol for 48 h; C, MTT assay of H187 small cell lung cancer cells with geldanamycin for 12 (●), 36 (○) and 60 (■) h; D, MTT assay of H889 cells treated with geldanamycin for 48 h; E, MTT assay of U87MG glioblastoma cells treated with geldanamycin for 48 h; F, H69 cells treated with geldanamycin for 48 h and assayed for viable (○) and total (●) cell counts using a Vi-cell XR cell viability analyzer. Error bars show the mean ± SE of three replicates.

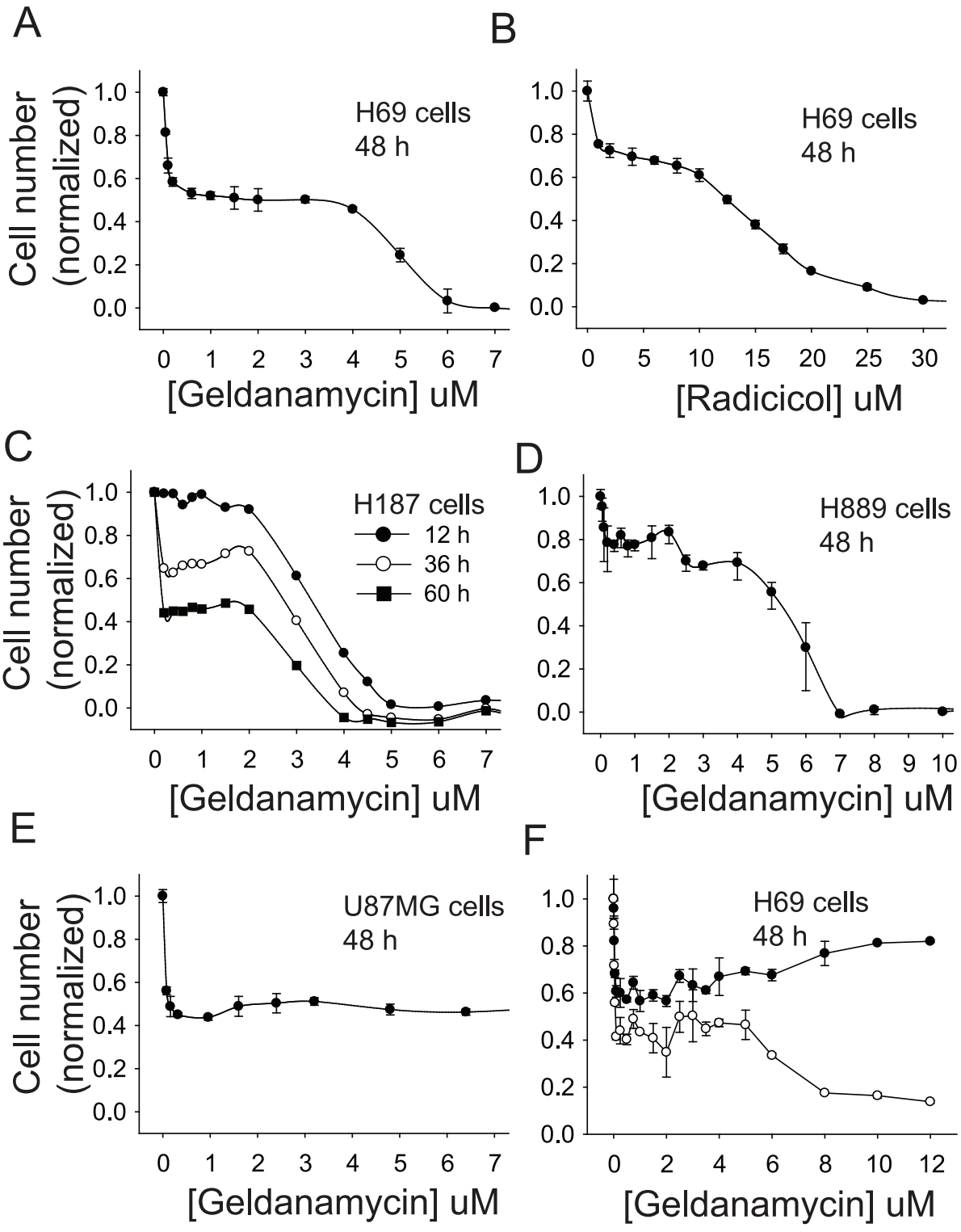
A
B
C
D
E
F
Cell number (normalized)
H69 cells
48 h
[Geldanamycin] uM
[Radicicol] uM
H187 cells
12 h
36 h
60 h
H889 cells
U87MG cells

induces proliferation arrest in H69 cells at low concentrations but induces cell death at high concentrations. The data in Figure 1C, which show MTT assays on H187 cells treated for different periods of time (12, 36 and 60 h) with geldanamycin, are consistent with this conclusion, as the first phase is only evident with longer treatments where there is time for significant cell proliferation to take place in the control. This also shows that the cell death at high geldanamycin concentrations happens relatively rapidly (*i.e.* in less than 12 h).

Response of H69 cells after withdrawal of Hsp90 inhibition: Proliferation arrest induced by drugs may be reversible or irreversible (*i.e.* senescence-like). To distinguish between these possibilities, H69 cells were treated with different concentrations of geldanamycin for two days. Drug was then removed and viable cell counts were monitored. Cell proliferation recovered from treatment with geldanamycin concentrations of 50 nM or less. However, after treatment with 100 nM geldanamycin, a population of viable cells remained that did not increase over a time period of greater than thirty days after removal of drug (Figure 2A). Similar results were obtained with the H187 and H889 small cell lung cancer cell lines (Figure 2B and Supplementary Figure 1A) and in H69 cells treated with the clinically-relevant Hsp90 inhibitor 17-AAG (Figure 2C). H69 cells required a minimum of 24 h of exposure to geldanamycin to induce irreversible proliferation arrest (Figure 2D) and the induction of irreversible proliferation arrest was unaffected by caspase inhibition (Figure 2E). For comparison the same experiment was performed on the U87MG human glioblastoma cell line (Figure 2F). These cells recover growth after treatment with 100 nM geldanamycin and also recover from a treatment with a ten-fold higher concentration of geldanamycin.

Figure 2. Proliferation after withdrawal of Hsp90 inhibitors. Cells were treated for 48 h with the indicated concentration of inhibitor, which was then removed. Viable cell counts were then determined at the indicated times after inhibitor removal. A, H69 cells treated with geldanamycin; B, H187 cells treated with geldanamycin; C, H69 cells treated with 17-AAG. D, H69 cells treated with 100 nM geldanamycin for 4, 12 or 24 h. E, H69 cells were treated for 48 h with 100 nM geldanamycin in the absence or presence of 100 μM Z-VAD-FMK, a general caspase inhibitor. Z-VAD-FMK treatment was started 1 h before the addition of geldanamycin. F, U87MG cells treated with geldanamycin.

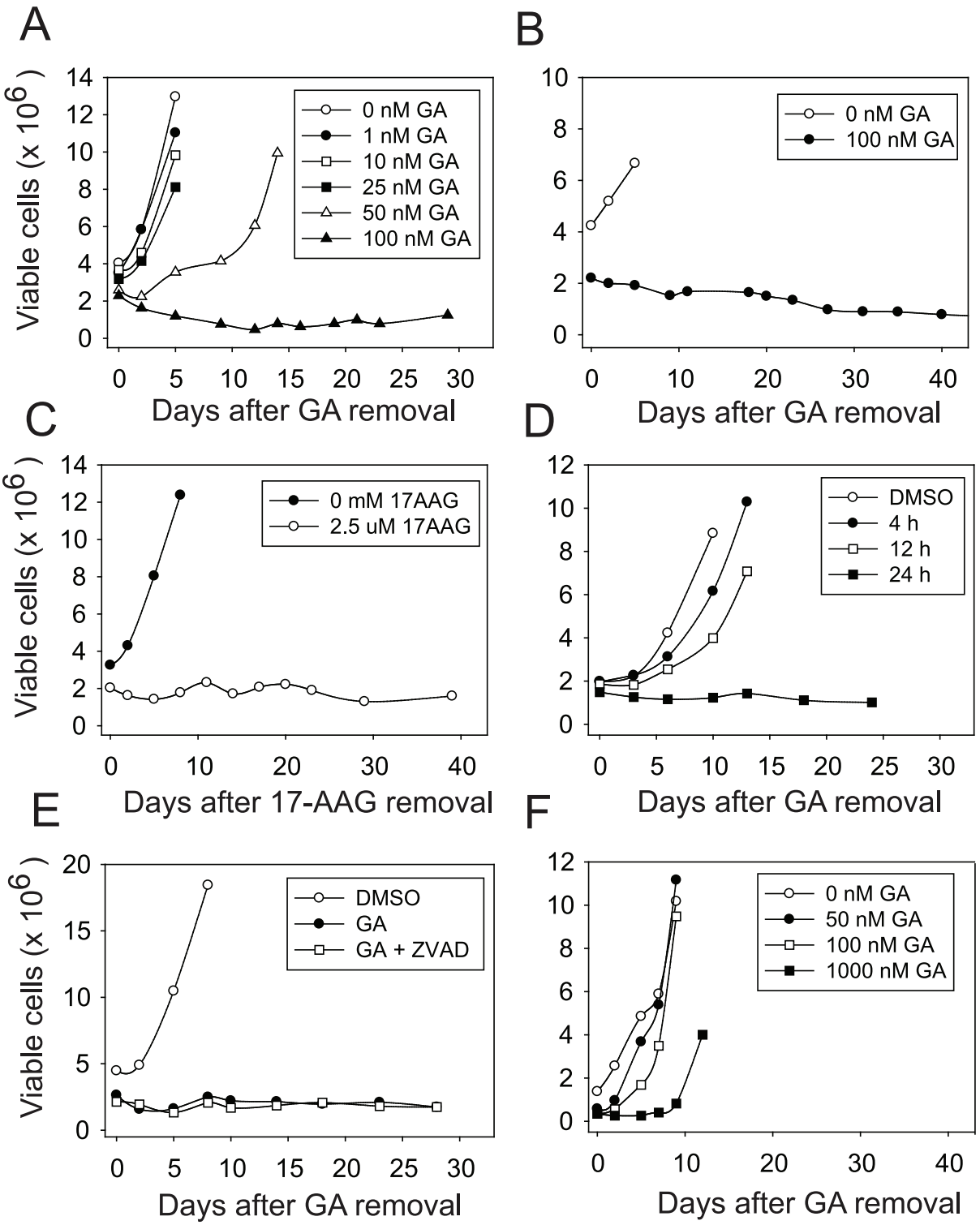
A
Viable cells (x 10^6)
Days after GA removal
0 nM GA
1 nM GA
10 nM GA
25 nM GA
50 nM GA
100 nM GA
B
Days after GA removal
0 nM GA
100 nM GA
C
Viable cells (x 10^6)
Days after 17-AAG removal
0 mM 17AAG
2.5 uM 17AAG
D
Days after GA removal
DMSO
4 h
12 h
24 h
E
Viable cells (x 10^6)
Days after GA removal
DMSO
GA
GA + ZVAD
F
Days after GA removal
0 nM GA
50 nM GA
100 nM GA
1000 nM GA

The sustained proliferation arrest induced by geldanamycin is therefore not a universal response of cancer cells but rather is cancer cell-type specific.

To confirm the sustained growth arrest by a second method, incorporation of BrdU into H69 cells that had been exposed to 100 nM geldanamycin was also assessed. Consistent with viable cell counts, this assay showed that H69 cells failed to recover their proliferative capacity after geldanamycin removal (Figure 3A).

Changes in Hsp90 client proteins and heat shock proteins in response to Hsp90 inhibition: The effects of different concentrations of geldanamycin on known Hsp90 clients were also assessed in H69 cells (Figure 3B, right four lanes of blot). Substantial depletion of the Hsp90 client proteins Cdk4 and Raf1 were seen at geldanamycin concentrations as low as 50 nM. A second well-described response of cells to Hsp90 inhibition is the induction of other heat shock proteins that occurs via activation of Hsf1 (19). As with client protein responses, geldanamycin concentrations as low as 50 nM caused increases in Hsp70, Hsp27 and Hsp90α/β. These geldanamycin concentrations parallel those that cause proliferation arrest, but are about 100 times less than the concentrations that cause substantial cell death.

U87MG and H69 cells showed very similar sensitivities to geldanamycin with respect to client protein decreases and heat shock protein increases (Figure 3B). This indicates that the difference in behavior between H69 and U87MG cells after removal of geldanamycin is not a consequence of differences in drug metabolism (*e.g.* multidrug transporter activity or diaphorase activity, both of which affect geldanamycin activity (20,21)). Rather it appears that the different responses of these cells after withdrawal of geldanamycin are due to differences that are downstream of Hsp90 inhibition.

Figure 3. BrdU incorporation and client protein responses in Hsp90 inhibitor-treated cells. A. H69 cells were treated for 48 h with 100 nM geldanamycin. Geldanamycin was then removed. Six or eight days after drug removal, 25,000 treated cells (GA) per well were plated in ninety-six well plates along with the same number of untreated H69 cells for comparison (no GA). Cells were allowed to uptake BrdU for 16 h and BrdU incorporation was then assayed as described in Materials and Methods. Results were normalized to the values for untreated cells. Data shown are the mean ± SD of six replicates. B. Cells were treated for 48 h with geldanamycin. Total cell lysates were then collected and analyzed by Western blotting using antibodies to the indicated proteins. The bottom panel shows a blot stained for total protein with amido black prior to antibody incubation. Equal amounts of DMSO were added to cells for each treatment, except in the leftmost lane, where DMSO was omitted.

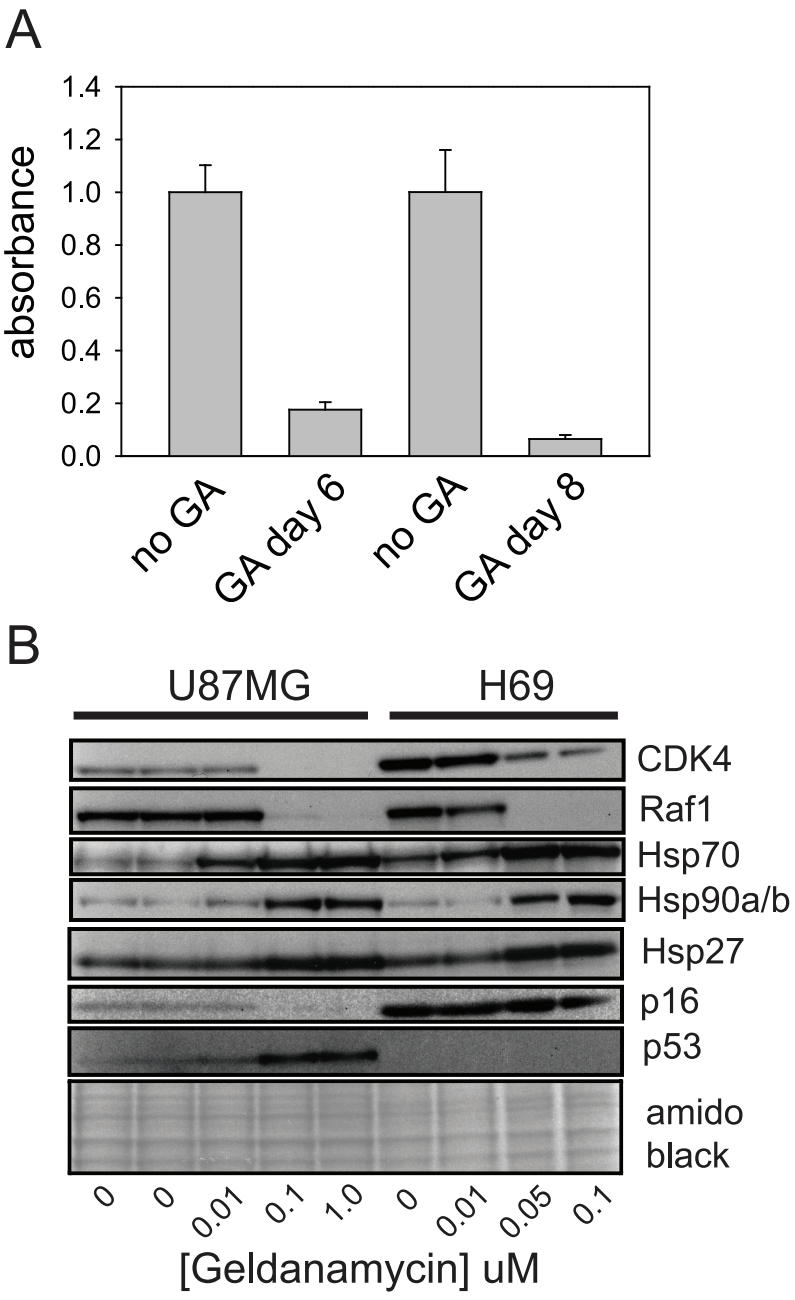
A
absorbance
1.4
1.2
1.0
0.8
0.6
0.4
0.2
0.0
no GA
GA day 6
no GA
GA day 8
B
U87MG
H69
CDK4
Raf1
Hsp70
Hsp90a/b
Hsp27
p16
p53
amido
black
0
0
0.01
0.1
1.0
0
0.01
0.05
0.1
[Geldanamycin] uM

Western blot analysis confirmed that H69 cells lacked detectable p53 (Figure 3B), in agreement with Smith *et al*., who showed that there is a stop mutation in *P53* exon 5 in this cell line (22). p16Ink4a was present in H69 cells and its levels were unaffected by treatment with geldanamycin for 48 h (Figure 3B).

Senescence markers in growth-arrested small cell lung cancer cells: The irreversible proliferation arrest induced by Hsp90 inhibition in small cell lung cancer cells suggested that these cells had become senescent. To assess this further, additional markers of senescence were assessed. Figure 4A shows the morphology of suspension cultures of untreated H69 cells eight days after geldanamycin removal. Treated cells show some enlargement and increased cytoplasmic granularity, characteristic features of senescent cells. Another common feature of senescent cells is the presence of senescence-associated heterochromatin foci (SAHF) (23). Consistent with senescence induction, inhibition of Hsp90 with geldanamycin led to the formation of SAHF in H69 cells as demonstrated by DAPI staining (Figure 4B). SAHF were maintained after removal of geldanamycin, as expected for a senescence marker (see Figure 6C) and were enriched in histone H3 methylated on lysine 9, consistent with previous studies (Supplemental Figure 1B)(24). Activation of a DNA damage response is an important feature of both replicative and premature senescence that contributes to the growth arrest phenotype of senescent cells(25). A central feature of the DNA damage response is the generation of phosphorylated histone H2AX (γH2AX) at sites adjacent to DNA damage. Both geldanamycin and radicicol treatments increased levels of γH2AX in H69 cells (Supplementary Figure 1C). γH2AX levels remained elevated for up to six days after geldanamycin removal, the longest time point assessed (Figure 4C). This is consistent

Figure 4. Senescence markers in Hsp90-inhibitor-treated small cell lung cancer cells. A. H69 cells were treated with DMSO alone or 100 nM geldanamycin for 48 h. Geldanamycin was then removed. Eight days later cells were allowed to settle onto poly-L-lysine-coated coverslips, fixed with paraformaldehyde and photographed under phase contrast using a 63X objective lens. B. SAHF formation after treatment of cells with Hsp90 inhibitors. H69 cells were treated with DMSO or 100 nM geldanamycin for 48 h. Cells were then fixed, stained with DAPI and examined by fluorescence microscopy. C. H69 cells were treated with DMSO (control) or 100 nM geldanamycin. DMSO and geldanamycin were then removed on Day 0. Total cell lysates were collected on the indicated days after geldanamycin removal and analyzed for γH2AX and H2AX levels by Western blotting.

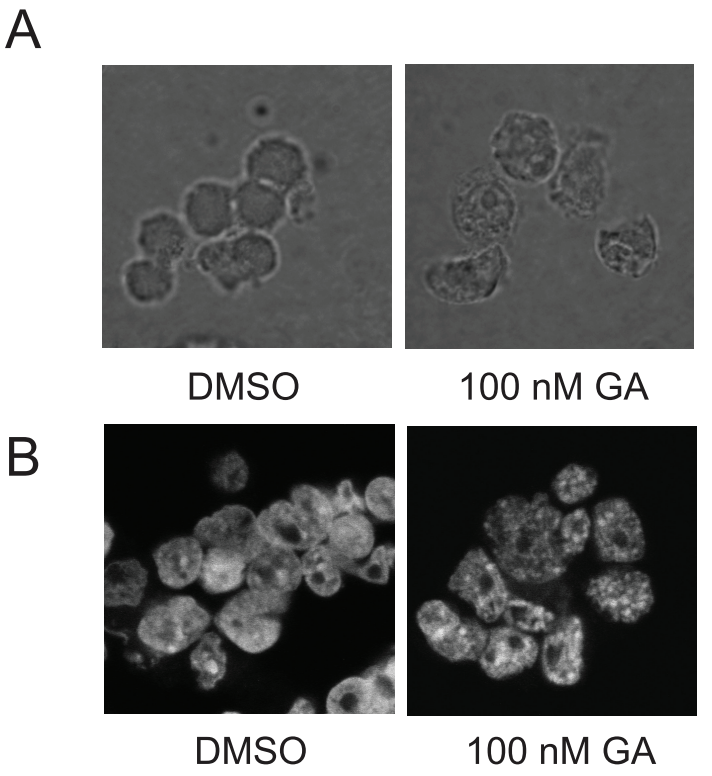
A
DMSO
100 nM GA
B
DMSO
100 nM GA
C
Control
GA treated
Day 2
Day 2
Day 4
Day 6
gH2AX
H2AX
normalized signal
0
1
2
3
4
5
DMSO
Day 2 GA
Day 4 GA
Day 6 GA

with reports that senescent cells maintain an activated DNA damage response for an extended period after the induction of senescence (25,26).

Isolation of variant H69 cells that bypass geldanamycin-induced senescence: While H69 cells maintained a proliferation-arrested state for more than thirty days after removal of geldanamycin, after approximately forty days a population of cells did start to proliferate in one experiment. We have designated this population as H69/41d cells. H69/41d cells have a distinct morphology: while H69 cells are non-adherent cells that form ragged aggregates, the variant cells, while also non-adherent, form tight spheres reminiscent of those seen with stem cell populations (Figure 5A). Upon retesting, these cells still underwent proliferation arrest in response to 100 nM geldanamycin, but were able to recover proliferative capacity upon removal of drug, similar to what we observed in glioblastoma cells (Figure 5B). H69/41d cells were also able to recover proliferative capacity after treatment with the Hsp90 inhibitor radicicol (Figure 5C). Compared to the parent H69 cell line, H69/41d cells showed similar responses to Hsp90 inhibition with respect to proliferation inhibition in the presence of drug, although cell death tended to occur at slightly lower concentrations than seen with H69 cells (Figure 5D). Degradation of client proteins and induction of other heat shock proteins was also similar in the two cell lines (Figure 6A). As above, this rules out differences in drug processing between the two cell populations, and indicates that the differences are due to events downstream of Hsp90 inhibition that specifically affect whether cells undergo reversible or irreversible proliferation arrest. SAHF formation was also impaired in H69/41d cells (Figure 6B). In H69 cells, SAHFs were detected maximally in approximately 35 % of cells (Figure 6C). In contrast, geldanamycin treatment only

Figure 5. Properties of variant H69 cells that recover growth after Hsp90 inhibitor withdrawal. A. Photographs of H69 and H69/41d cells under phase microscopy, at low (top panels) and high (bottom panels) magnification; B. H69 and H69/41d cells were treated with 100 nM geldanamycin for 48 h. Geldanamycin was then removed and numbers of viable cells were assessed at the indicated times after drug removal. C. H69 and H69/41d cells were treated with 5 mM radicicol for 48 h. Radicicol was then removed and numbers of viable cells were assessed at the indicated times after drug removal. D. MTT assay of H69/41d cells treated for 48 h with geldanamycin.

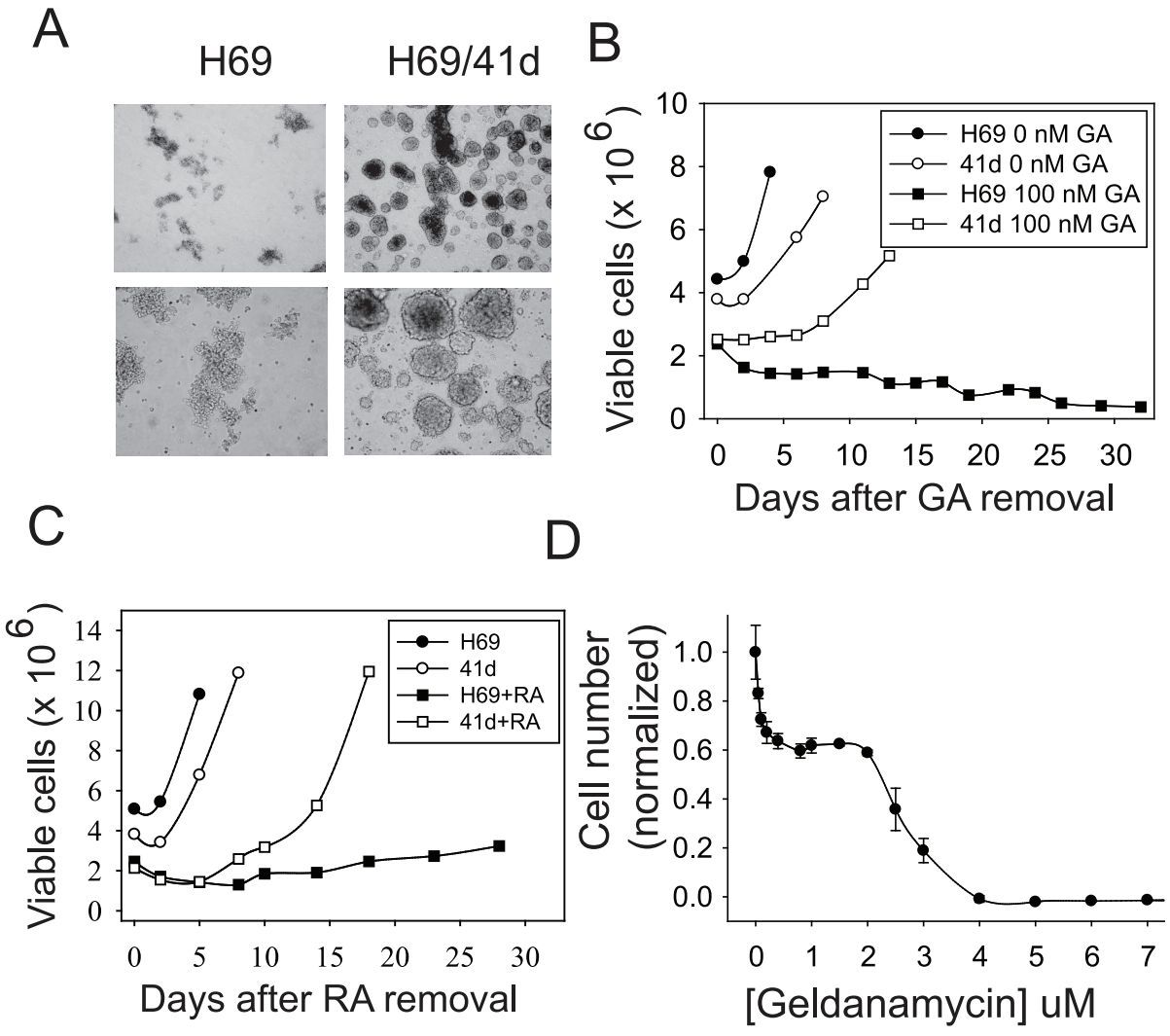
A
H69
H69/41d
B
Viable cells (x 10^6)
H69 0 nM GA
41d 0 nM GA
H69 100 nM GA
41d 100 nM GA
Days after GA removal
C
Viable cells (x 10^6)
H69
41d
H69+RA
41d+RA
Days after RA removal
D
Cell number (normalized)
[Geldanamycin] uM

Figure 6. Client protein degradation and SAHF induction markers in H69/41d cells. H69 and H69/41d cells were treated for 48 h with geldanamycin or DMSO as vehicle control. A. Total cell lysates were collected after 48 h treatment and analyzed by Western blotting as in Figure 3. B. DMSO-treated cells were stained for SAHFs 2 days after removing the DMSO. Geldanamycin-treated cells were stained for SAHFs 2, 4 and 6 days after drug removal. Representative fluorescence microscopy images of H69 and H69/41d cell nuclei, two days after removal of geldanamycin, are shown. C. SAHFs in H69 (light gray) and H69/41d cells (dark gray) were counted at the indicated times after drug removal. Data are expressed as the percent of nuclei that are SAHF positive. Bars show the mean percentage ± SE. D. Total cell extracts of untreated H69 and H69/41d cells were analyzed for expression of p21 protein by Western blotting.

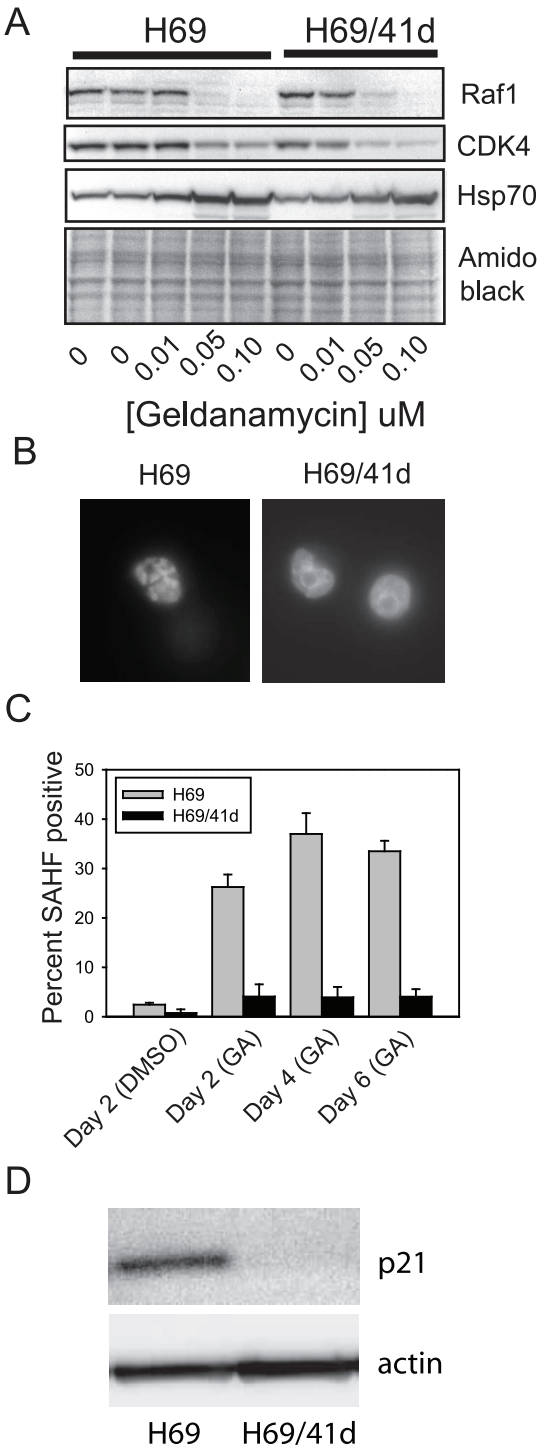
A
H69
H69/41d
Raf1
CDK4
Hsp70
Amido black
0 0 0.01 0.05 0.10 0 0.01 0.05 0.10
[Geldanamycin] uM
B
H69
H69/41d
C
Percent SAHF positive
50
40
30
20
10
0
H69
H69/41d
Day 2 (DMSO)
Day 2 (GA)
Day 4 (GA)
Day 6 (GA)
D
p21
actin
H69
H69/41d

caused a modest increase in SAHFs in H69/41d cells and SAHFs were detected in 4.5 % of cells maximally (Figure 6C).

To directly assess the genetic relationship of H69 cells with H69/41d cells, DNA was isolated from both cell lines and analyzed using Affymetrix Genome-Wide Human SNP Array 6.0 chips, which contain probes for 900,000 single nucleotide polymorphism and a similar number of probes to assess copy number variation. Supplementary Figure 2 shows karyotypes of the two cell lines reconstructed from this data (each is compared to an Affymetrix reference karyotype). H69 cells show extensive chromosomal aberrations as expected for cancer cells. These losses, gains and regions of amplification/ copy number variation are very similar between H69 and H69/41d cells, showing unequivocally that they are clonally related. Some differences were evident between the two cell lines. These include a 4.8 Mbp deletion on the single copy of chromosome 2 that contains approximately nineteen genes and a 9.6 Mbp deletion on one copy of chromosome 11 that contains approximately 83 genes. There is also a gain of the long arm of chromosome 3 and a loss of a partial long arm of chromosome 15. However, the SNP/copy number analysis did not point to a single defined genetic locus that might explain why H69/41d cells are able to evade Hsp90 inhibitor-induced senescence. As a second approach to determine the mechanism by which these cells evade Hsp90 inhibitor-induced senescence, cells were screened for a number of proteins known that have previously been shown to have important roles in senescence. p21 (CDKN1A, p21Waf1/Cip1) is one such protein that is of particular interest as it has been shown to induce senescence in cancer cells lacking p53 (27). p21 is expressed in H69 cells but is undetectable in H69/41d cells (Figure 6D). Given its known role in the

induction and maintenance of senescence (26), the loss of p21 expression provides a plausible explanation for the failure of H69/41d cells to undergo senescence in response to Hsp90 inhibitors.

DISCUSSION

In previous studies, the most commonly described response of cancer cells to Hsp90 inhibition has been cell cycle arrest. This cell cycle arrest has generally been assumed to be reversible in nature, although most studies did not address this directly. Growth arrest can occur at either the G1/S or G2/M transition (28,29) and is likely to be a consequence of the Hsp90 dependence of proteins such as CDK4, cdc2 and polo-like kinase (30-32). In a subset of cancer cell types, Hsp90 inhibitors have been shown to induce apoptosis. These include small cell lung cancer cells and multiple myeloma cells (18,33).

Aside from transient cell cycle arrest and cell death, a third cellular fate for cancer cells is senescence. For cancer cells, this is sometimes referred to as "premature" or "accelerated" cellular senescence to distinguish it from the replicative senescence that normal cells undergo upon reaching their Hayflick limit (34,35). Senescence in cancer has been studied in two contexts: the first of these is the senescence seen in response to oncogene activation, where it may play a role in protecting organisms from developing cancer; the second of these is as a response to cancer therapeutics (36). Chemotherapy agents that damage DNA appear to induce senescence to a much greater extent than agents that target microtubules (37). This is more likely to occur with exposure to lower doses of drug, with higher doses causing apoptosis. Chemotherapy-induced senescence has been observed both in cell culture and in animal models (38).

The key, defining features of senescent cells are that they remain metabolically active but undergo a sustained withdrawal from the cell cycle that is not reversed by standard mitogenic stimuli. After transient exposure to low concentrations of

geldanamycin, small cell lung cancer cells remained alive and metabolically active (as indicated by trypan blue exclusion and MTT assays). However these cells underwent a proliferation arrest that was sustained for greater than thirty days, in spite of the regular addition of fresh media containing fetal calf serum, a rich source of mitogens. The proliferation arrest was evident both from live cell counts and from BrdU incorporation assays.

In addition to permanent proliferation arrest, additional markers of the senescent state have been developed, although none of these is currently seen as being a definitive marker of the senescent state (39). A characteristic set of morphological changes have been described for senescent cells that include cell enlargement and an increased granularity of the cytoplasm (40). These features were evident in H69 small cell lung cancer cells in which sustained proliferation arrest had been induced by Hsp90 inhibitors. (They do not show the flattening described for adherent cells, as the small cell lung cancer cells used in this study grow in suspension.) SAHF are another marker that is commonly observed in senescent cells and that are thought to have a role in maintaining the senescent phenotype. SAHF were present in small cell lung cancer cells in which sustained proliferation arrest had been induced by Hsp90 inhibitors. Expression of SAHF was maintained for up to six days after removal of Hsp90 inhibitor (the longest time point examined) and the time course for their appearance was similar to previous studies on the induction of premature senescence by various agents (41,42). Activation of the DNA damage response is also commonly observed in senescence, where it has a role in both the initiation and maintenance of the senescent phenotype (25,26). Hsp90 inhibitors (both geldanamycin and radicicol)

activated a DNA damage response that was maintained after inhibitor removal. This finding is also consistent with a senescence phenotype and also provides a mechanism by which these inhibitors activate senescence.

DNA damage, either telomeric or non-telomeric, is the most widely characterized inducer of senescence. As well as being a marker of senescence, the activation of the DNA damage response by Hsp90 inhibitors also provides a mechanism by which they induce senescence in small cell lung cancer cells. Previous studies have also pointed to a link between Hsp90 and DNA damage: both telomerase and the Fanconi anemia DNA damage response pathway are dependent on Hsp90 for their activity (43,44).

Senescence-associated β-galactosidase (SAβgal) has also been widely used as a senescence marker (35). SAβgal activity is detected as a consequence of the expansion of the lysosomal compartment in senescent cells, but is not required for senescence induction or maintenance (45). Small cell lung cancer cells treated with Hsp90 inhibitors were not positive for SAβgal. Adriamycin also did not induce SAβgal in small cell lung cancer cells when used a concentrations that induced this marker in other cancer cell types. This suggests that SAβgal may not be a useful marker of senescence in small cell lung cancer. A possible explanation is that these cells have scant cytoplasm and are specialized secretory cells that may have a relatively small lysosomal compartment.

Taken together, the above data show that Hsp90 inhibitors induce a sustained proliferation arrest that has features consistent with premature senescence. This premature senescence occurred at concentrations of geldanamycin that correlated

closely with the concentrations required to induce the degradation of well-established Hsp90 client proteins and to induce the expression of other heat shock proteins (a widely used marker of Hsp90 inhibition). Premature senescence was also induced by 17-AAG (tanespimycin; 17-allylamino-17-demethoxygeldanamycin), a geldanamycin derivative that has been tested in clinical trials (46). 17-AAG induced senescence at a concentration that is similar to the concentrations achieved in the plasma of patients treated at the maximum tolerated dose of this compound (12), suggesting that this response is clinically relevant. Senescence induction by Hsp90 inhibitors requires neither p53 nor Rb, as both of these tumor suppressors are known to be mutated in the H69 cell line used in this study.

In some experiments, populations of cells did start to grow after long term culture of senescent H69 cells. One of these cell populations, designated H69/41d, was characterized in detail. SNP and copy number analysis of these cells shows that while they are clearly derived from H69 cells they have a distinct set of genetic changes. These cells show similar responses to Hsp90 inhibition as the parent H69 cells with respect to proliferation inhibition in the presence of drug and induction of cell death at high geldanamycin concentrations. However they undergo a reversible, rather than irreversible proliferation arrest in response to Hsp90 inhibition. H69/41d cells also show identical responses to the parent cell line with respect to degradation of Hsp90 client proteins and induction of other heat shock proteins. Thus this form of "resistance" to Hsp90 inhibition is clearly distinct from that described in previous studies, where resistance was due to alterations in drug metabolizing enzymes and was reflected in a requirement for higher doses to see cellular effects (47). The isolation of

these cells demonstrates that, in principle, small cell lung cancer cells with additional genetic alterations can evade Hsp90-induced premature senescence. p21 (CDKN1A) has previously been shown to be an important regulator of senescence, a property that appears to be independent of its inhibitory activity against cyclin-dependent kinases (48). p21 is regulated by both p53 and p53-independent mechanisms and can induce senescence in cells that lack p53 (as is the case for H69 cells) (27). The absence of p21 in H69/41d cells provides a mechanism by which these cells evade premature senescence in response to Hsp90 inhibition.

We observed two distinct responses to Hsp90 inhibitors in small cell lung cancer cells, the first being the premature senescence described above and the second being cell death, which is seen at much higher concentrations of Hsp90 inhibitors. The two responses are temporally distinct, in that cell death is maximal after only 12 h of exposure to Hsp90 inhibitor, while premature senescence requires a minimum of 24 h exposure to drug. These two responses were reflected in a biphasic dose response curve in MTT assays, which was very distinct with geldanamycin but was more subtle with radicicol (see below). The biphasic response is only evident when a detailed analysis of the dose effects of Hsp90 inhibitors at low concentrations is performed and when long treatments with drug are used, where there is sufficient time for cell proliferation to occur in untreated samples. The induction of cell death that we observed is consistent with previous observations, where it was shown that Hsp90 inhibitors activate the intrinsic pathway of apoptosis in small cell lung cancer cells (18). However we find that the concentration of geldanamycin required to induce cell death is approximately 100 times higher than that required to inhibit cytosolic Hsp90,

as assessed by degradation of Hsp90 client proteins and induction of heat shock proteins. The cell death seen in small cell lung cancer cells is therefore due to inhibition of a target other than cytosolic Hsp90; likely alternate targets include either the endoplasmic reticulum Hsp90 paralog Grp94 or the mitochondrial Hsp90 paralog Trap1. Geldanamycin binds to purified Grp94 and Trap1 with dissociation constants in the 1-2 μM range (8,10); the IC_{50} for the second phase of the curve in our geldanamycin MTT assays is approximately 5 μM, consistent with either Grp94 or Trap1 as alternate targets. The large difference in the affinity of geldanamycin for cytosolic Hsp90 in cancer cells (low nanomolar range) and either Grp94 or Trap1 may explain why a biphasic dose response is clearly seen with this compound in MTT assays; for compounds where the affinities are relatively close, this would not be observed as readily. In the previous report linking small cell lung cancer cell apoptosis to inhibition of cytosolic Hsp90, the Grp94 and Trap1 binding affinities of the compounds used were not assessed (18). Previous work has indicated that inhibition of Trap1 (along with mitochondrial Hsp90) is cytotoxic to cancer cells (49,50). Similarly, inhibition of Grp94 can also induce cell death under some conditions (51). Trap1 and Grp94 are therefore candidate alternate targets for the effects of Hsp90 inhibitors on small cell lung cancer cells both on the basis of their known affinities for Hsp90 inhibitors and their established roles in the prevention of cell death.

Our studies support the earlier conclusion that small cell lung cancer may be a candidate for treatment with Hsp90 inhibitors (18). However we find that a senescence-like proliferation arrest is the primary response of these cells to concentrations of Hsp90 inhibitors that inhibit cytosolic Hsp90. This suggests that

disease stabilization may be a more likely outcome in patients rather than tumor regression, and that small populations of cancer cells with additional genetic alterations may be able to escape senescence induction. If, as our data suggests, the apoptotic effect of Hsp90 inhibitors in small cell lung cancer is due to inhibition of other Hsp90 family members, such as Grp94 or Trap1, it will be important to develop new drugs that are optimized for selectivity and potency for these targets.

MATERIALS AND METHODS

Chemicals and antibodies: Geldanamycin and radicicol were from Sigma-Aldrich Canada Ltd. (Oakville, ON, Canada). 17-AAG (17-(Allylamino)-17-demethoxygeldanamycin) and the caspase inhibitor Z-VAD-FMK were from Calbiochem (San Diego, CA, USA). MTT reagent (3-(4,5-dimethylthiazol-2-yl)-2,5-diphenyl tetrazolium bromide) was from Sigma-Aldrich Canada Ltd. (Oakville, ON, Canada). Cdk4 and Hsp70 mouse monoclonal antibodies were from Neomarkers (Fremont, CA, USA). Raf1 rabbit polyclonal antibody was from Santa Cruz Biotechnology Inc. (Santa Cruz, CA, USA). Hsp90α/β mouse monoclonal and Hsp27 rabbit polyclonal antibodies were from Stressgen (Ann Arbor, MI, USA). Actin mouse monoclonal antibody was from Sigma-Aldrich Canada Ltd. (Oakville, ON, Canada). Antibodies to γH2AX (phospho-Histone H2A.X (Ser139)) and histone H2A.X were from Millipore (Billerica, MA, USA). Rabbit polyclonal antibody to histone H3 tri-methylated K9 was from Abcam (Cambridge, MA, USA).

Cell lines: Human H69, H187 and H889 small cell lung cancer cell lines were from American Type Culture Collection (Manassas, VA, USA). All cell lines were passaged for less than six months continuously and were routinely checked for mycoplasma contamination. Small cell lung cancer cell lines were grown as suspension cultures in RPMI-1640 medium containing 25 mM HEPES and L-glutamine (Invitrogen, Carlsbad, CA, USA) supplemented with 100 units/ml penicillin, 100 µg/ml streptomycin, 1 mM sodium pyruvate and 10% (v/v) fetal bovine serum. The human U87MG glioblastoma cell line was obtained from Dr. W. Cavenee (Ludwig Institute for Cancer Research, La Jolla, CA, USA) and was cultured in Dulbecco's modified Eagle's medium (DMEM) supplemented with 100 units/ml penicillin, 100 µg/ml streptomycin, 2 mM glutamine

and 10% (v/v) of a 2:1 mixture of donor bovine serum and fetal bovine serum. All cell lines were cultured at 37ºC and 5% CO_2.

Cell counts: Total and viable cell numbers were measured using a Vi-cell XR cell viability analyzer from Beckman Coulter Canada Inc. (Mississauga, ON, Canada).

Growth assays: Cells were added to 5 ml of media in T25 tissue culture flasks and 24 h later were treated with drug or the drug vehicle DMSO (dimethyl sulfoxide) for the specified time. Cells were pelleted by centrifugation, media with drug was removed, and cells were washed with sterile PBS and centrifuged again. Cells were then added to new flasks with fresh media (day 0). Aliquots were counted for total and viable cell numbers on the specified days and fresh media was added to replenish and maintain the total volume of media in the flask. Cell proliferation was also assessed using the BrdU Cell Proliferation Assay kit from Calbiochem (San Diego, CA, USA).

MTT assays: Cells were added to 100 µl media in 96-well tissue culture plates and 24 h later were treated with drug or the drug vehicle DMSO for the specified time. 25 µl of MTT reagent was added (5 mg/ml in sterile PBS) and incubated for 24 h at 37ºC and 5% CO_2. The cells were lysed and the formazan product was dissolved for 30 min with 100 µl of lysis detergent (20% SDS (BioShop Canada Inc., Burlington, ON, Canada) and 40% DMF (VWR International, Mississauga, ON, Canada). The absorbance was measured at 570 nm using a Dynex MRX microplate reader (Dynex Technologies, Chantilly, VA, USA).

Western blot analysis: Western blotting was performed as described previously (52). To ensure equal loading and transfer, blots were stained with amido black prior to blocking and incubation with primary antibody.

SAHF staining: H69 cells were centrifuged, washed twice with cold PBS for 5 min, fixed in 4% paraformaldehyde at room temperature for 30 min, and washed twice with PBS for 5 min. Cells were stained for 4 min with 0.13 µg/µl DAPI (4´,6-diamidino-2-phenylindole, Invitrogen, Carlsbad, CA, USA). Cells were then washed twice with PBS for 5 min and mounted on slides in 5 µl PBS and 5 µl of ProLong Gold mounting medium (Invitrogen, Carlsbad, CA, USA). Fluorescence microscopy was performed using an AxioSkop 2 MOT microscope with a Zeiss FluoArc mercury lamp and Zeiss AxioVision release 3.1 software (Carl Zeiss Canada Ltd., Toronto, ON, Canada). Percentages of cells containing SAHFs were determined by counting total and SAHF-containing nuclei under a 100X objective. A minimum of three randomly-chosen fields containing a minimum total of 100 nuclei were scored independently by two reviewers and averaged. For detection of histone H3 trimethylated on lysine 9, H69 cells were allowed to settle onto cover slips coated with 0.1% poly-L-lysine (Sigma-Aldrich, St. Louis MO) and fixed with paraformaldehyde as above. Immunofluorescence was then performed as described previously using anti-histone H3 tri-methylated K9 antibody at a 1:5000 dilution (5).

Microarray-based DNA analysis : DNA was isolated using the DNeasy Blood and Tissue kit from Qiagen (Mississauga, ON, Canada). Analysis using Genome-Wide Human SNP Array 6.0 chips from Affymetrix Inc. (Santa Clara, CA, USA) was performed at the Centre for Applied Genomics at the Hospital for Sick Children, Toronto, ON, Canada.

Data analysis was performed using the Genotyping Console software version 3.0.1 from Affymetrix Inc. (Santa Clara, CA, USA).

ACKNOWLEDGEMENTS

This work was supported by grants from the Canadian Institutes of Health Research and the Canadian Cancer Society (grant #020121). IL holds the J. Adrien and Eileen Leger Chair in Cancer Research at the Ottawa Hospital Research Institute. The authors would like to thank Dr. Scott Findlay at the University of Ottawa for his many contributions to this project at its early stages.

REFERENCES

1. Wandinger SK, Richter K, Buchner J (2008) The Hsp90 chaperone machinery. J Biol Chem 283, 18473-18477.

2. Pearl LH, Prodromou C (2006) Structure and mechanism of the Hsp90 molecular chaperone machinery. Annu Rev Biochem 75, 271-294.

3. Pearl LH, Prodromou C, Workman P (2008) The Hsp90 molecular chaperone: an open and shut case for treatment. Biochem J 410, 439-453.

4. Xu Y, Singer MA, Lindquist S (1999) Maturation of the tyrosine kinase c-src as a kinase and as a substrate depends on the molecular chaperone Hsp90. Proc Natl Acad Sci U S A 96, 109-114.

5. Lavictoire SJ, Parolin DA, Klimowicz AC, Kelly JF, Lorimer IA (2003) Interaction of Hsp90 with the nascent form of the mutant epidermal growth factor receptor EGFRvIII. J Biol Chem 278, 5292-5299.

6. Sawai A, Chandarlapaty S, Greulich H, Gonen M, Ye Q et al. (2008) Inhibition of Hsp90 down-regulates mutant epidermal growth factor receptor (EGFR) expression and sensitizes EGFR mutant tumors to paclitaxel. Cancer Res 68, 589-596.

7. Kamal A, Thao L, Sensintaffar J, Zhang L, Boehm MF et al. (2003) A high-affinity conformation of Hsp90 confers tumour selectivity on Hsp90 inhibitors. Nature 425, 407-410.

8. Xu W, Mimnaugh E, Rosser MF, Nicchitta C, Marcu M et al. (2001) Sensitivity of mature Erbb2 to geldanamycin is conferred by its kinase domain and is mediated by the chaperone protein Hsp90. J Biol Chem 276, 3702-3708.

9. Schulte TW, Akinaga S, Murakata T, Agatsuma T, Sugimoto S et al. (1999) Interaction of radicicol with members of the heat shock protein 90 family of molecular chaperones. Mol Endocrinol 13, 1435-1448.

10. Felts SJ, Owen BA, Nguyen P, Trepel J, Donner DB et al. (2000) The hsp90-related protein TRAP1 is a mitochondrial protein with distinct functional properties. J Biol Chem 275, 3305-3312.

11. Taldone T, Gozman A, Maharaj R, Chiosis G (2008) Targeting Hsp90: small-molecule inhibitors and their clinical development. Curr Opin Pharmacol 8, 370-374.

12. Goetz MP, Toft D, Reid J, Ames M, Stensgard B et al. (2005) Phase I trial of 17-allylamino-17-demethoxygeldanamycin in patients with advanced cancer. J Clin Oncol 23, 1078-1087.

13. Grem JL, Morrison G, Guo XD, Agnew E, Takimoto CH et al. (2005) Phase I and pharmacologic study of 17-(allylamino)-17-demethoxygeldanamycin in adult patients with solid tumors. J Clin Oncol 23, 1885-1893.

14. Banerji U, O'Donnell A, Scurr M, Pacey S, Stapleton S et al. (2005) Phase I pharmacokinetic and pharmacodynamic study of 17-allylamino, 17-demethoxygeldanamycin in patients with advanced malignancies. J Clin Oncol 23, 4152-4161.

15. Modi S, Stopeck AT, Gordon MS, Mendelson D, Solit DB (2007) Combination of trastuzumab and tanespimycin (17-AAG, KOS-953) is safe and active in trastuzumab-refractory HER-2 overexpressing breast cancer: a phase I dose-escalation study. J Clin Oncol 25, 5410-5417.

16. Sher T, Dy GK, Adjei AA (2008) Small cell lung cancer. Mayo Clin Proc 83, 355-367.

17. Cook RM, Miller YE, Bunn PA Jr (1993) Small cell lung cancer: etiology, biology, clinical features, staging, and treatment. Curr Probl Cancer 17, 69-141.

18. Rodina A, Vilenchik M, Moulick K, Aguirre J, Kim J et al. (2007) Selective compounds define Hsp90 as a major inhibitor of apoptosis in small-cell lung cancer. Nat.Chem.Biol., 3, 498-507.

19. Bagatell R, Paine-Murrieta GD, Taylor CW, Pulcini EJ, Akinaga S et al. (2000) Induction of a heat shock factor 1-dependent stress response alters the cytotoxic activity of hsp90-binding agents. Clin Cancer Res 6, 3312-3318.

20. Kelland LR, Sharp SY, Rogers PM, Myers TG, Workman P (1999) DT-Diaphorase expression and tumor cell sensitivity to 17-allylamino, 17-demethoxygeldanamycin, an inhibitor of heat shock protein 90. J Natl Cancer Inst 91, 1940-1949.

21. Guo W, Reigan P, Siegel D, Zirrolli J, Gustafson D et al. (2005) Formation of 17-allylamino-demethoxygeldanamycin (17-AAG) hydroquinone by NAD(P)H:quinone oxidoreductase 1: role of 17-AAG hydroquinone in heat shock protein 90 inhibition. Cancer Res, 65, 10006-10015.

22. Smith PJ, Wiltshire M, Chin SF, Rabbitts P, Soues S (1999) Cell cycle checkpoint evasion and protracted cell cycle arrest in X-irradiated small-cell lung carcinoma cells. Int J Radiat Biol 75, 1137-1147.

23. Funayama R, Ishikawa F (2007) Cellular senescence and chromatin structure. Chromosoma 116, 431-440.

24. Narita M, Nunez S, Heard E, Narita M, Lin AW et al. (2003) Rb-mediated heterochromatin formation and silencing of E2F target genes during cellular senescence. Cell, 113, 703-716.

25. d'Adda dF, Reaper PM, Clay-Farrace L, Fiegler H, Carr P, von Zglinicki T et al. (2003) A DNA damage checkpoint response in telomere-initiated senescence. Nature 426, 194-198.

26. Passos JF, Nelson G, Wang C, Richter T, Simillion C et al. (2010) Feedback between p21 and reactive oxygen production is necessary for cell senescence. Mol.Syst Biol 6, 347.

27. Fang L, Igarashi M, Leung J, Sugrue MM, Lee SW et al. (1999) p21Waf1/Cip1/Sdi1 induces permanent growth arrest with markers of replicative senescence in human tumor cells lacking functional p53. Oncogene 18, 2789-2797.

28. Srethapakdi M, Liu F, Tavorath R, Rosen N (2000) Inhibition of Hsp90 function by ansamycins causes retinoblastoma gene product-dependent G1 arrest. Cancer Res 60, 3940-3946.

29. Kim HR, Lee CH, Choi YH, Kang HS, Kim HD (1999) Geldanamycin induces cell cycle arrest in K562 erythroleukemic cells. IUBMB Life 48, 425-428.

30. Stepanova L, Leng X, Parker SB, Harper JW (1996) Mammalian p50Cdc37 is a protein kinase-targeting subunit of Hsp90 that binds and stabilizes Cdk4. Genes Dev 10, 1491-1502.

31. Munoz MJ, Jimenez J (1999) Genetic interactions between Hsp90 and the Cdc2 mitotic machinery in the fission yeast Schizosaccharomyces pombe. Mol Gen Genet 261, 242-250.

32. de Carcer G (2004) Heat shock protein 90 regulates the metaphase-anaphase transition in a polo-like kinase-dependent manner. Cancer Res 64, 5106-5112.

33. Davenport EL, Moore HE, Dunlop AS, Sharp SY, Workman P et al. (2007) Heat shock protein inhibition is associated with activation of the unfolded protein response pathway in myeloma plasma cells. Blood 110, 2641-2649.

34. Soengas MS (2008) Cancer: Ins and outs of tumour control. Nature 454, 586-587.

35. Campisi J, d'Adda dF (2007) Cellular senescence: when bad things happen to good cells. Nat Rev Mol Cell Biol 8, 729-740.

36. Shay JW, Roninson IB (2004) Hallmarks of senescence in carcinogenesis and cancer therapy. Oncogene 23, 2919-2933.

37. Chang BD, Broude EV, Dokmanovic M, Zhu H, Ruth A et al. (1999) A senescence-like phenotype distinguishes tumor cells that undergo terminal proliferation arrest after exposure to anticancer agents. Cancer Res 59, 3761-3767.

38. Schmitt CA, Fridman JS, Yang M, Lee S, Baranov E et al. (2002) A senescence program controlled by p53 and p16INK4a contributes to the outcome of cancer therapy. Cell 109, 335-346.

39. Schmitt CA (2007) Cellular senescence and cancer treatment. Biochim Biophys Acta 1775, 5-20.

40. Gewirtz DA, Holt SE, Elmore LW (2008) Accelerated senescence: an emerging role in tumor cell response to chemotherapy and radiation. Biochem.Pharmacol 76, 947-957.

41. Zhang R, Poustovoitov MV, Ye X, Santos HA, Chen W et al. (2005) Formation of MacroH2A-containing senescence-associated heterochromatin foci and senescence driven by ASF1a and HIRA. Dev Cell 8, 19-30.

42. Denoyelle C, Abou-Rjaily G, Bezrookove V, Verhaegen M, Johnson TM et al. (2006) Anti-oncogenic role of the endoplasmic reticulum differentially activated by mutations in the MAPK pathway. Nat Cell Biol, 8, 1053-1063.

43. Keppler BR, Grady AT, Jarstfer MB (2006) The biochemical role of the heat shock protein 90 chaperone complex in establishing human telomerase activity. J Biol Chem 281, 19840-19848.

44. Oda T, Hayano T, Miyaso H, Takahashi N, Yamashita T (2007) Hsp90 regulates the Fanconi anemia DNA damage response pathway. Blood 109, 5016-5026.

45. Lee BY, Han JA, Im JS, Morrone A, Johung K et al. (2006) Senescence-associated beta-galactosidase is lysosomal beta-galactosidase. Aging Cell 5, 187-195.

46. Erlichman,C. (2009) Tanespimycin: the opportunities and challenges of targeting heat shock protein 90. Expert Opin Investig Drugs, 18, 861-868.

47. Gaspar N, Sharp SY, Pacey S, Jones C, Walton M et al. (2009) Acquired resistance to 17-allylamino-17-demethoxygeldanamycin (17-AAG, tanespimycin) in glioblastoma cells. Cancer Res 69, 1966-1975.

48. Macip S, Igarashi M, Fang L, Chen A, Pan ZQ et al. (2002) Inhibition of p21-mediated ROS accumulation can rescue p21-induced senescence. EMBO J 21, 2180-2188.

49. Kang BH, Plescia J, Dohi T, Rosa J, Doxsey SJ, Altieri DC (2007) Regulation of tumor cell mitochondrial homeostasis by an organelle-specific Hsp90 chaperone network. Cell 131, 257-270.

50. Kang BH, Plescia J, Song HY, Meli M, Colombo G et al. (2009) Combinatorial drug design targeting multiple cancer signaling networks controlled by mitochondrial Hsp90. J Clin Invest 119, 454-464.

51. Ostrovsky O, Ahmed NT, Argon Y (2009) The chaperone activity of GRP94 toward insulin-like growth factor II is necessary for the stress response to serum deprivation. Mol Biol Cell 20, 1855-1864.

52. Baldwin RM, Garratt-Lalonde M, Parolin DA, Krzyzanowski PM, Andrade MA et al. (2006) Protection of glioblastoma cells from cisplatin cytotoxicity via protein kinase Ciota-mediated attenuation of p38 MAP kinase signaling. Oncogene 25, 2909-2919.

Figure S1. A. H889 human small lung cancer cells were treated with 100 nM geldanamycin for 48 h. Viable cell numbers were determined at the indicated days after geldanamycin removal as indicated in Figure 2. **B.** H69 were treated with 100 nM geldanamycin for 48 h. Four days after removal of the drug, cells were allowed to settle onto poly-L-lysine-coated coverslips and fixed with paraformaldehyde. Histone H3 trimethylated on lysine 9 was then detected by immunofluorescence (red) with counterstaining of nuclei using DAPI (green). **C.** H69 cells were treated with DMSO, geldanamycin (GA), or radicicol (RA) for 48 hours. Total cell lysates were collected on the indicated days after geldanamycin removal and analyzed for γH2AX and H2AX levels by Western blotting.

A

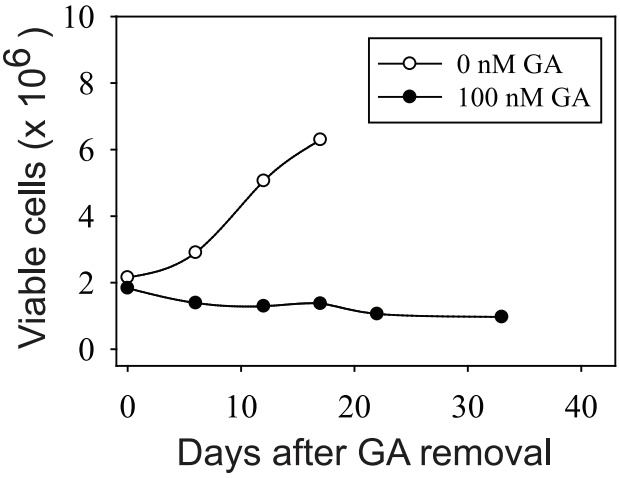
Viable cells (x 10^6)
10
8
6
4
2
0
0 nM GA
100 nM GA
0
10
20
30
40
Days after GA removal

B

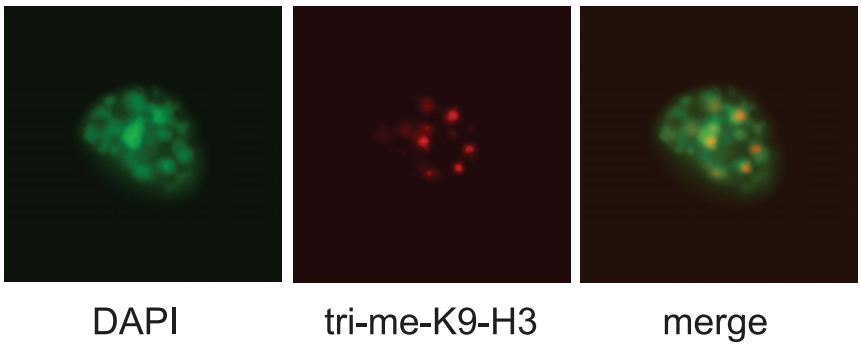
DAPI
tri-me-K9-H3
merge

C

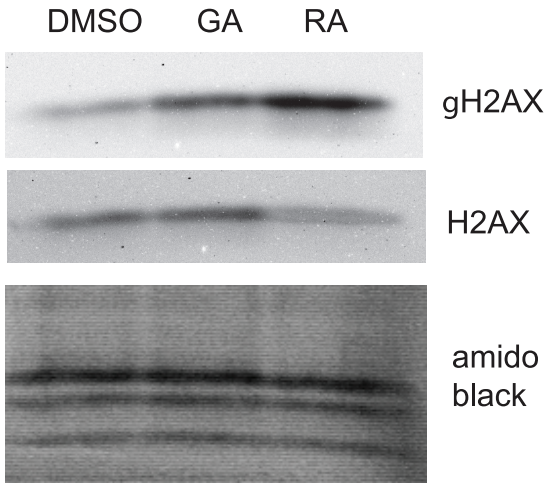
DMSO
GA
RA
gH2AX
H2AX
amido
black

Figure S2. *Karyotypes of H69 and H69/41d cells.* DNA was isolated from H69 and H69/41d cells and analyzed using Affymetrix Genome-Wide Human SNP Array 6.0 chips. The labels above each column indicate the chromosomes depicted by each small panel (*e.g.* column one has five small panels that show data for chromosomes one, at the top of the column, through five, at the bottom). Each small panel shows copy number on a scale of one to five for H69 cells (in blue) and H69/41d cells (in green) for one chromosome, displayed using the smoothsignal display option in Affymetrix Genotyping Console software. Data files are available from the authors on request.

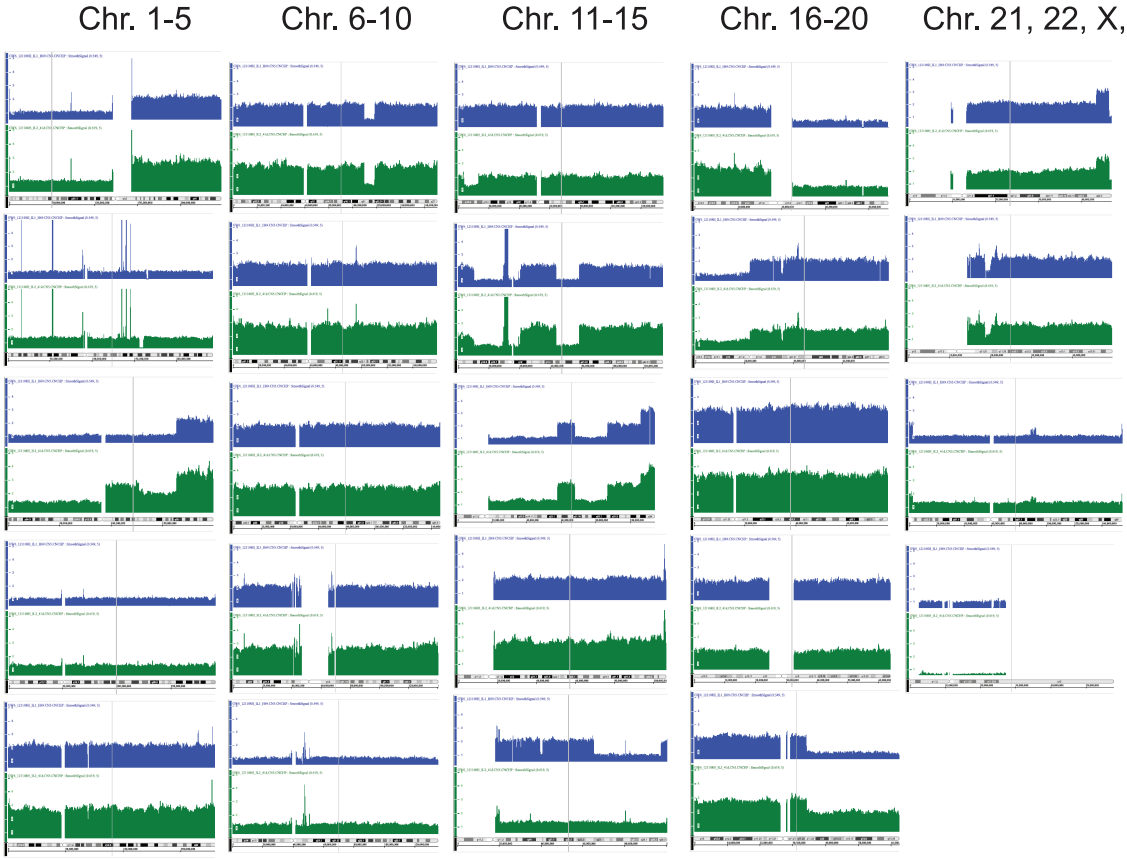
Chr. 1-5
Chr. 6-10
Chr. 11-15
Chr. 16-20
Chr. 21, 22, X, Y

3. REPRESSION OF CANCER CELL SENESCENCE BY PKCι

Judith A Paget[1,2,*], Ian J Restall[1,2,*], Manijeh Daneshmand[1], Julie A Mersereau[1], Manon A Simard[1], Doris A E Parolin[1], Sylvie J Lavictoire[1], Md. Sharier Amin[3], Shahidul Islam[3] and Ian AJ Lorimer[1,2,4]

[1]Centre for Cancer Therapeutics, Ottawa Hospital Research Institute;
[2]Department of Biochemistry, Microbiology and Immunology, University of Ottawa, Ottawa, Ontario, Canada
[3]Department of Pathology, Ottawa Hospital, Ottawa, Canada
[4]Department of Medicine, University of Ottawa, Ottawa, Ontario, Canada

* JAP and IJR contributed equally to this manuscript.

Address correspondence to: Ian A. J. Lorimer, Ottawa Hospital Regional Cancer Centre, Centre for Cancer Therapeutics

Running Title: Repression of senescence by PKCι

Contribution of Authors
This manuscript was contributed to equally by I.J. Restall and J.A. Paget. I.J. Restall contributed the work regarding glioblastoma and the initial finding for the role of PKCι in senescence. The content of this manuscript regarding glioblastoma was written by I.J. Restall with the help of Dr. I.A.J. Lorimer. All of the experiments regarding glioblastoma in Figures 8 to 10 presented in this manuscript are the work of I.J. Restall with the exception of Figure 10D. Figure 10D was performed by M.A. Simard (Co-op student of I.A.J. Lorimer).

Published: Oncogene. 2012; 31(31): 3584-3596

Abstract

Senescence is an irreversible growth arrest phenotype adopted by cells that has a key role in protecting organisms from cancer. There is now considerable interest in therapeutic strategies that reactivate this process to control the growth of cancer cells. Protein kinase C iota (PKCι) is a member of the atypical protein kinase C family and an important downstream mediator in the phosphoinositide 3-kinase pathway. PKCι expression was found to be upregulated in a subset of breast cancers and breast cancer cell lines. Activation of the phosphoinositide 3-kinase pathway by the introduction of mutant, oncogenic *PIK3CA* into breast mammary epithelial cells increased both the expression and activation of PKCι. In breast cancer cells lines overexpressing PKCι, depletion of PKCι increased the number of senescent cells, as assessed by senescence-associated β-galactosidase, morphology and bromodeoxyuridine incorporation. This phenomenon was not restricted to breast cancer cells, as it was also seen in glioblastoma cells in which PKCι is activated by loss of *PTEN*. Senescence occurred in the absence of a detectable DNA damage response, was dependent on p21, and was enhanced by the aurora kinase inhibitor VX-680, suggesting that senescence is triggered by defects in mitosis. Depletion of PKCι had no effect on senescence in normal mammary epithelial cell lines. We conclude that PKCι is overexpressed in a subset of cancers where it functions to suppress premature senescence. This function appears to be restricted to cancer cells and inhibition of PKCι may therefore be an effective way to selectively activate premature senescence in cancer cells.

Keywords: Atypical protein kinase C; PIK3CA; breast cancer; glioblastoma; senescence; Aurora kinase

Introduction

Cellular senescence is a state of permanent proliferation arrest that cannot be overcome by the addition of mitogenic stimuli. In addition to this loss of proliferation potential, adherent senescent cells show a characteristic set of morphological changes that includes flattening, enlargement and an increase in cytoplasmic granularity and vacuolization. Senescence was originally described as a phenomenon that primary (non-transformed) cells underwent after serial passage in cell culture. This is now known to be due to the gradual loss of telomeric repeats from the ends of chromosomes during cell divisions. This ultimately leads to the activation of a DNA damage response that triggers a sustained state of proliferation arrest (d'Adda et al, 2003). This senescence phenomenon is now referred to more specifically as replicative senescence to distinguish it from a related phenomenon known as premature senescence, which has overlapping features with replicative senescence (Schmitt, 2007). Premature senescence can occur in response to either oncogene activation or stress. Thus, for example, the introduction of mutant, oncogenic *KRAS* into many primary cell types induces an irreversible proliferation arrest, along with similar morphological and biochemical changes to those seen in cells undergoing replicative senescence. This phenomenon, referred to as oncogene-induced senescence, appears to be an important endogenous cancer control mechanism in the human body. The best example of this are the cells found in the naevi (moles) present on the skin of many humans. These often have oncogenic mutations but have undergone senescence and therefore fail to develop into malignant cancers (Pollock et al, 2003;Michaloglou et al, 2005).

Cancer cells clearly develop the ability to evade both replicative and premature senescence. However there is substantial evidence that this can be overcome under specific circumstances and that senescence induction is a legitimate additional strategy to block cancer cell proliferation (Schmitt, 2007). This was first shown with DNA-damaging chemotherapy agents, which can induce premature senescence in many cancer cell types (Gewirtz et al, 2008). It appears that oncogenic mutations increase the threshold for a DNA damage-triggered senescence response in these cells, but do not completely abrogate the senescence response. A second strategy to induce senescence in cancer cells may be simply to turn off the suppression of oncogene-induced senescence (Ventura et al, 2007;Wu et al, 2007). An exciting aspect of this approach is that it provides a mechanism for selectivity for cancer cells over normal cells, as oncogenic signals unique to the cancer cells can drive them into senescence.

The phosphoinositide 3-kinase pathway is aberrantly activated in the majority of cancers, either by activation of receptor tyrosine kinases, loss of the tumor suppressor PTEN or mutational activation of PI 3-kinase itself. Mutational activation of PI 3-kinase most frequently occurs as a result of point mutations in the *PIK3CA* gene, which are found in 25-30% of breast cancers and at a lower frequency in other cancer types (Karakas et al, 2006). Amplification of the *PIK3CB* gene has also been reported, although this appears to be a relatively rare event (Crowder et al, 2009). All of these events lead to the generation of the second messenger phosphoinositide 3,4,5 trisphosphate on the inner leaflet of the plasma membrane. This leads to the activation of multiple downstream kinases via phosphoinositide-dependent kinase 1 (PDK1).

While PKB/Akt is the most widely studied of these kinases, multiple other kinases also require PDK1 phosphorylation for their activation, including the atypical PKCs (Peifer et al, 2008).

There are two members of the atypical PKC family, PKCζ and PKCι (PKCλ in mice). Both of the atypical PKCs are distinguished from other members of the PKC family by their lack of dependence on diacylglycerol for activation. PKCι is activated by PDK1 phosphorylation either on its own or in association with a complex of an activated member of the Cdc42 family of GTPases and Par6 (Kanzaki et al, 2004). Of the two enzymes, PKCι is the most ubiquitously expressed and there is now considerable evidence linking PKCι to the transformed phenotype (Fields et al, 2007). It is overexpressed in multiple cancer types and studies in both mouse models and human cancer cell lines show an important role in the growth, invasion and resistance to apoptosis of a variety of cancer cell types. In glioblastoma, PKCι represses apoptosis and promotes invasion (Baldwin et al, 2006;Baldwin et al, 2008). PKCι also has a key role in the pathogenesis of lung, ovarian and pancreatic cancer (Eder et al, 2005;Zhang et al, 2006;Regala et al, 2005).

Several previous studies have provided evidence for a role for the PI 3-kinase pathway in senescence. In cultured mouse embryonic fibroblasts, the PI 3-kinase inhibitors LY294002 and wortmannin induce senescence (Collado et al, 2000). In mouse models of melanoma, while *BRAF* activation in melanocytes mimics the generation of senescent cells described in human naevi, *BRAF* activation in mice deleted for *PTEN* leads to the formation of malignant tumours (Dankort et al, 2009). In contrast to these studies that indicate a role for the PI 3-kinase pathway in suppressing oncogene-induced senescence, other studies have indicated a role for the PI 3-kinase

pathway in driving oncogene-induced senescence. Chen *et al*. have shown that in mouse models of prostate cancer, loss of PTEN drives cells into senescence (Chen et al, 2005). Yuan *et al*. have shown data indicating that high levels of PI 3-kinase activity can drive breast epithelial cells into senescence (Yuan et al, 2011). These differences may be a reflection of the striking tissue-specific effects of relatively small changes in signaling through the PI 3-kinase pathway (Carracedo et al, 2011). Here we show that PKCι is overexpressed in breast cancer cells and that this overexpression is driven, in part, by mutational activation of *PIK3CA*. Overexpressed PKCι functions to suppress oncogene-induced senescence in breast cancer cells, and also in glioblastoma cells where PKCι is activated by loss of *PTEN*.

Results

PKCι expression in breast cancer: PKCι expression in breast cancer was assessed by immunohistochemistry. The monoclonal antibody used for this recognizes a single band on Western blots of breast cancer cell lines and, unlike some polyclonal antibodies, is specific for PKCι and does not bind PKCζ. Three different commercial tissue microarrays were analyzed for PKCι expression. These were: a tissue microarray with cores from 36 breast cancer cases and 12 cases of non-malignant breast cancer tissue; a tissue microarray with cores from 50 breast cancer cases and matched lymph node metastases; a tissue microarray with 5 cases of normal tissue, 12 hyperplasia cases, 12 carcinoma *in situ*, and 12 invasive carcinomas. Scoring of stained slides was done by two pathologists using scanned digital images of slides and TMA Software from Aperio. Representative examples of staining are shown in Figure 1. In normal breast tissue there were very low levels of PKCι cytoplasmic staining in both luminal and myoepithelial cells of the duct, as well as the surrounding stromal cells. The distribution of scores for hyperplasia, ductal carcinoma *in situ*, invasive ductal carcinoma and lymph node metastases is shown in Figure 1. Cytoplasmic staining for PKCι was somewhat higher in hyperplasia than in normal tissue. PKCι expression was not significantly different between ductal carcinoma *in situ*, invasive ductal carcinoma and lymph node metastases; however PKCι expression was significantly higher in all of these when compared to hyperplasia ($p<0.05$ for each of the three comparisons, see Supplementary Table 1). Cytoplasmic PKCι expression is therefore increased at an early stage in breast cancer development and is maintained in metastatic disease.

Figure 1. PKCι expression in breast cancer. Panels on the left show examples of PKCι immunohistochemistry in (from top to bottom): normal breast tissue; hyperplasia; ductal carcinoma *in situ* (DCIS); invasive ductal carcinoma (IDC); breast cancer lymph node metastases (LNM). Bar graphs on the right show the distribution of immunohistochemistry scores for hyperplasia, ductal carcinoma *in situ*, invasive ductal carcinoma and lymph node metastases cases.

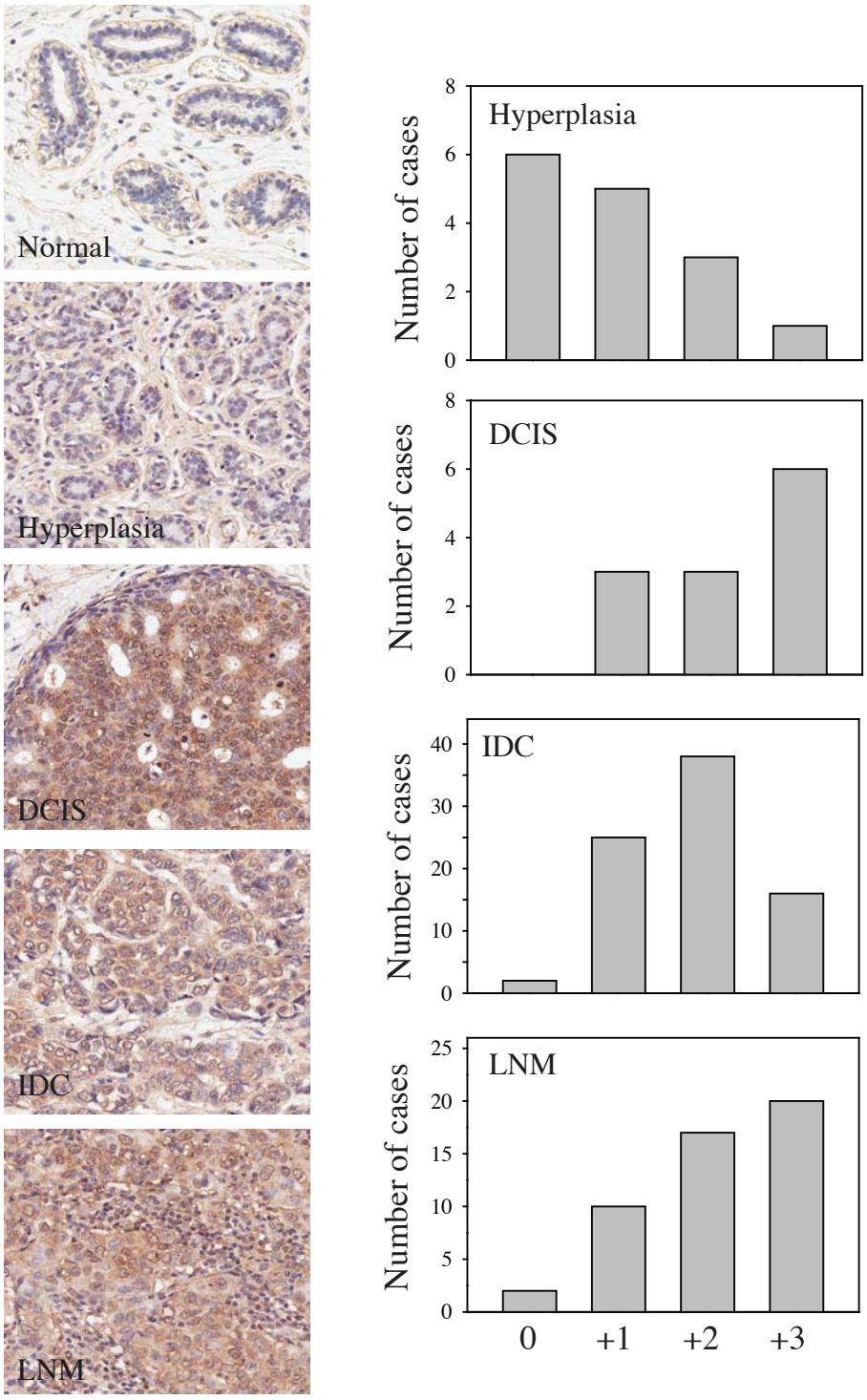
Normal
Hyperplasia
DCIS
IDC
LNM
Hyperplasia
Number of cases
0
2
4
6
8
DCIS
Number of cases
0
2
4
6
8
IDC
Number of cases
0
10
20
30
40
LNM
Number of cases
0
5
10
15
20
25
0
+1
+2
+3

PKCι expression in breast cancer cell lines: Levels of PKCι were assessed in four different breast cancer cell lines (MCF7, T47D, MDA-MB-231 and BT549) by Western blotting and compared to expression levels in two breast epithelial cell lines, MCF10A and human mammary epithelial cells transduced with telomerase (hTert-HMEC). Expression levels were similar between the two breast epithelial cell lines (Figure 2A). Levels of PKCι protein were higher in three of the four breast cancer cell lines analyzed. To determine if these reflected increased activity of PKCι, Western blots were also probed with an antibody specific for PKCι phosphorylated at Thr555. Phosphorylation of this site, in the turn motif of the PKCι catalytic domain, is a feature of activation of this and other AGC kinase family members (Freeley et al, 2011). Two of the four breast cancer cell lines (MCF7 and T47D) also showed marked increases in the levels of phosphorylated PKCι. Normalizing this to total PKCι levels showed that there was an increase in the proportion of PKCι that is activated in these two cell lines (Figure 2B).

PIK3CA mutations increase the expression and activation of PKCι: The two cell lines that showed the highest expression and activation of PKCι have been shown previously to have *PIK3CA* mutations and this was confirmed in our lab (E545K for MCF7 and H1047R for T47D). To directly assess the effects of *PIK3CA* mutations on PKCι expression and activation, MCF10A cells expressing wild-type and the E545K and H1047R mutants of *PIK3CA* were made using retroviral transduction, as described previously. Figure 2C shows a Western blot analysis of PKCι expression and activation status in these cells grown in the absence of growth factors. Both *PIK3CA* mutants, but not wild-type *PIK3CA*, increased levels of PKCι reproducibly (Figure 2D). This effect

Figure 2. PKCι expression in breast cancer cell lines and activation by PIK3CA. A. Total cell lysates from the breast epithelial cell lines MCF10A and hTert-HMEC, and the breast cancer cells lines MCF7, T47D, MDA MB-231 and BT549 were analyzed by Western blotting for PKCι phosphorylated at Thr555, total PKCι and actin (as a loading control). **B.** PKCι levels were quantitated and normalized to actin levels (upper plot). Mean values determined from two independent experiments are shown and are expressed relative to levels in MCF10A cells. Phosphorylated PKCι levels were quantitated and divided by total PKCι levels (lower plot). Mean values determined from two independent experiments are shown and are expressed relative to levels in MCF10A cells. **C.** Total cell lysates from MCF10A cells transduced with empty vector (JP1520), wild-type *PIK3CA* cDNA, E454K mutant *PIK3CA* cDNA or H1047R mutant *PIK3CA* cDNA were analyzed by Western blotting for levels of phosphorylated and total PKCι and PKB/Akt. **D.** Quantitation of levels of total PKCι protein. Data shown are the mean ± SE from three separate experiments.

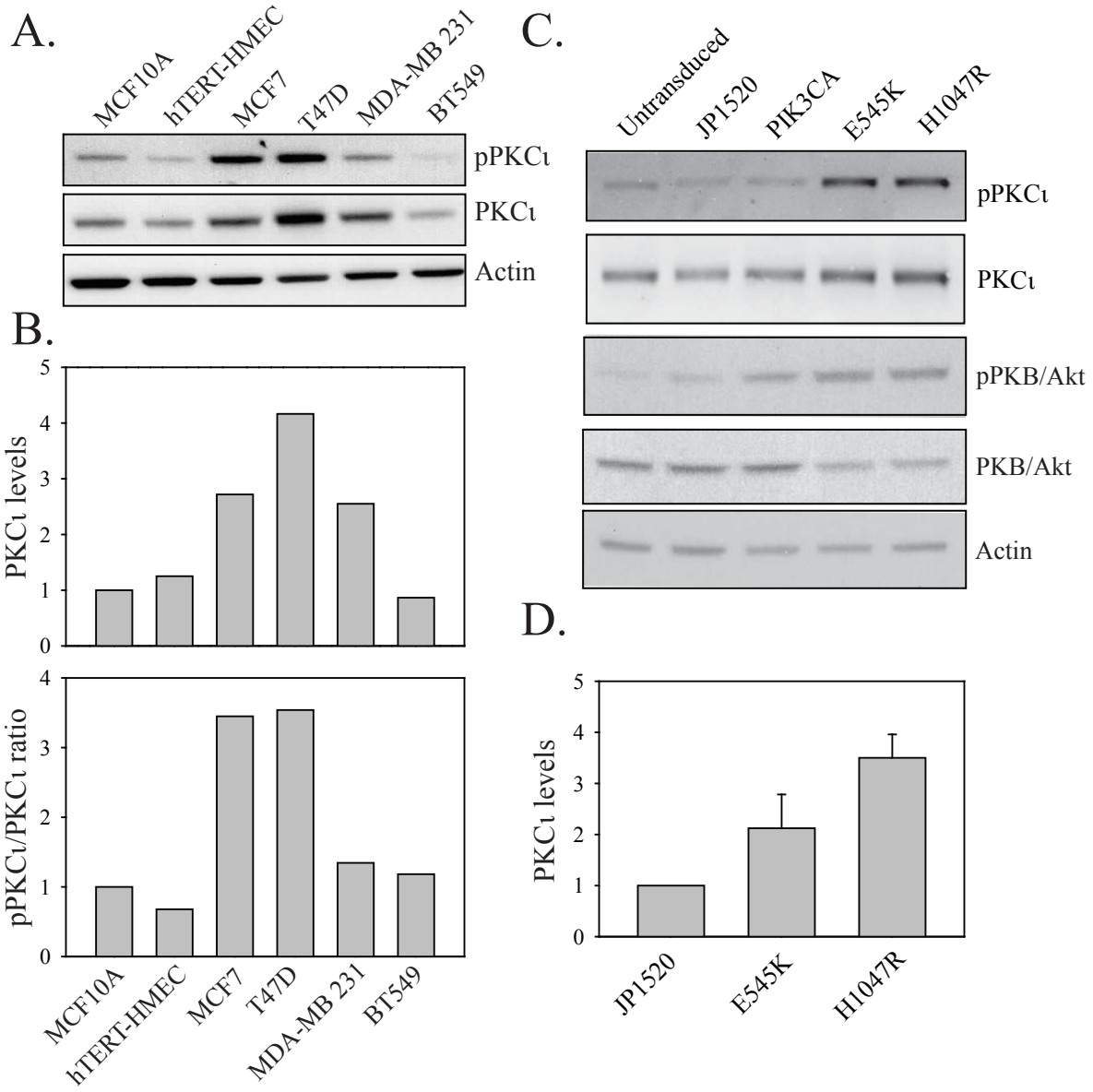
A.
MCF10A
hTERT-HMEC
MCF7
T47D
MDA-MB 231
BT549
pPKCι
PKCι
Actin
B.
PKCι levels
pPKCι/PKCι ratio
MCF10A
hTERT-HMEC
MCF7
T47D
MDA-MB 231
BT549
C.
Untransduced
JP1520
PIK3CA
E545K
H1047R
pPKCι
PKCι
pPKB/Akt
PKB/Akt
Actin
D.
PKCι levels
JP1520
E545K
H1047R

was more marked with the H1047R mutant, consistent with the very high expression seen in T47D cells that also have this specific mutation. Both mutant forms of *PIK3CA*, but not wild-type, also increased the levels of phosphorylated PKCι. Constitutively active *PIK3CA* mutants therefore increase both the expression and activation of PKCι.

PKCι promotes breast cancer cell proliferation by repressing senescence: Transient transfection of RNA duplexes targeting PKCι effectively reduced its levels in both MCF7 cells and T47D cells (Figure 3A). Levels of PKCι remained low for up to six days after transfection (the longest time point tested). Depletion of PKCι with two different RNA duplexes decreased the proliferation in MCF7 and T47D cells (Figure 3B). This occurred in the absence of any detectable increase in cell death, as assessed by flow cytometry. Cultures of MCF7 and T47D cells depleted of PKCι also showed a decrease in the percentage of cells incorporating BrdU, consistent with decreased cell division causing the decrease in viable cell numbers observed (Figure 3C).

One possible explanation for the reduced proliferation of breast cancer cells upon depletion of PKCι was that there was an increase in the number of cells undergoing senescence. To assess this, cells were assessed for the activity of senescence-associated βgalactosidase (SA-β-gal), a widely used marker of senescence (Debacq-Chainiaux et al, 2009). PKCι depletion significantly increased the percentage of SA-β-gal -positive cells in both MCF7 and T47D cells (Figure 4A). Cells that were SA-β-gal -positive showed an enlarged, flattened morphology (Figure 4B) and these cells were negative for BrdU incorporation (Figure 4C), all consistent with the senescent phenotype.

Figure 3. Depletion of PKCι decreases breast cancer cell proliferation. A. Western blots showing depletion of PKCζ in total cell lysates of breast cancer cells using RNA interference. The left panel shows the levels of PKCζ, PKCζ phosphorylated at Thr555 (pPKCι) and actin (as loading control) in MCF7 cells 2 days after mock transfection, transfection with a control RNA duplex or transfection of two different RNA duplexes targeting PKCζ. The right panel shows transfection of T47D cells. Samples were collected on days 2, 4 and 6 after transfection to assess the duration of PKCζ depletion. **B.** The indicated cell types were either mock-transfected, transfected with a control RNA duplex or transfected with two different RNA duplexes targeting PKCζ. The numbers of viable cells were then determined on the indicated days after transfection. **C.** MCF7 and T47D cells were transfected as above. Six days after transfection, incorporation of BrdU was assessed. The data shown are the means±s.e. of three separate experiments. * indicates a P value <0.05.

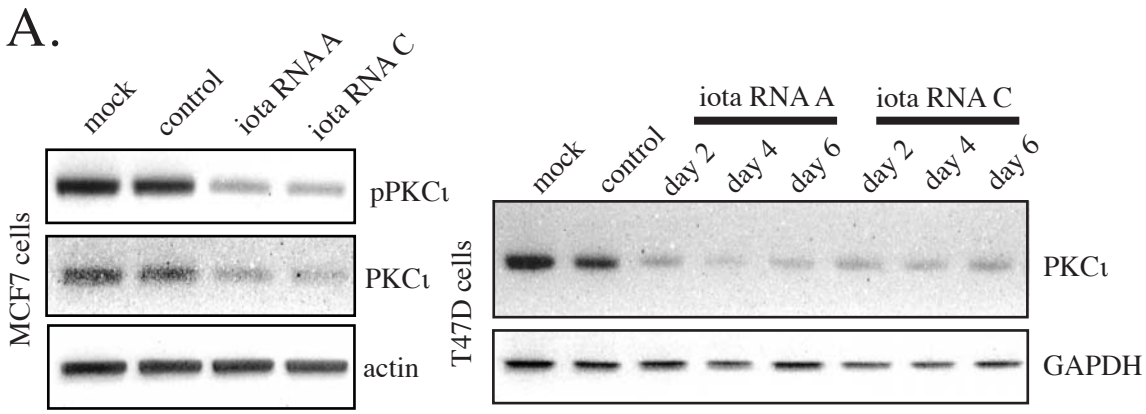
A.
mock
control
iota RNA A
iota RNA C
MCF7 cells
pPKCι
PKCι
actin
iota RNA A
iota RNA C
mock
control
day 2
day 4
day 6
day 2
day 4
day 6
T47D cells
PKCι
GAPDH

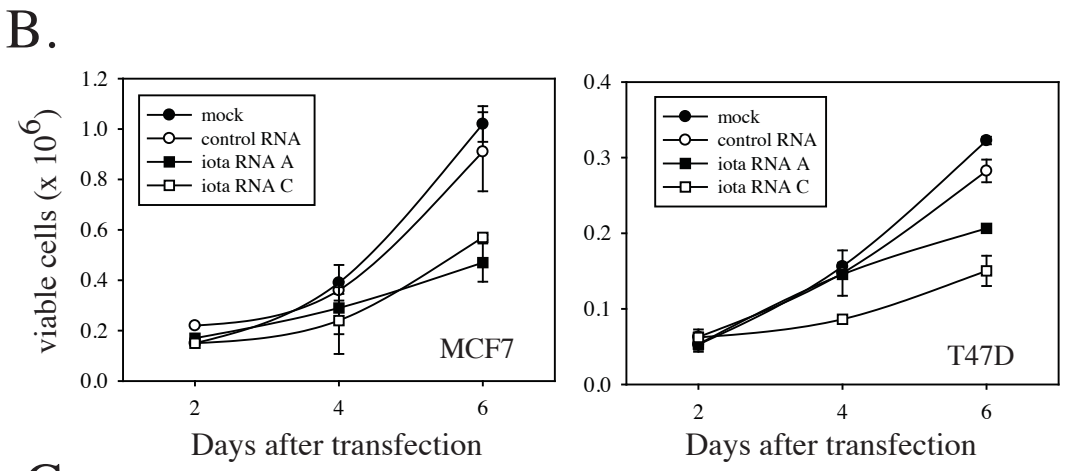
B.
viable cells (x 10^6)
mock
control RNA
iota RNA A
iota RNA C
MCF7
T47D
Days after transfection
Days after transfection

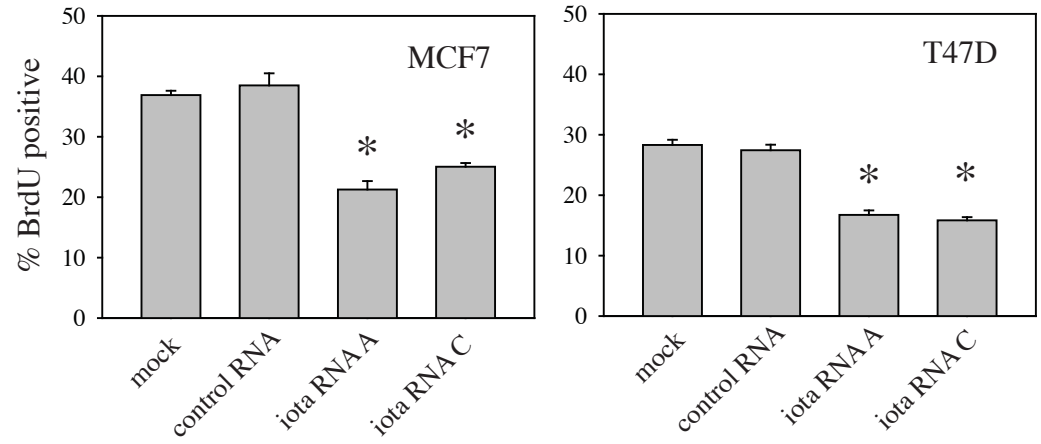
C.
% BrdU positive
MCF7
T47D
mock
control RNA
iota RNA A
iota RNA C

Figure 4. Depletion of PKCι induces senescence in breast cancer cell lines. A. Indicated cell types were either mock-transfected, transfected with a control RNA duplex, or transfected with two different RNA duplexes targeting PKCι. Six days after transfection, cells were stained for SA-β-gal activity. Percentages of SA-β-gal positive cells were determined as described in Materials and Methods. Data shown are from three independent experiments. **B.** Morphology of cells staining positive for SA-β-gal. Cells were photographed under bright-field microscopy. **C.** Cells with senescent morphology do not incorporate BrdU. Superimposed images of phase contrast, DAPI staining (blue) and BrdU staining (red) are shown.

A.

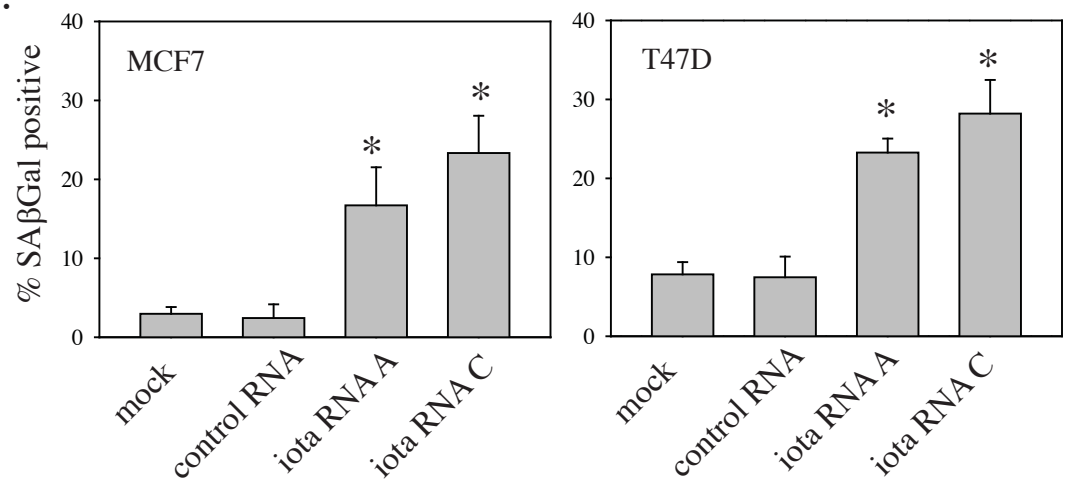
% SAβGal positive
MCF7
T47D
40
30
20
10
0
*
mock
control RNA
iota RNA A
iota RNA C

B.

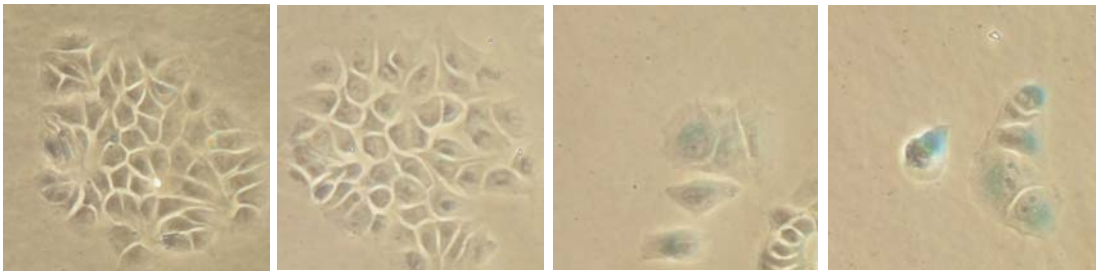
Mock
Control
iotaRNAA
iotaRNAC

C.

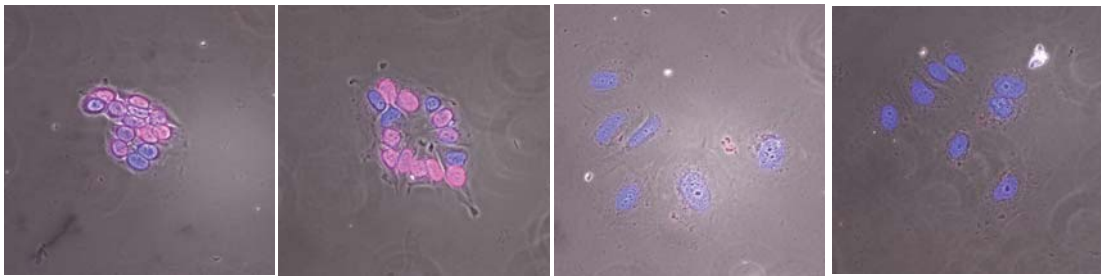
Mock
Control
iotaRNAA
iotaRNAC

DNA damage (either telomeric in the case of replicative senescence or non-telomeric in the case of premature senescence) is a common, although not universally observed (Denoyelle et al, 2006;Lin et al, 2010), feature of senescence and DNA damage responses have an important role in the initiation and maintenance of the senescent phenotype (Passos et al, 2010). To assay whether DNA damage response pathways were activated upon PKCι depletion in breast cancer cells, the presence of γH2AX foci was assessed by immunofluorescence microscopy. As a positive control, cells were treated with adriamycin, which has been shown previously to induce senescence via DNA damage and induced senescence in the cell lines used in this study. As expected with adriamycin treatment, cells showed the presence of numerous nuclear foci staining positive for γH2AX that were still present five days after adriamycin treatment. However in MCF7 cells in which senescence was induced by PKCι depletion, numbers of γH2AX foci were not significantly higher than in control cells (Figure 5A).

Multiple studies have indicated a key role for the cell cycle inhibitory protein p21 in senescence induction. To assess the role of p21 in the senescence induction after PKCι depletion, siRNA targeting p21 and PKCι were used either separately or in combination to simultaneously deplete cells of both proteins (Figure 5B). Depletion of p21 levels in MCF7 cells prevented senescence induction with PKCι depletion, demonstrating an essential role for p21 in this process (Figure 5C).

Previous data has linked impaired mitosis to senescence activation (Baker et al, 2004;Lin et al, 2010) and our recent data has indicated a role for PKCι in mitosis (Baldwin et al, 2010). As an alternate means to impair mitosis, the effects of Aurora kinase inhibition on senescence were assessed, both in the absence and presence of

Figure 5. Role of the DNA damage response and p21 in senescence induction. A. MCF7 cells were either mock-transfected, transfected with a control RNA duplex, or transfected with two different RNA duplexes targeting PKCι. Five days after transfection, cells were fixed on coverslips and assessed for the presence of γH2AX foci by immunofluorescence microscopy. As a positive control, cells were also treated with either 500 nM adriamycin for 24 h and assessed five days later for the presence of γH2AX foci. **B**. MCF7 cells were transfected with the indicated duplexes targeting either PKCι or p21. Two days after transfection, total cell lysates were collected and analyzed for levels of p21, PKCι and GAPDH by Western blotting. **C.** MCF7 cells were transfected with RNA duplexes targeting PKCι or p21 as in B. Five days after transfection, cells were stained for SA-β-gal activity.

A.

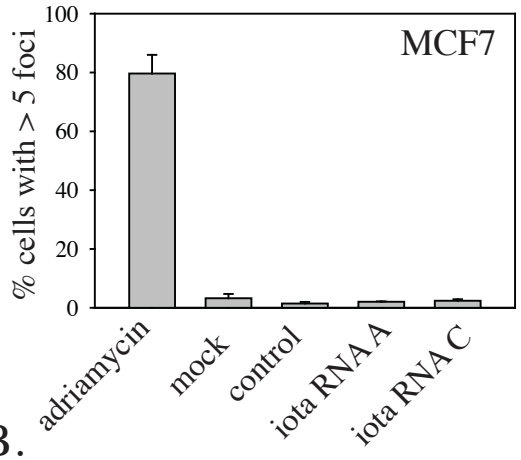
MCF7
% cells with > 5 foci
100
80
60
40
20
0
adriamycin
mock
control
iota RNA A
iota RNA C

B.

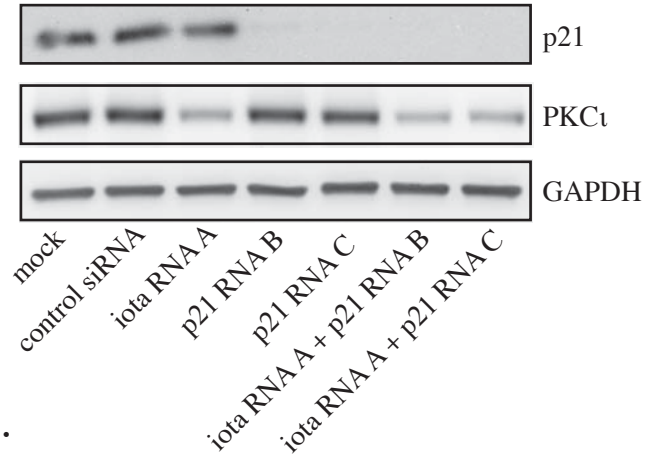
p21
PKCι
GAPDH
mock
control siRNA
iota RNA A
p21 RNA B
p21 RNA C
iota RNA A + p21 RNA B
iota RNA A + p21 RNA C

C.

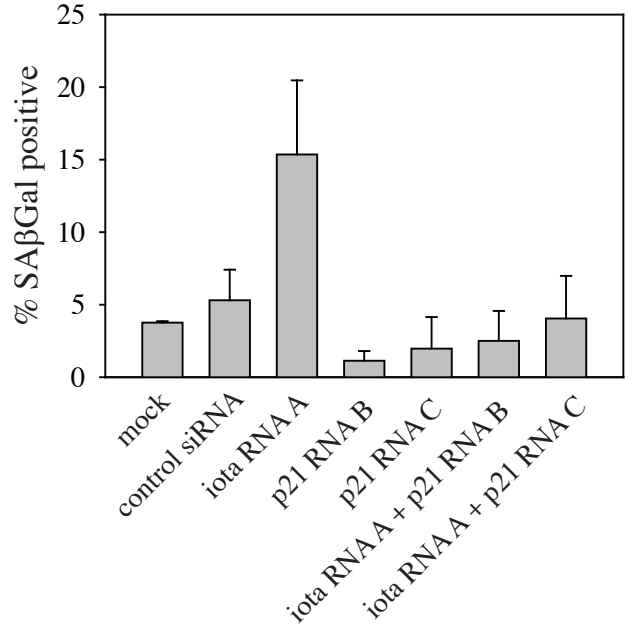
% SAβGal positive
25
20
15
10
5
0
mock
control siRNA
iota RNA A
p21 RNA B
p21 RNA C
iota RNA A + p21 RNA B
iota RNA A + p21 RNA C

PKCι depletion. The Aurora kinases are known to have a central role in the control of mitosis (Barr et al, 2007). The pan-aurora kinase inhibitor VX-680 was used for these experiments (Harrington et al, 2004). VX-680 on its own caused an increase in the number of senescent MCF7 cells and also enhanced the effects of PKCι depletion on senescence induction (Figure 6A). VX-680, either alone or in combination with PKCι depletion, did not increase numbers of γH2AX foci beyond those seen in control cells, suggesting that the two treatments promote senescence by similar mechanisms (Figure 6B). Consistent with results reported for the aurora kinase A selective inhibitors MLN8237 and MLN8054 (Gorgun et al, 2010;Huck et al, 2010), VX-680 also increased levels of p21 in MCF7 cells prior to the onset of the senescence phenotype (Figure 6C and D).

PKCι depletion does not induce senescence in normal breast epithelial cells. In hTert-HMEC cells, depletion of PKCι had no effect on proliferation (Figures 7A and B). These cells had undetectable basal levels of SA-βgal positivity and no increase in positivity was seen upon PKCι depletion (Figure 7C). Similarly, PKCι depletion did not have a significant effect on SA-βgal positivity in MCF10A normal breast epithelial cells, even though these cells had relatively high basal levels of SA-βgal positivity (similar to levels seen in T47D cells)(Figure 7C).

PKCι represses senescence in glioblastoma: PKCι depletion also increased the proportion of SA-β-gal -positive cells in three different glioblastoma cell lines (U87MG, A172 and DBTRG)(Figure 8A and B). In these cells, PKCι is activated by loss of *PTEN* rather than by *PIK3CA* mutation (Baldwin et al, 2008). Glioblastoma cells that were SAβgal-positive

Figure 6. Senescence induction upon PKCι depletion combined with Aurora kinase inhibition. A. MCF7 were transfected as above to deplete PKCι. Two days after transfection, cells were treated for the indicated time with 400 nM VX-680. Media with VX-680 was then removed and fresh media was added. Cells were stained for SA-β-gal activity five days after the start of transfection. **B.** MCF7 cells were treated as above. Five days after transfection, cells were fixed and assessed for the presence of γH2AX foci by immunofluorescence microscopy. **C** and **D.** MCF7 cells were treated with DMSO control or 400 nM VX-680 for the indicated times. Total cell lysates were then analyzed by Western blotting for levels of p21 and GAPDH (as a loading control). A representative blot is shown in C. Quantitation of changes in p21 levels (normalized to vehicle-treated controls) is shown in D. Data shown are the mean ± SE from three independent experiments.

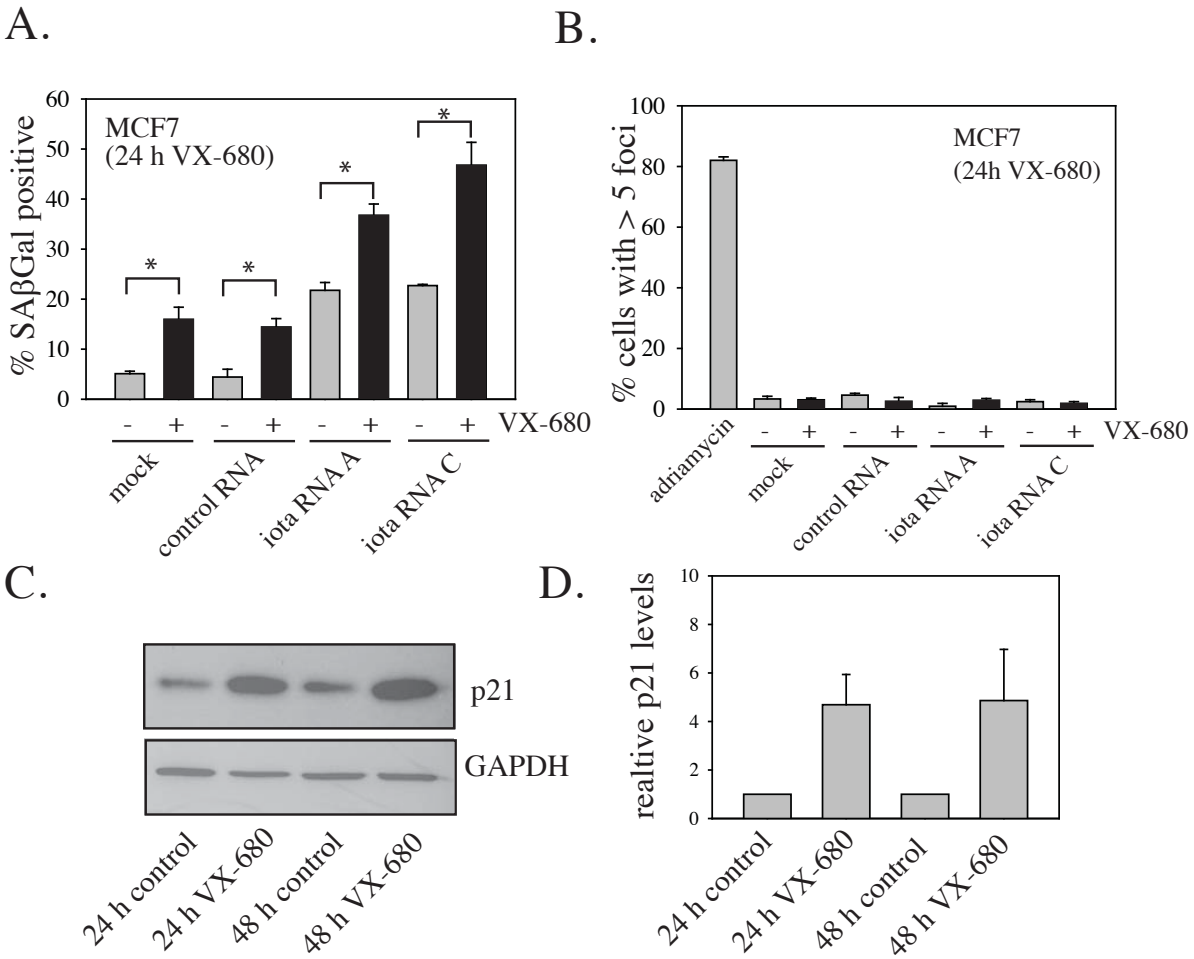
A.
B.
C.
D.
% SAβGal positive
MCF7
(24 h VX-680)
VX-680
mock
control RNA
iota RNA A
iota RNA C
% cells with > 5 foci
MCF7
(24h VX-680)
adriamycin
p21
GAPDH
realtive p21 levels
24 h control
24 h VX-680
48 h control
48 h VX-680

Figure 7. Effects of PKCι depletion in normal breast epithelial cell lines. A. hTert-HMEC cells were transfected as described in Figure 1. Total cell lysates were prepared on the indicated days after transfection and analyzed by Western blotting for levels of PKCι and GAPDH (as a loading control). **B.** hTert-HMEC cells were transfected with the indicated RNA duplexes and numbers of viable cells were then determined on the indicated days after transfection. **C.** hTert-HMEC and MCF10A cells were transfected with RNA duplexes as indicated and assessed for SA-βGal activity five days after transfection. MCF10A cells transduced with retroviral vectors expressing *PIK3CA* cDNA with either E545K or H1047R mutations were also analyzed for SA-βGal activity in parallel with MCF10A cells.

A.

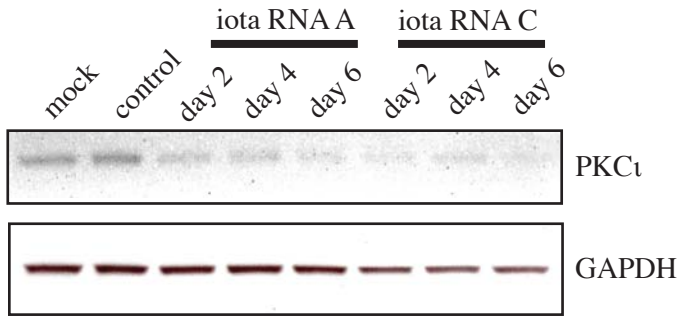
iota RNA A
iota RNA C
mock
control
day 2
day 4
day 6
day 2
day 4
day 6
PKCι
GAPDH

B.

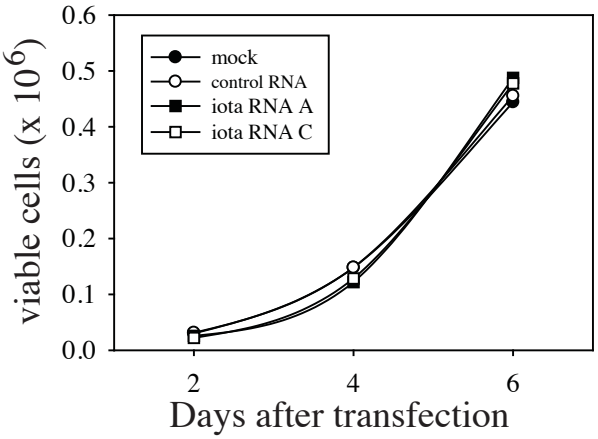
mock
control RNA
iota RNA A
iota RNA C
viable cells (x 10^6)
0.0
0.1
0.2
0.3
0.4
0.5
0.6
2
4
6
Days after transfection

C.

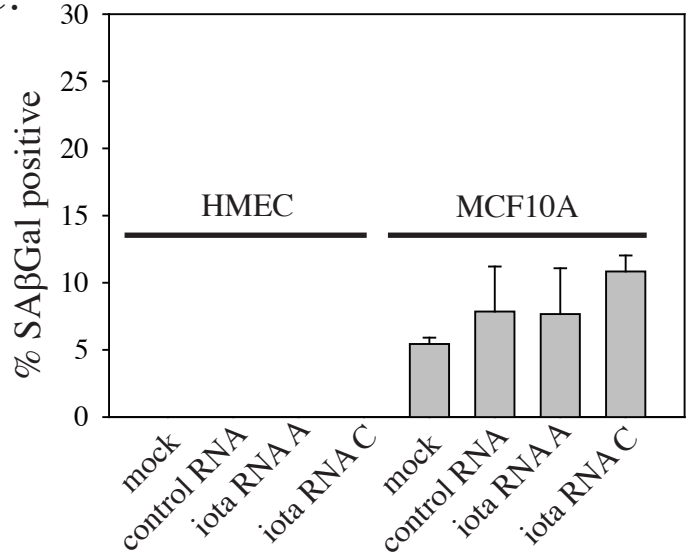
% SAβGal positive
0
5
10
15
20
25
30
HMEC
MCF10A
mock
control RNA
iota RNA A
iota RNA C
mock
control RNA
iota RNA A
iota RNA C

Figure 8. Depletion of PKCι induces senescence in glioblastoma cell lines. **A.** U87MG cells were either mock-transfected, transfected with a control RNA duplex, or transfected with two different RNA duplexes targeting PKCι. Two days after transfection, total cell lysates were collected and analyzed for expression of PKCι and GAPDH. **B.** Glioblastoma cell lines U87MG, A172 and DBTRG were transfected as in A. Six days after transfection, cells were stained for SA-βGal activity. Percentages of SA-βGal positive cells were determined as described in Materials and Methods. Data shown are the mean ±SE from three independent experiments**. B.** Morphology of SA-βGal positive U87MG glioblastoma cells six days after PKCι depletion.

A.

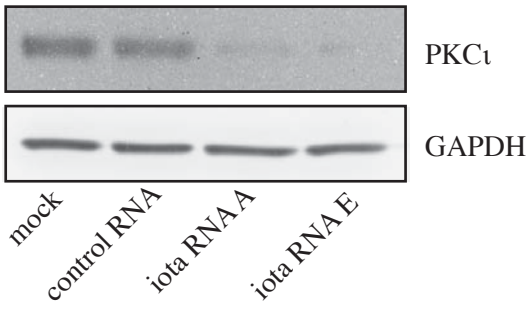
PKCι
GAPDH
mock
control RNA
iota RNA A
iota RNA E

B.

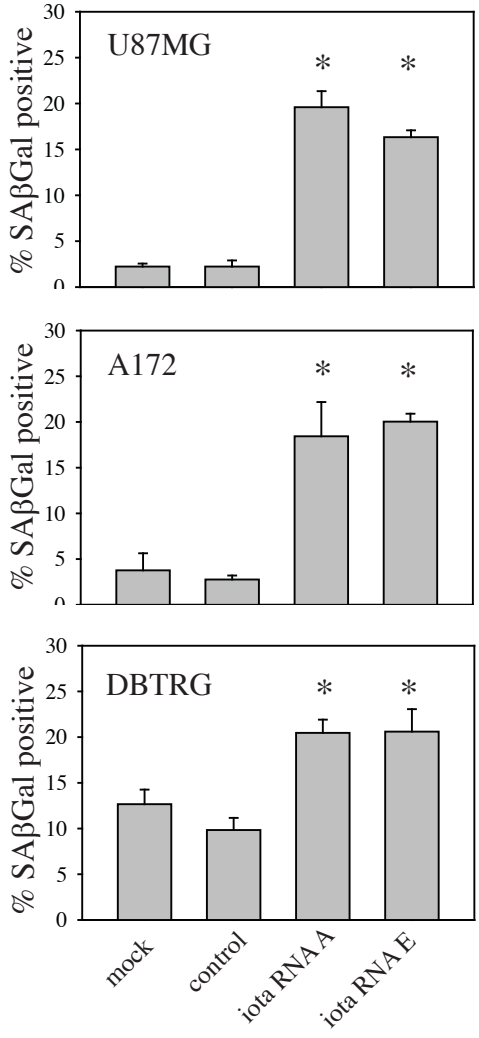
U87MG
A172
DBTRG
% SAβGal positive
0
5
10
15
20
25
30
*
mock
control
iota RNA A
iota RNA E

C.

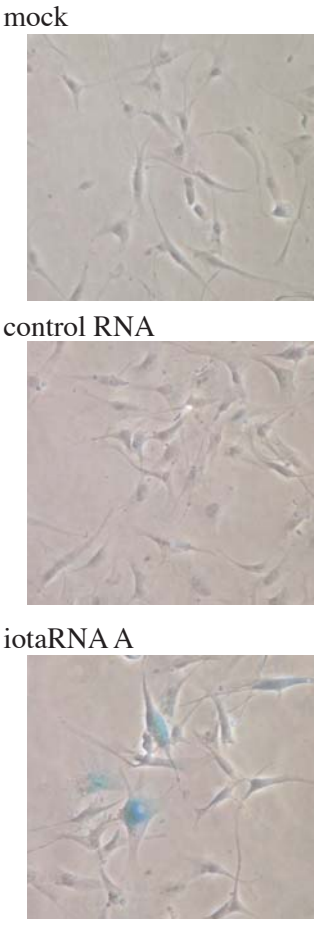
mock
control RNA
iotaRNA A

also showed an enlarged, flattened morphology, confirming that they were senescent (Figure 8C). As with MCF7 breast cancer cells, senescence occurred in the absence of a detectable DNA damage response (Figure 9A and B) and was dependent on the presence of p21 (Figure 9C and D). VX-680 also caused an increase in the number of senescent U87MG cells (Figure 10A), although only with longer (72 h) exposures to the drug. With shorter (24 h) exposures, VX-680 treatment did not give a statistically significant increase in senescence U87MG cells, but did sensitize them to senescence induction upon PKCι depletion (Figure 10B). This also occurred without any evidence for activation of the DNA damage response (Figure 10C). VX-680 treatment also caused an increase in p21 levels in U87MG cells, although as with senescence induction this was only evident with longer exposures to VX-680 (Figure 10D).

Figure 9. Role of the DNA damage response and p21 in senescence induction in glioblastoma cells. A. U87MG cells were either mock-transfected, transfected with a control RNA duplex, or transfected with two different RNA duplexes targeting PKCι. Five days after transfection, cells were fixed on coverslips and assessed for the presence of γH2AX foci by immunofluorescence microscopy. As a positive control, cells were also treated with either 200 nM adriamycin for 24 h and assessed five days later for the presence of γH2AX foci. **B**. Representative images of nuclei from U87MG cells that have undergone senescence after treatment with PKCι-targeted RNA duplexes or adriamycin. A nucleus from a non-senescent cell treated with a control RNA duplex is shown for comparison. DAPI staining of nuclei is shown in blue and γH2AX staining is shown in red. **C.** U87MG cells were transfected with RNA duplexes targeting PKCι or p21 as indicated. Two days after transfection, total cell lysates were collected and analyzed for the expression of p21, PKCι and GAPDH by Western blotting. **D.** U87MG cells were transfected as in C. Five days after transfection, cells were stained for SA-β-gal activity.

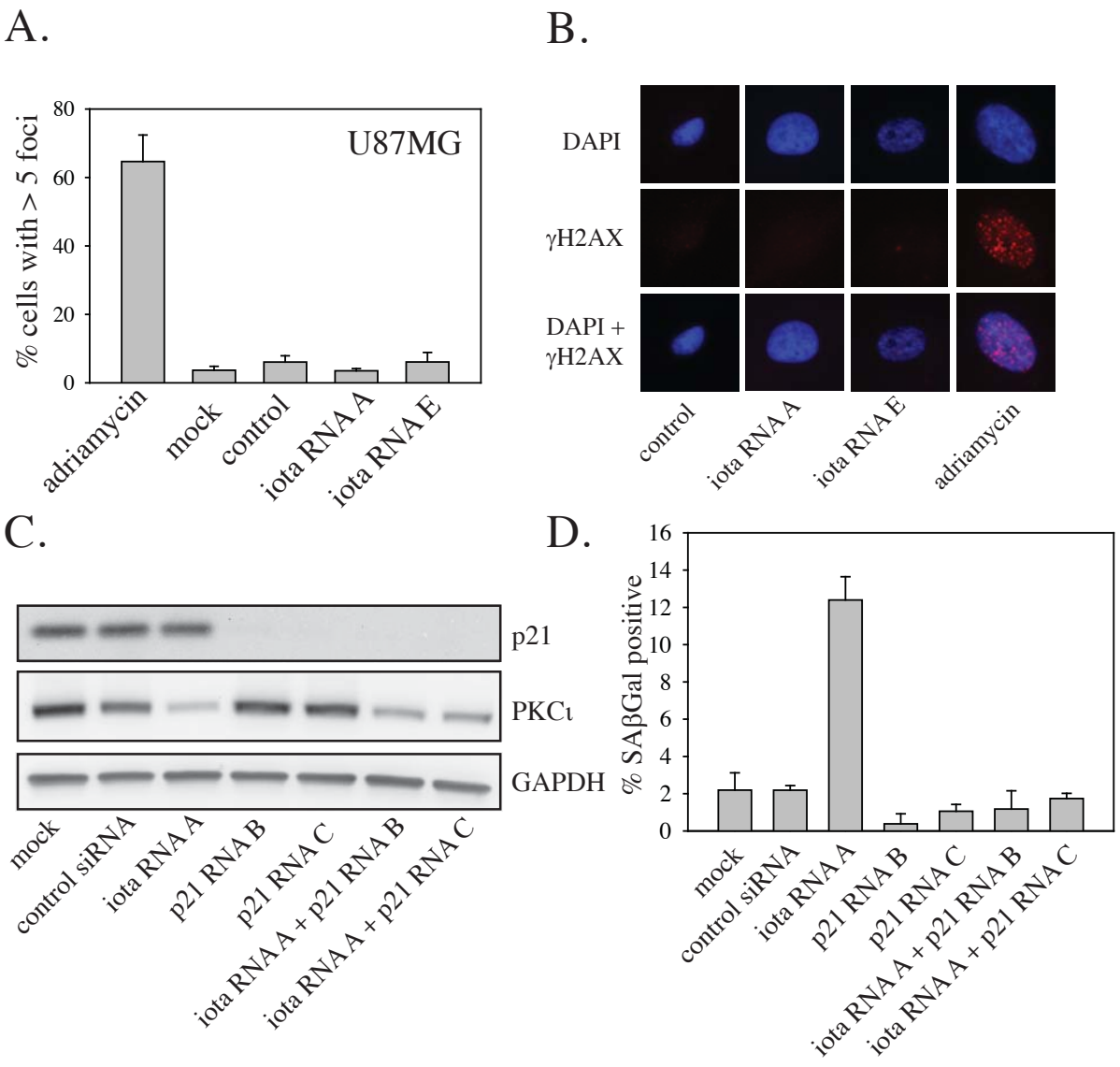
A.
B.
C.
D.
U87MG
% cells with > 5 foci
adriamycin
mock
control
iota RNA A
iota RNA E
DAPI
γH2AX
DAPI + γH2AX
control
iota RNA A
iota RNA E
adriamycin
p21
PKCι
GAPDH
mock
control siRNA
iota RNA A
p21 RNA B
p21 RNA C
iota RNA A + p21 RNA B
iota RNA A + p21 RNA C
% SAβGal positive

Figure 10. Senescence induction upon PKCι depletion combined with Aurora kinase inhibition in glioblastoma cells. A and B. U87MG cells were transfected as above to deplete PKCι. Two days after transfection, cells were treated for 72 h (A) or 24 h (B) with 400 nM VX-680. Media with VX-680 was then removed and fresh media was added. Cells were stained for SA-β-gal activity five days after the start of transfection. **C.** U87MG cells were treated as in A above. Five days after transfection, cells were fixed and assessed for the presence of γH2AX foci by immunofluorescence microscopy. **D.** U87MG cells were treated with DMSO control or 400 nM VX-680 for the indicated times. Total cell lysates were then analyzed by Western blotting for levels of p21. The bar graph shows quantitation of p21 levels (normalized to vehicle-treated controls) from three independent experiments. A representative blot is also shown, with lanes aligned to correspond to the labels on the graph.

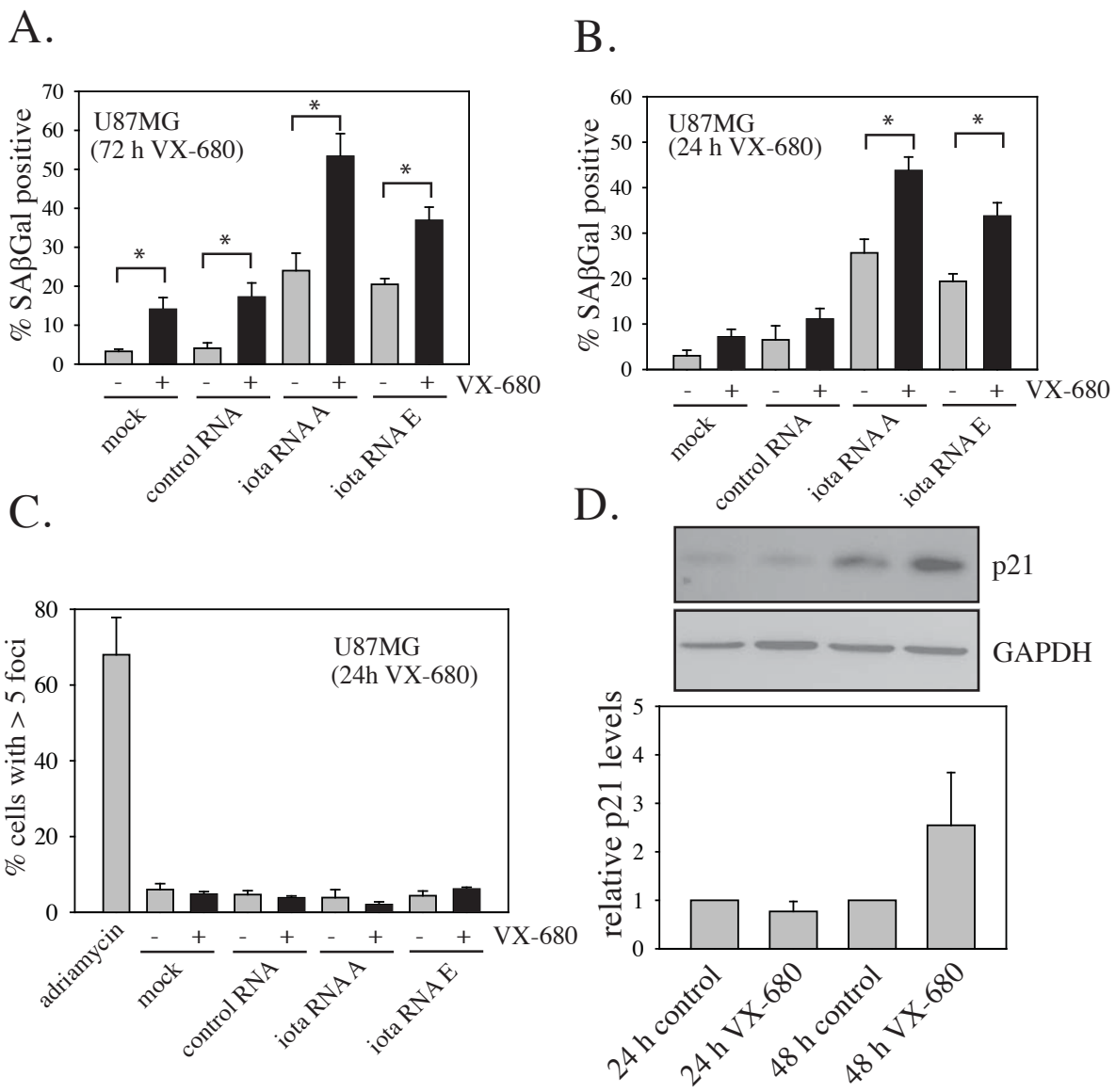
A.
U87MG
(72 h VX-680)
% SAβGal positive
VX-680
mock
control RNA
iota RNA A
iota RNA E
B.
U87MG
(24 h VX-680)
% SAβGal positive
VX-680
mock
control RNA
iota RNA A
iota RNA E
C.
U87MG
(24h VX-680)
% cells with > 5 foci
VX-680
adriamycin
mock
control RNA
iota RNA A
iota RNA E
D.
p21
GAPDH
relative p21 levels
24 h control
24 h VX-680
48 h control
48 h VX-680

Discussion:

Overexpression of PKCι in breast cancer has been reported previously by Kojima *et al*. (Kojima et al, 2008). Our findings are consistent with the results of this previous study, except that we observed PKCι overexpression in ductal carcinoma *in situ*. We also found that PKCι is overexpressed in lymph node metastases (76%), which were not assessed in the study by Kojima *et al*. The causes of increased PKCι expression in breast cancer have not been previously studied in detail. To address this, we evaluated PKCι expression in breast cancer cell lines. A subset of breast cancer cell lines also overexpressed PKCι and showed increased activation of this kinase. Both the overexpression and activation could be induced by mutant, constitutively-active *PIK3CA. PIK3CA* mutations are present in 25-30 % of breast cancers (Karakas et al, 2006). As we and others have observed overexpression of PKCι in 70-80% of breast cancers, additional factors are probably also able to drive this overexpression. Likely candidates are *PTEN* loss and Her2 activation, both of which also constitutively activate the PI 3-kinase pathway. This suggests that elevated PKCι levels might be a general marker of enhanced PI 3-kinase signalling in breast cancer cells. PKCι levels could therefore be a useful biomarker for identifying patients that benefit from therapeutics targeting this pathway, although clearly this requires further study. Increases in PKCι mRNA levels were not sufficient to explain the increases in PKCι protein levels (Supplementary Figure 1A). A likely explanation for the increase in PKCι protein levels is that phosphorylation stabilizes the enzyme, as has been shown for other members of the PKC family (Bornancin et al, 1996;Freeley et al, 2011).

The finding that *PIK3CA* mutations activate PKCι emphasizes the point made previously in the literature that while Akt is a major downstream mediator in the PI 3-kinase pathway, multiple other downstream signalling events are also important (Vanhaesebroeck et al, 2000). Recent data show that the activation of Akt downstream of mutant *PIK3CA* is not observed robustly in all cell types, further emphasizing the importance of additional downstream signalling events (Vasudevan et al, 2009). While both PKCι and PKB/Akt are activated by PI 3-kinase signalling there are potential differences in the details of their activation mechanism. Notably, the atypical PKCs, have an acidic amino acid in place of a serine in their hydrophobic motif region (Vanhaesebroeck and Alessi, 2000). In most other AGC kinases, including PKB/Akt, serine phosphorylation at this site by the mTORC2 complex primes the kinase for PI 3-kinase activation (Pearce et al, 2010). The presence of an acidic residue allows the atypical PKCs to constitutively associate with PDK1 (Balendran et al, 2000). In addition, this acidic residue should render the atypical PKCs resistant to the protein phosphatase PHLPP, which inactivates Akt by dephosphorylating its hydrophobic motif (Gao et al, 2005).

The consequences of increased PKCι in breast cancer have also not been previously studied in detail. We used RNA interference to deplete breast cancer cells of this enzyme. In agreement with our previous results in glioblastoma cells, and the results of others in breast cancer cells (Nolan et al, 2008), we found that PKCι depletion reduced the growth rate of breast cancer cells. As this was due to decreased proliferation rather than increased cell death, we investigated whether PKCι affected senescence in these cells. We found that PKCι depletion lead to increased numbers of

senescent cells. This was initially assessed using assays for SA-β-gal. The senescent phenotype of these cells was confirmed by their flattened morphology and their lack of BrdU incorporation. PKCι depletion promoted senescence in MCF7 and T47D breast cancer cells, both of which have *PIK3CA* mutations, but did not promote senescence in MDA-MB-231 cells which lack this mutation (Supplementary Figure 1B). We extended these findings, showing that PKCι depletion also promotes senescence in three different glioblastoma cells lines, in which the PI 3-kinase pathway is activated by *PTEN* loss rather than by *PIK3CA* mutation (Ishii et al, 1999).

PKCι depletion induced senescence in T47D cells, which have mutant p53 (O'Connor et al, 1997), and in MCF7 and U87MG cells, which are mutated at the INK4a/ARF locus (Herman et al, 1995;Ishii et al, 1999). Thus there is no absolute requirement for p53, p16 or ARF in the senescent pathway involved (although it is formally possible that they could enhance senescence via this pathway). Activation of a DNA damage response is a feature of replicative senescence and is also a feature of some forms of oncogene-induced senescence (Di Micco et al, 2006). We did not see any evidence for activation of the DNA damage response with PKCι depletion in either breast cancer or glioblastoma cells. Other groups have also described senescence that occurs in the absence of detectable DNA damage response pathway activation (Denoyelle et al, 2006;Lin et al, 2010). The lack of a requirement for p53 and p16, along with the absence of activation of a DNA damage response, suggest a novel mechanism for senescence induction upon PKCι depletion.

We have previously shown that depletion of PKCι results in defects in mitosis (Baldwin et al, 2010). A recent paper has described senescence activation in the

absence of DNA damage in mice that have cell cycle defects due to loss of Skp2 expression (Lin et al, 2010). Mice that are hypomorphic for the spindle checkpoint kinase Bub1 also show enhanced senescence (Baker et al, 2004). It therefore seems possible that there is a second mechanism for senescence induction that is triggered by mitosis defects and that is independent of activation of the DNA damage response pathway. Consistent with this hypothesis, we found that impairment of mitosis with the Aurora kinase inhibitor VX-680 also promotes senescence in both breast and brain cancer cells. Shorter VX-680 exposures sensitized glioblastoma cells to the effects of PKCι depletion on senescence, suggesting that PKCι depletion and VX-680 treatment induce senescence by related mechanisms. Also consistent with a related mechanism, both treatments induced senescence in the absence of a detectable DNA damage response.

Senescence induction with PKCι depletion was markedly dependent on the presence of the cell cycle regulatory protein p21. Many studies have demonstrated a role for p21 in promoting senescence, although often this has been as a consequence of its activation via the DNA damage response pathway and p53 (Schmitt, 2007). p21 has previously been shown to be a direct substrate for the atypical PKCs, which appear to inactivate p21 by phosphorylation at a serine residue in the carboxy terminus (Scott et al, 2002). This suggests a model for senescence induction by PKCι depletion in which decreased PKCι phosphorylation leads to p21 activation directly, without the need for p21 activation via the DNA damage response pathway and p53. Aurora kinase inhibition with VX-680 increased levels of p21, presumably by preventing its degradation at the initiation of mitosis. VX-680 treatment and PKCι depletion may

therefore cooperate to promote cancer cell senescence by simultaneously increasing p21 levels and p21 activation, respectively, in cancer cells attempting to initiate mitosis.

We did not observe any effects of PKCι depletion on senescence in two normal breast cancer cell lines, showing that depletion of PKCι induces cancer cell-specific reactivation of oncogene-induced senescence. Given the evidence that PI 3-kinase pathway activation may either promote or repress senescence, two possible models can be proposed. In the first model, PKCι could be mediating downstream anti-senescent activity of the PI 3-kinase pathway that prevents oncogene-induced senescence by a second oncogenic pathway. This model is suggested by the data from mouse models of melanoma, where PI 3-kinase pathway signalling appears to prevent oncogene-induced senescence driven by mutant *BRAF* (Dankort et al, 2009). In an alternate model, PKCι might attenuate oncogene-induced senescence driven by the PI 3-kinase pathway itself. This model is suggested by the pro-senescent effects of PTEN loss in mouse models of prostate cancer (Chen et al, 2005). We only observed senescence induction after PKCι depletion in cells with mutations in *PIK3CA* or with loss of *PTEN*. If the second model is correct, it provides a straightforward explanation as to why this phenomenon is apparently restricted to cells with these mutations.

In summary, we have identified a novel role for PKCι in repressing oncogene-induced senescence. PKCι fulfills this role in cells in which the PI 3-kinase pathway is activated by mutations in either *PIK3CA* or in *PTEN*. Inhibition of PKCι activated senescence in cancer cells by a mechanism that did not require activation of a DNA-damage response, but may instead be triggered by defects in the initiation of mitosis.

Materials and Methods:

Antibodies and inhibitors: PKCι mouse monoclonal and phospho-threonine 555 PKCι rabbit polyclonal antibodies were from BD Transduction Laboratories (Mississauga, ON, Canada) and Invitrogen (Carlsbad, CA, USA) respectively. The Akt goat polyclonal and pAKT (Ser473) rabbit polyclonal antibodies were from Santa Cruz Biotechnology (Santa Cruz, CA, USA) and Cell Signaling Technology (Danvers, MA, USA) respectively. GAPDH antibody was from AbCam (Cambridge, MA, USA). Antibodies to γH2AX (phospho-Histone H2A.X (Ser139)) were from Millipore (Billerica, MA, USA). Rabbit monoclonal antibody to p21 was from Cell Signalling Technology (Danvers, MA, USA). The mouse monoclonal actin antibody was purchased from Sigma-Aldrich Canada (Oakville, ON, Canada). All secondary antibodies were purchased from Jackson Immunoresearch Laboratories (West Grove, PA, USA). VX-680 was from Selleck Chemicals (Houston, TX, USA). Adriamycin was from the Ottawa Hospital Cancer Centre Pharmacy.

Cell Culture: MCF-10A, HTERT-HMEC, MDA-MB-231, MCF7, BT549,T47D, A172 and DBTRG cell lines were all purchased from ATCC. The human U87MG glioblastoma cell line was obtained from Dr. W. Cavenee (Ludwig Institute for Cancer Research, La Jolla, CA, USA). All cell lines were passaged for less than six months continuously and were routinely checked for mycoplasma contamination.

Expression constructs and retroviral transduction: The JP1520 vector was purchased from Harvard Institute of Proteomics (Boston, MA, USA). JP1520/*PIK3CA*, JP1520/E545K and JP1520/H1047R constructs were created by Isakoff SJ *et al*.(Isakoff et al, 2005), and purchased from Addgene (Addgene plasmids 14570, 14571, 14572).

Replication-incompetent retroviruses were made as described previously(Lorimer et al, 2000) and used to transduce MCF10A cells. All experiments were done using transduced populations of cells that were selected with 1μg/mL puromycin.

Immunohistochemistry: Tissue microarray slides were purchased from US Biomax Company (Maryland, USA). For PKCι staining, antigen retrieval was performed using sodium citrate pH 6 and microwave treatment. Primary mouse monoclonal PKCι antibody was used at a concentration of 10 μg/ml and was detected with the Envision Polymer Detection System (Dako, Mississauga, Canada). A scoring system from 0 to 3+ based on the intensity of cytoplasmic staining of tumour cells was used, with 3+ being the strongest staining. Scoring was performed independently by a general pathologist (MD) and a surgical oncologist (SA).

Western Blot Analysis: Western blots were performed as described previously (Baldwin, Garratt-Lalonde, Parolin, Krzyzanowski, Andrade, and Lorimer, 2006). Quantification of Western blots by densitometry was performed using the GeneGnome chemiluminescent system and Syngene software or the Alpha Innotech Fluorchem system and Alphaview software.

RNA interference: RNA duplexes with the following sense strand sequences were used to target PKCι: duplex A, 5'-GTGCATCAACTGCAAACTC-3'(Baldwin, Garratt-Lalonde, Parolin, Krzyzanowski, Andrade, and Lorimer, 2006); duplex C, 5'-CTTCCTGAAGAACATGCCA-3'(Xu et al, 2006); duplex E, 5'-GCCTGGATACAATTAACCATT-3'(Scotti et al, 2010). Sense strand sequences of RNA duplexes targeting p21 were; duplex B, 5'- GCCTTAGTCTCAGTTTGTGTG; duplex C, 5'-GATGGAACTTCGACTTTGT. All duplexes were purchased from Dharmacon (Lafayette, CO, USA).

SiGENOME Non-Targeting siRNA #2 and #3 from Dharmacon were used as controls. RNA transfections were done as described previously (Baldwin et al, 2006).

Proliferation assays: RNA transfections performed 24 h after plating cells. Viable cells were counted at the indicated times after transfection using a Vi-Cell XR cell counter (Beckman Coulter, Mississauga, Ontario).

SA-β-Gal Staining: Cells were plated on gelatin-coated coverslips in each well of a 6 well dish. 24 hrs later, transfection of RNA duplexes was performed as described above. Media was refreshed every 48 hours. At the indicated number of days after transfection, cells were fixed in 4% paraformaldehyde and assayed for SA-β-gal activity as described(Debacq-Chainiaux, Erusalimsky, Campisi, and Toussaint, 2009). Slides were analyzed using a Zeiss Axioskop 2 microscope. Total and SA-β-gal -positive cells were counted in a minimum of three separate fields for each condition.

Morphology: Slides were analyzed using a Nikon Eclipse TE 2000-U microscope using 20x magnification. Representative pictures were taken using a Coolpix MDC lens (Nikon) and Nikon 5400 digital camera.

BrdU incorporation: MCF7 and T47D cells were plated on gelatin-coated coverslips and transfected with RNA duplexes the following day. Media was refreshed every 48 hours. Six days after transfection, BrdU (Sigma) was added to fresh media on cells at a concentration of 10 μM. After two hours, cells were fixed with 70% ethanol. Incorporated BrdU was detected using BrdU mouse monoclonal antibody from Cell Signalling and AlexaFluor 555 goat anti-mouse antibody as the secondary antibody. Total and BrdU positive nuclei were counted under a Zeiss Axioplan 2 microscope. A minimum of 3 fields and 250 nuclei were counted for each condition.

Immunofluorescent staining for γH2AX: Cells on gelatin coated cover slips were fixed for 30 min with 4% paraformaldehyde and permeabilized for 10 min using 0.2% Triton X-100. After blocking in 5% normal goat serum in PBS, cells were incubated with anti-γH2AX antibody for 1 hr at a 1:800 dilution in 5% normal goat serum. This was followed with a 1 h incubation with AlexaFluor 555 goat anti-mouse secondary at 2μg/ml in 5% normal goat serum. A minimum of 100 cells over a minimum of 4 fields were counted and nuclei with 5 or more foci were considered positive, as proposed by Lawless et al, 2010.

Statistical analysis: Unless otherwise indicated, all values are represented as the average of three independent experiments, with error bars indicating standard error of the mean. Statistical significance was determined by a two tailed t-test. Values were considered significant when $P<0.05$.

Conflict of Interest: The authors declare no conflict of interest.

Acknowledgments: This work was supported by grants from the Canadian Institutes of Health Research and the Ottawa Regional Cancer Foundation (to IAJL). JP was supported by a Canadian Institutes of Health Research Banting and Best M.Sc. Scholarship. IR is supported by an Ontario Graduate Scholarship in Science and Technology. Thanks to Sharon Rowan and Mara Coiciu for their work on the initial characterization of PKCι activation in breast cancer cells.

References

Baker DJ, Jeganathan KB, Cameron JD, Thompson M, Juneja S, Kopecka A et al. (2004). BubR1 insufficiency causes early onset of aging-associated phenotypes and infertility in mice. *Nat Genet* **36**:744-749.

Baldwin RM, Barrett GM, Parolin DA, Gillies JK, Paget JA, Lavictoire SJ, et al. (2010). Coordination of glioblastoma cell motility by PKCiota. *Mol Cancer* **9**:233.

Baldwin RM, Garratt-Lalonde M, Parolin DA, Krzyzanowski PM, Andrade MA, and Lorimer IA (2006). Protection of glioblastoma cells from cisplatin cytotoxicity via protein kinase Ciota-mediated attenuation of p38 MAP kinase signaling. *Oncogene* **25**:2909-2919.

Baldwin RM, Parolin DA, and Lorimer IA (2008). Regulation of glioblastoma cell invasion by PKC iota and RhoB. *Oncogene* **27**:3587-3595.

Balendran A, Biondi RM, Cheung PC, Casamayor A, Deak M, and Alessi DR (2000). A 3-phosphoinositide-dependent protein kinase-1 (PDK1) docking site is required for the phosphorylation of protein kinase Czeta (PKCzeta) and PKC-related kinase 2 by PDK1. *J Biol Chem* **275**:20806-20813.

Barr AR and Gergely F (2007). Aurora-A: the maker and breaker of spindle poles. *J Cell Sci* **120**:2987-2996.

Bornancin F and Parker PJ (1996). Phosphorylation of threonine 638 critically controls the dephosphorylation and inactivation of protein kinase Calpha. *Curr Biol* **6**:1114-1123.

Carracedo A, Alimonti A, and Pandolfi PP (2011). PTEN level in tumor suppression: how much is too little? *Cancer Res* **71**:629-633.

Chen Z, Trotman LC, Shaffer D, Lin HK, Dotan ZA, Niki M, et al. (2005). Crucial role of p53-dependent cellular senescence in suppression of Pten-deficient tumorigenesis. *Nature* **436**:725-730.

Collado M, Medema RH, Garcia-Cao I, Dubuisson ML, Barradas M, Glassford J, et al. (2000). Inhibition of the phosphoinositide 3-kinase pathway induces a senescence-like arrest mediated by p27Kip1. *J Biol Chem* **275**:21960-21968.

Crowder RJ, Phommaly C, Tao Y, Hoog J, Luo J, Perou CM, et al. (2009). PIK3CA and PIK3CB inhibition produce synthetic lethality when combined with estrogen deprivation in estrogen receptor-positive breast cancer. *Cancer Res* **69**:3955-3962.

d'Adda dF, Reaper PM, Clay-Farrace L, Fiegler H, Carr P, von Zglinicki T, et al. (2003). A DNA damage checkpoint response in telomere-initiated senescence. *Nature* **426**:194-198.

Dankort D, Curley DP, Cartlidge RA, Nelson B, Karnezis AN, Damsky WE, Jr., et al. (2009). Braf(V600E) cooperates with Pten loss to induce metastatic melanoma. *Nat Genet* **41**:544-552.

Debacq-Chainiaux F, Erusalimsky JD, Campisi J, and Toussaint O (2009). Protocols to detect senescence-associated beta-galactosidase (SA-betagal) activity, a biomarker of senescent cells in culture and in vivo. *Nat Protoc* **4**:1798-1806.

Denoyelle C, Abou-Rjaily G, Bezrookove V, Verhaegen M, Johnson TM, Fullen DR, et al. (2006). Anti-oncogenic role of the endoplasmic reticulum differentially activated by mutations in the MAPK pathway. *Nat Cell Biol* **8**:1053-1063.

Di Micco R, Fumagalli M, Cicalese A, Piccinin S, Gasparini P, Luise C, et al. (2006). Oncogene-induced senescence is a DNA damage response triggered by DNA hyper-replication. *Nature* **444**:638-642.

Eder AM, Sui X, Rosen DG, Nolden LK, Cheng KW, Lahad JP, et al. (2005). Atypical PKCiota contributes to poor prognosis through loss of apical-basal polarity and cyclin E overexpression in ovarian cancer. *Proc Natl Acad Sci U S A* **102**:12519-12524.

Fields AP and Regala RP (2007). Protein kinase C iota: human oncogene, prognostic marker and therapeutic target. *Pharmacol Res* **55**:487-497.

Freeley M, Kelleher D, and Long A (2011). Regulation of Protein Kinase C function by phosphorylation on conserved and non-conserved sites. *Cell Signal* **23**:753-762.

Gao T, Furnari F, and Newton AC (2005). PHLPP: a phosphatase that directly dephosphorylates Akt, promotes apoptosis, and suppresses tumor growth. *Mol Cell* **18**:13-24.

Gewirtz DA, Holt SE, and Elmore LW (2008). Accelerated senescence: an emerging role in tumor cell response to chemotherapy and radiation. *Biochem Pharmacol* **76**:947-957.

Gorgun G, Calabrese E, Hideshima T, Ecsedy J, Perrone G, Mani M, et al. (2010). A novel Aurora-A kinase inhibitor MLN8237 induces cytotoxicity and cell-cycle arrest in multiple myeloma. *Blood* **115**:5202-5213.

Harrington EA, Bebbington D, Moore J, Rasmussen RK, Ajose-Adeogun AO, Nakayama T, et al. VX-680, a potent and selective small-molecule inhibitor of the Aurora kinases, suppresses tumor growth in vivo. *Nat Med* **10**:262-267.

Herman JG, Merlo A, Mao L, Lapidus RG, Issa JP, Davidson NE, et al. (1995). Inactivation of the CDKN2/p16/MTS1 gene is frequently associated with aberrant DNA methylation in all common human cancers. *Cancer Res* **55**:4525-4530.

Huck JJ, Zhang M, McDonald A, Bowman D, Hoar KM, Stringer B, et al. (2010). MLN8054, an inhibitor of Aurora A kinase, induces senescence in human tumor cells both in vitro and in vivo. *Mol Cancer Res* **8**:373-384.

Isakoff SJ, Engelman JA, Irie HY, Luo J, Brachmann SM, Pearline RV, et al. (2005). Breast cancer-associated PIK3CA mutations are oncogenic in mammary epithelial cells. *Cancer Res* **65**:10992-11000.

Ishii N, Maier D, Merlo A, Tada M, Sawamura Y, Diserens AC, Van Meir EG (1999). Frequent co-alterations of TP53, p16/CDKN2A, p14ARF, PTEN tumor suppressor genes in human glioma cell lines. *Brain Pathol* **9**:469-479.

Kanzaki M, Mora S, Hwang JB, Saltiel AR, and Pessin JE (2004). Atypical protein kinase C (PKCzeta/lambda) is a convergent downstream target of the insulin-stimulated phosphatidylinositol 3-kinase and TC10 signaling pathways. *J Cell Biol* **164**:279-290.

Karakas B, Bachman KE, and Park BH (2006). Mutation of the PIK3CA oncogene in human cancers. *Br J Cancer* **94**:455-459.

Kojima Y, Akimoto K, Nagashima Y, Ishiguro H, Shirai S, Chishima T, et al. (2008). The overexpression and altered localization of the atypical protein kinase C lambda/iota in breast cancer correlates with the pathologic type of these tumors. *Hum Pathol* **39**:824-831.

Lawless C, Wang C, Jurk D, Merz A, Zglinicki TV, and Passos JF (2010). Quantitative assessment of markers for cell senescence. *Exp Gerontol*. **45**:772-778.

Lin HK, Chen Z, Wang G, Nardella C, Lee SW, Chan CH, et al. (2010). Skp2 targeting suppresses tumorigenesis by Arf-p53-independent cellular senescence. *Nature* **464**:374-379.

Lorimer IA and Lavictoire SJ (2000). Targeting retrovirus to cancer cells expressing a mutant EGF receptor by insertion of a single chain antibody variable domain in the envelope glycoprotein receptor binding lobe. *J Immunol Methods* **237**:147-157.

Michaloglou C, Vredeveld LC, Soengas MS, Denoyelle C, Kuilman T, van der Horst CM, et al. (2005). BRAFE600-associated senescence-like cell cycle arrest of human naevi. *Nature* **436**:720-724.

Nolan ME, Aranda V, Lee S, Lakshmi B, Basu S, Allred DC, and Muthuswamy SK (2008). The polarity protein Par6 induces cell proliferation and is overexpressed in breast cancer. *Cancer Res* **68**:8201-8209.

O'Connor PM, Jackman J, Bae I, Myers TG, Fan S, Mutoh M, et al. (1997). Characterization of the p53 tumor suppressor pathway in cell lines of the National Cancer Institute anticancer drug screen and correlations with the growth-inhibitory potency of 123 anticancer agents. *Cancer Res* **57**:4285-4300.

Passos JF, Nelson G, Wang C, Richter T, Simillion C, Proctor CJ, et al. (2010). Feedback between p21 and reactive oxygen production is necessary for cell senescence. *Mol Syst Biol* **6**:347.

Pearce LR, Komander D, and Alessi DR (2010). The nuts and bolts of AGC protein kinases. *Nat Rev Mol Cell Biol* **11**:9-22.

Peifer C and Alessi DR (2008). Small-molecule inhibitors of PDK1. *Chem Med Chem* **3**:1810-1838.

Pollock PM, Harper UL, Hansen KS, Yudt LM, Stark M, Robbins CM, et al. (2003). High frequency of BRAF mutations in nevi. *Nat Genet* **33**:19-20.

Regala RP, Weems C, Jamieson L, Khoor A, Edell ES, Lohse CM, Fields AP (2005). Atypical protein kinase C iota is an oncogene in human non-small cell lung cancer. *Cancer Res* **65**:8905-8911.

Schmitt CA (2007). Cellular senescence and cancer treatment. *Biochim Biophys Acta* **1775**:5-20.

Scott MT, Ingram A, and Ball KL (2002). PDK1-dependent activation of atypical PKC leads to degradation of the p21 tumour modifier protein. *EMBO J* **21**:6771-6780.

Scotti ML, Bamlet WR, Smyrk TC, Fields AP, and Murray NR (2010). Protein kinase Ciota is required for pancreatic cancer cell transformed growth and tumorigenesis. *Cancer Res* **70**:2064-2074.

Vanhaesebroeck B and Alessi DR (2000). The PI3K-PDK1 connection: more than just a road to PKB. *Biochem J* **346**:561-576.

Vasudevan KM, Barbie DA, Davies MA, Rabinovsky R, McNear CJ, Kim JJ, et al. (2009). AKT-independent signaling downstream of oncogenic PIK3CA mutations in human cancer. *Cancer Cell* **16**:21-32.

Ventura A, Kirsch DG, McLaughlin ME, Tuveson DA, Grimm J, Lintault L, et al. (2007). Restoration of p53 function leads to tumour regression in vivo. *Nature 445*:661-665.

Wu CH, van Riggelen J, Yetil A, Fan AC, Bachireddy P, Felsher DW (2007). Cellular senescence is an important mechanism of tumor regression upon c-Myc inactivation. *Proc Natl Acad Sci U S A* **104**:13028-13033.

Xu L and Deng X (2006). Protein kinase Ciota promotes nicotine-induced migration and invasion of cancer cells via phosphorylation of micro- and m-calpains. *J Biol Chem* **281**:4457-4466.

Yuan TL, Wulf G, Burga L, and Cantley LC (2011). Cell-to-cell variability in PI3K protein level regulates PI3K-AKT pathway activity in cell populations. *Curr Biol* **21**:173-183.

Zhang L, Huang J, Yang N, Liang S, Barchetti A, Giannakakis A, et al. (2006). Integrative genomic analysis of protein kinase C (PKC) family identifies PKCiota as a biomarker and potential oncogene in ovarian carcinoma. *Cancer Res* **66**:4627-4635.

	0	+1	+2	+3	total	p value vs hyperplasia
Hyperplasia	6	5	3	1	15	
DCIS	0	3	3	6	12	0.001
IDC	2	25	38	16	81	0.0001
LNM	2	10	17	20	49	0.00003

Supplementary Table 1. Scoring of PKCι immunohistochemistry. The number of cases that scored either 0, +1, +2 or +3 for hyperplasia, ductal carcinoma insitu (DCIS), invasive ductal carcinoma (IDC) and breast cancer lymph node metastases (LNM) are shown, along with p values for comparisons with hyperplasia scores.

Supplementary Figure 1: A. RT-PCR analysis of PKCι mRNA levels. Total RNA was isolated from MCF10A, MCF10A-H1047R and MCF10A-E545K cell lines using RNEasy Plus Mini Kits (Qiagen Inc., Mississauga, ON, Canada). cDNA from each cell type was synthesized from 1.0ug total RNA using Qiagen Quantitect RT Kits. qPCR was performed to amplify PKCι cDNA and PUM1 cDNA (used as a reference) using the Rotor-Gene SYBR Green PCR Kit and a Roche LightCycler thermocycler. PKCι primers were: 5' GTC CGG GTG AAA GCC TAC TAC 3' and 5' ACG GGT CTC CTT CCT CAT CT 3'. PUM1 primers were: 5'TGA GGT GTG CAC CAT GAA C 3' and 5' CAG AAT GTG CTT GCC ATA GGG 3'. Standard curves were created for both PKCι and PUM1using RNA from MCF10A cells and used to determine relative amounts of PKCι and PUM1 mRNAs. Data shown are means ± SE from three independent experiments. **B.** MCF7 and MDA-MB-231 cells were either mock-transfected, transfected with a control RNA duplex, or transfected with two different RNA duplexes targeting PKCι. Six days after transfection, cells were stained for SA-βGal activity. Percentages of SA-βGal positive cells were determined as described in Materials and Methods. No basal or induced SA-βGal activity was detected in MDA-MB-231 cells. Shown is a representative example from three independent experiments.

A.

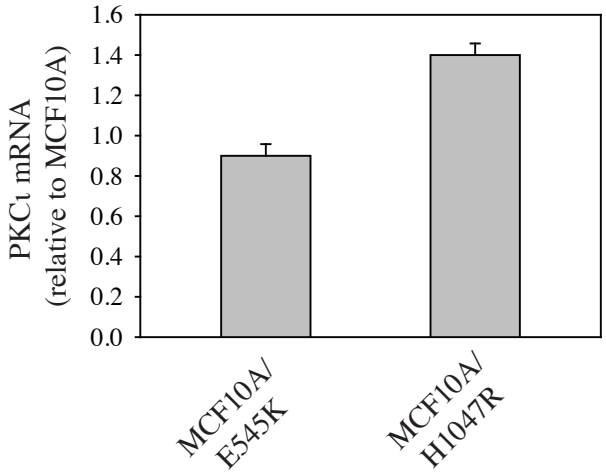
PKCι mRNA
(relative to MCF10A)
1.6
1.4
1.2
1.0
0.8
0.6
0.4
0.2
0.0
MCF10A/
E545K
MCF10A/
H1047R

B.

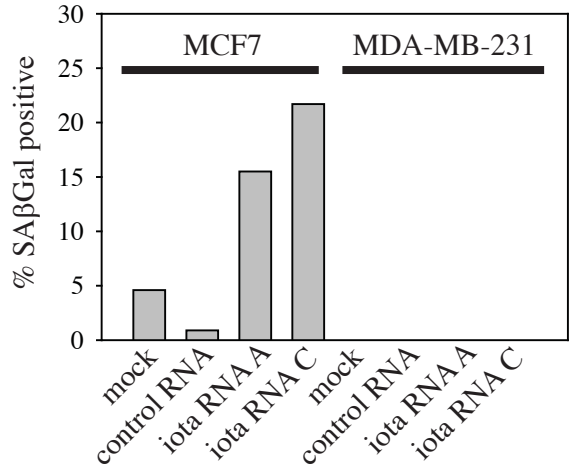
% SAβGal positive
30
25
20
15
10
5
0
MCF7
MDA-MB-231
mock
control RNA
iota RNA A
iota RNA C
mock
control RNA
iota RNA A
iota RNA C

4. PKCι DEPLETION INITIATES MITOTIC SLIPPAGE-INDUCED SENESCENCE IN GLIOBLASTOMA

Ian J Restall[1,2], Doris A E Parolin[1], Manijeh Daneshmand[1], Jennifer E L Hanson[1], Sylvie J Lavictoire[1], and Ian A J Lorimer[1,2,3]

[1]Centre for Cancer Therapeutics, Ottawa Hospital Research Institute;
[2]Department of Biochemistry, Microbiology and Immunology, University of Ottawa, Ottawa, Ontario, Canada
[3]Department of Medicine, University of Ottawa, Ottawa, Ontario, Canada

Address correspondence to: Ian A. J. Lorimer, Ottawa Hospital Regional Cancer Centre, Centre for Cancer Therapeutics

Running Title: PKCι depletion initiates mitotic slippage-induced senescence

Contribution of Authors

The content of this manuscript was written by I.J. Restall with minor edits from Dr. I.A.J. Lorimer. All of the experiments presented in this manuscript are the work of I.J. Restall done with the assistance of D.A.E. Parolin with the exception of Figures 7, 8, and 9. Experiments in Figure 8 were done with the assistance of M. Daneshmand. Experiments in Figures 7, 8, and 9 were done with the assistance of J.E.L. Hanson.

In preparation for submission

Abstract

Cellular senescence is a tumor suppressor mechanism where cells enter a permanent growth arrest following cellular stress. Oncogene-induced senescence (OIS) is induced in normal cells following the expression of an oncogene or repression of a tumor suppressor. Previously, we have show that PKCι depletion induces premature senescence in glioblastoma cells. In this study, we showed that senescent glioblastoma cells have aberrant centrosomes. This was observed in basal levels of senescence, in p21-induced senescence, and in PKCι depletion-induced senescence. Senescent glioblastoma cells were also Ki-67 negative, polyploid and were arrested at the G1/S checkpoint. These markers are consistent with cells that have undergone mitotic slippage. Mitotic slippage occurs when mitotic cells do not satisfy the spindle assembly checkpoint (SAC) and eventually exit mitosis into the G1 phase of the cell cycle. Although in G1, these cells have the replicated DNA and centrosome content of a cell that has entered mitosis and failed to divide. PKCι was also depleted in established glioblastoma xenograft tumors using a doxycycline-inducible shRNA. After 14 days on a doxycycline diet, glioblastoma tumors depleted of PKCι had decreased staining for the proliferation marker Ki-67 and a trend towards increased SAβGal staining. With a longer-term depletion of PKCι, established glioblastoma xenografts in mice had a decrease in tumor growth and improved survival. We conclude that PKCι initiates mitotic slippage-induced senescence in glioblastoma cells. Moreover, PKCι depletion in established glioblastoma xenografts decreased tumor growth and provided further evidence for the targeting of PKCι in cancer.

Introduction

Cellular senescence is induced as a response to sustained cellular stress. The major consequence of cellular senescence is the permanent cessation of cell proliferation. Replicative senescence of cultured primary human fibroblasts was first described in 1961 by Hayflick and Moorhead (Hayflick and Moorhead, 1961). The observation of replicative senescence was the first demonstration that normal fibroblasts had a limited replicative potential in culture. These senescent cells developed an enlarged spread out morphology and abnormally large interphase nuclei. Nearly three decades later the mechanism behind replicative senescence was experimentally shown to be due to the gradual shortening of telomere ends during cell division (Harley et al., 1990). The ability to override the shortening of telomeres and continue to divide is an essential hallmark of cancer (Hanahan and Weinberg, 2011). This depicts replicative senescence as a tumor suppressor mechanism that limits the immortalization of cancer cells. Oncogene-induced senescence (OIS) is a form of premature senescence that is driven by the expression of an oncogene in an otherwise normal cell and has also been termed a tumor suppressor mechanism. Serrano *et al* first described this form of cellular senescence as the mechanism behind the inability of oncogenic Ras expression to transform otherwise normal human diploid fibroblasts (Serrano et al., 1997). Senescent cells are present in premalignant tissue but lost in malignant tumors in mouse models of lung cancer and melanoma (Collado et al., 2005; Dankort et al., 2007; Dhomen et al., 2009). Additionally, OIS has been observed in association with oncogenic events in human biopsies of premalignant dermal neurofibroma and melanocytic nevi (Courtois-Cox et al., 2006; Michaloglou et al., 2005).

Both replicative senescence and OIS are potent tumor suppressor mechanisms.

An exciting area of senescence research involves the induction, or re-activation, of senescence in tissue that has already reached malignancy. This has been shown in mice where the p53 tumor suppressor was re-activated in established sarcomas and tumor regression was observed following the induction of senescence but not apoptosis (Ventura et al., 2007; Xue et al., 2007). Our laboratory has previously shown that knockdown of protein kinase C iota (PKCι) in human breast cancer and glioblastoma multiforme cell lines re-activates premature senescence (Paget et al., 2011). Treatment with chemotherapeutics or irradiation also induces premature senescence in a variety of human cancer cell lines (Gewirtz et al., 2008). Furthermore, the induction of premature senescence has been observed in human malignant tissue in the clinic following treatment with chemotherapeutics (Roberson et al., 2005; te Poele et al., 2002). Induction of premature senescence as an outcome following the treatment of malignant tissue is an area of great interest.

Sustained cellular stress and an inability to progress through the cell cycle is a major driver of premature senescence. The spindle assembly checkpoint (SAC) is responsible for ensuring the proper attachment of microtubules to the kinetochores of all chromosomes (Foley and Kapoor, 2012). When the SAC is not satisfied it inhibits the activity of the anaphase promoting complex/cyclosome (APC/C) E3 ubiquitin ligase and interrupts the progression to anaphase. An inability to progress through the SAC does not result in a permanent arrest in metaphase. Following an extended period of arrest by the SAC, a slow degradation of cyclin B eventually results in the early exit from mitosis (Brito and Rieder, 2006). The degradation of cyclin B is due to the residual

activity of the APC/C and results in mitotic slippage (Lee et al., 2010). Cells that undergo mitotic slippage exit into interphase and result in a tetraploid G1 cell with double the expected number of centrosomes (Rieder and Maiato, 2004; Schneider et al., 2007).

Glioblastoma multiforme (GBM) is the most common and most aggressive adult primary malignant brain tumor. The invasive nature and frequent relapse of GBM contribute to its poor prognosis. The current therapy of surgery followed by radiotherapy and temozolomide treatment results in an average survival of only 12-14 months (Kanu et al., 2009; Stupp et al., 2005). There is therefore a necessity for the development of novel therapeutic strategies.

An integrative analysis of the core pathways of GBM, performed by The Cancer Genome Atlas Research Network, has provided an important overview of the genetic alterations in GBM (Cancer Genome Atlas Research, 2008). The phosphoinositide 3-kinase (PI3K) pathway is frequently activated in cancer. In GBM, 36% of samples had a mutation in or homozygous deletion of PTEN and 86% of samples had at least one genetic alteration in the PI3K pathway (Cancer Genome Atlas Research, 2008). Activation of the PI3K pathway results in 3-phosphoinositide dependent protein kinase-1 (PDK1) mediated phosphorylation and activation of the AGC kinases. The atypical protein kinase C family members PKCι and PKCζ are one subgroup of kinases activated by PDK1 (Chou et al., 1998; Le Good et al., 1998). PKCι was the first member of the PKC family to be classified as an oncogene (Regala et al., 2005). Furthering its role in cancer, elevated levels of PKCι have been detected in many tumor types and in multiple tumors high PKCι levels predicted poor survival (Murray et al., 2011).

PKCι has important roles in the malignant phenotype of GBM. Previously, we have demonstrated that in GBM cells PKCι: represses cisplatin-induced apoptosis; is necessary for invasion and motility; co-ordinates leading edge lamellipod formation; and is necessary for the progression through mitosis (Baldwin et al., 2010; Baldwin et al., 2006; Baldwin et al., 2008). We then expanded on the observed importance of PKCι in mitosis and demonstrated that knockdown of PKCι in GBM cell lines induces premature senescence (Paget et al., 2011). The premature senescence induced by PKCι depletion was independent of a DNA-damage response and was dependent on p21. This current study shows that senescent GBM cells in culture and following the overexpression of p21 have aberrant centrosomes, an increase in ploidy, and arrest in the G1 phase of the cell cycle. These are all properties of having undergone mitotic slippage. Senescence induced by depletion of PKCι also shows markers of mitotic slippage. In established GBM tumor xenografts, PKCι depletion results in decreased cell proliferation and tumor growth.

Results

Senescent glioblastoma cells have aberrant centrosomes.

A basal level of senescence is observed in untreated cultured cell lines. As reported previously, SAβGal staining showed that the U87MG, A172 and DBTRG glioblastoma cell lines have basal senescence levels of approximately 2%, 3%, and 11% respectively (Paget et al., 2011). In this study, aberrant centrosomes were identified as either supernumerary centrosomes (more than two centrosomes) or as having two clearly separated centrosomes in a cell with an uncondensed interphase nuclear morphology. Normal cells were defined as having a single average size nucleus, normal cytoplasmic size, and being negative for SAβGal stain. Senescent cells were defined as having a single enlarged nucleus, enlarged cytoplasm, and staining positive for SAβGal. Senescent U87MG cells had an aberrant centrosome phenotype, as detected by immunofluorescence of γ-tubulin (Figure 1A). Almost all normal U87MG cells in culture had two attached centrosomes, whereas the majority of senescent U87MG cells had more than two and as many as twelve centrosomes (Figure 1B). The U87MG, A172 and DBTRG glioblastoma cell lines all showed a marked increase in centrosome aberrations in senescent cells when compared to normal cells (Figure 1C).

p21-induced senescent glioblastoma cells have aberrant centrosomes.

U87MG and A172 cells that are senescent after p21 overexpression also show centrosome aberrations (Figure 2A, Supp. Figure 1A). When compared to cells that have a normal cell phenotype, senescent U87MG and A172 cells in the p21 overexpressing population have a greater number of centrosome aberrations (Figure 2B). Overexpression of p21 in these cells resulted in approximately 60% SAβGal

Figure 1. Senescent glioblastoma cells have aberrant centrosomes. A. Representative images of untreated normal and senescent cells. Centrosomes stained by immunofluorescent staining for γ-tubulin (1:800, white) and nuclei stained with DAPI (blue), inset is a magnification of the centrosomes. To the right is the brightfield grayscale image of the cells showing the presence or absence of SAβGal stain. Normal cells are characterized by a single nucleus of average size, a typical cytoplasmic size and are negative for SAβGal stain. Senescent cells are characterized by a single enlarged nucleus, increased cytoplasmic size and are positive for SAβGal stain. **B.** A histogram showing the centrosome number in normal and senescent U87MG cells. A minimum of 50 cells normal and senescent cells were counted following immunofluorescent staining for γ-tubulin. **C.** Percent of normal and senescent cells with aberrant centrosomes in three glioblastoma cell lines (U87MG, A172, DBTRG). Centrosomes were classified as aberrant if either supernumerary or separated in an interphase cell. Minimum of 50 cells counted per condition and per cell type.

A.

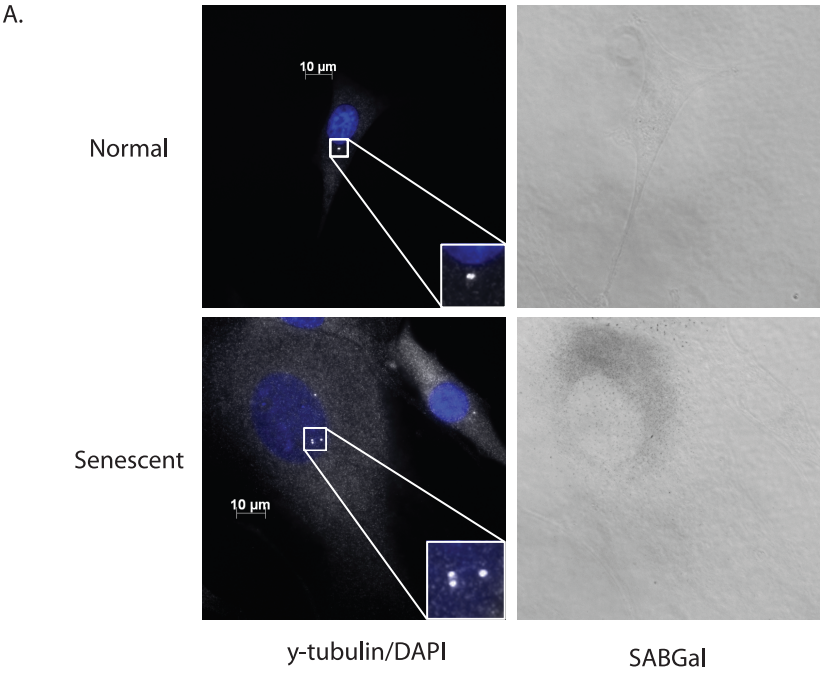
Normal
Senescent
10 µm
10 µm
y-tubulin/DAPI
SABGal

B.

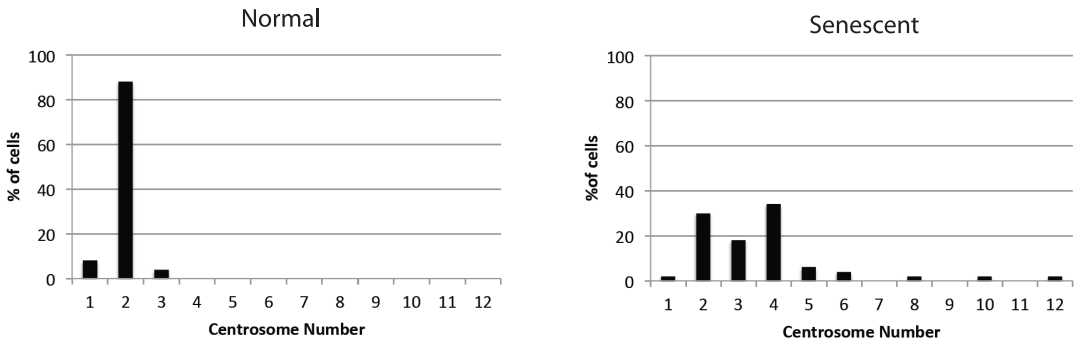
Normal
% of cells
Centrosome Number
Senescent
%of cells
Centrosome Number

C.

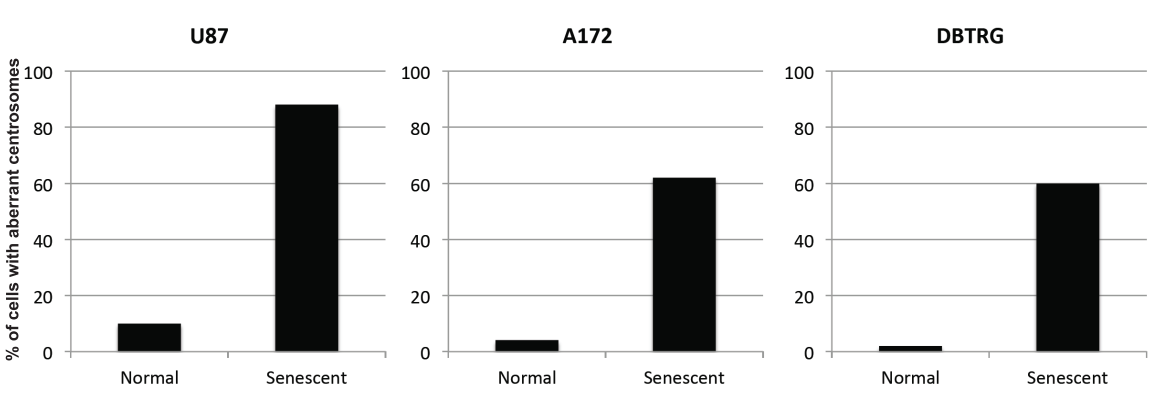
U87
A172
DBTRG
% of cells with aberrant centrosomes
Normal
Senescent

Figure 2. p21-induced senescent glioblastoma cells have aberrant centrosomes. A. Representative images of p21-induced senescent U87MG and A172 glioblastoma cells after overexpression of p21. Cells underwent immunofluorescence staining for γ-tubulin (white). Nuclei were stained with DAPI (blue) and a brightfield grayscale image of SAβGal stain is included to the right. Cells were transduced with a p21 lentivirus overnight, washed and fixed for staining four days later (five days after transduction). Inset is a magnification of the centrosomes. **B.** Quantification of normal and senescent (same criteria used in Figure 1) glioblastoma cells (U87MG, A172) with aberrant centrosomes after overexpression of p21.

A.

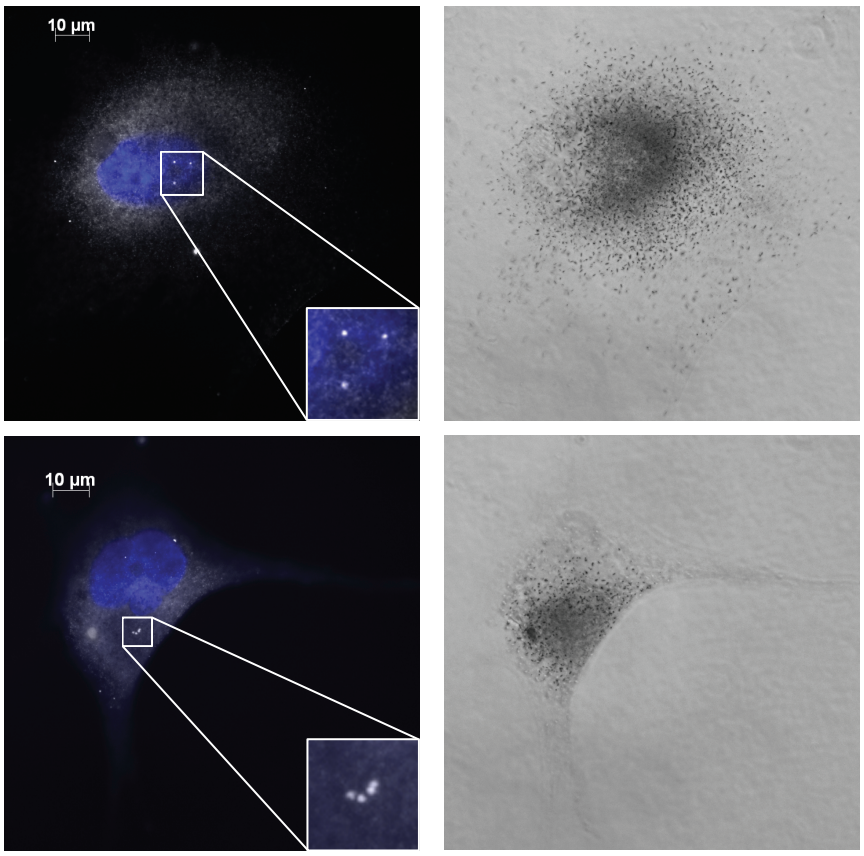
10 µm
10 µm
U87MG
A172
y-tubulin/DAPI
SABGal

B.

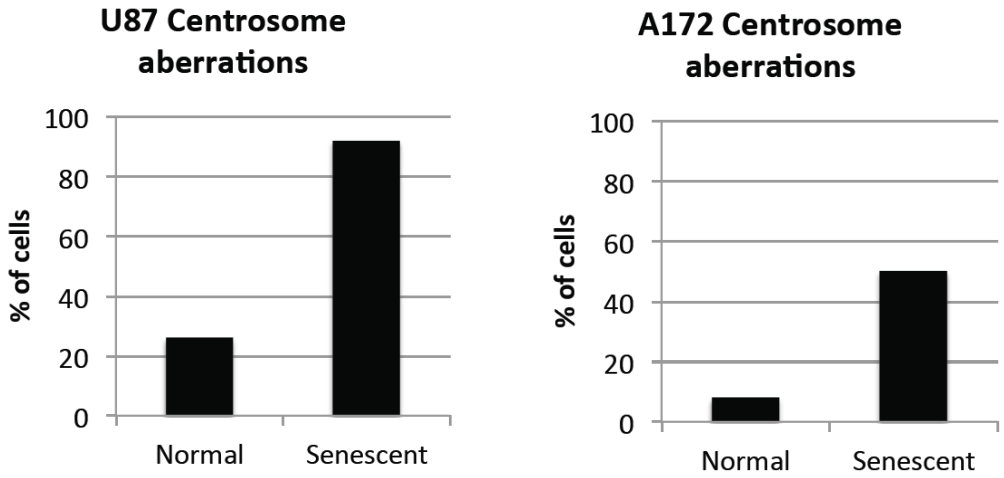
U87 Centrosome aberrations
% of cells
100
80
60
40
20
0
Normal
Senescent
A172 Centrosome aberrations
% of cells
100
80
60
40
20
0
Normal
Senescent

positive cells, whereas mock transduced cells were approximately 2% SAβGal positive (Suppl. Figure 1B). Therefore, basal senescence and p21-induced senescence both show centrosome aberrations.

Senescent U87MG cells are polyploid.

After mitotic slippage occurs there is an irregular DNA content within the cell. Chromogenic *in situ* hybridization labeling of the centromere of chromosome 7 demonstrated that senescent U87MG cells, based on an enlarged nucleus and cytoplasm, are polyploid when compared to cells with a normal cell morphology (Figure 3A). U87MG cells with a normal cell morphology predominantly had three signals of the chromosome 7 centromere, whereas the majority of senescent cells had 6 copies (Figure 3B). This suggests that the enlarged nuclear morphology associated with senescence is due to an increase in cell ploidy.

Cyclin expression in senescent glioblastoma cells.

Cells that have failed to progress through mitosis and have slipped into the G1 phase of the cell cycle will arrest at the G1/S checkpoint. Normal U87MG cells have increasingly higher levels of Cyclin B1 in the G2 phase of the cell cycle, peaking during metaphase (Figure 4A, left). Senescent U87MG cells in culture, based on a large flattened morphology, do not have high levels of Cyclin B1, suggesting that they are not arrested at the G2/M checkpoint (Figure 4A, right). Senescent U87MG cells, based on an enlarged morphology and positive staining for SAβGal, are negative for the proliferation marker Ki-67 and stain positive for Cyclin E (Figure 4B). This demonstrates that senescent U87MG cells are arrested at the G1/S checkpoint, where Cyclin E levels are at the highest point in the cell cycle.

Figure 3. Senescent U87MG cells are polyploid. A. Chromogenic in situ hybridization (CISH) using a probe for the centromere of chromosome 7. Representative images of normal and senescent (by morphology) U87MG cells. Senescent cells are shown at ½ the scale to be able to show the entire cells. **B.** Quantification of CISH staining in U87MG cells (n=30).

A.

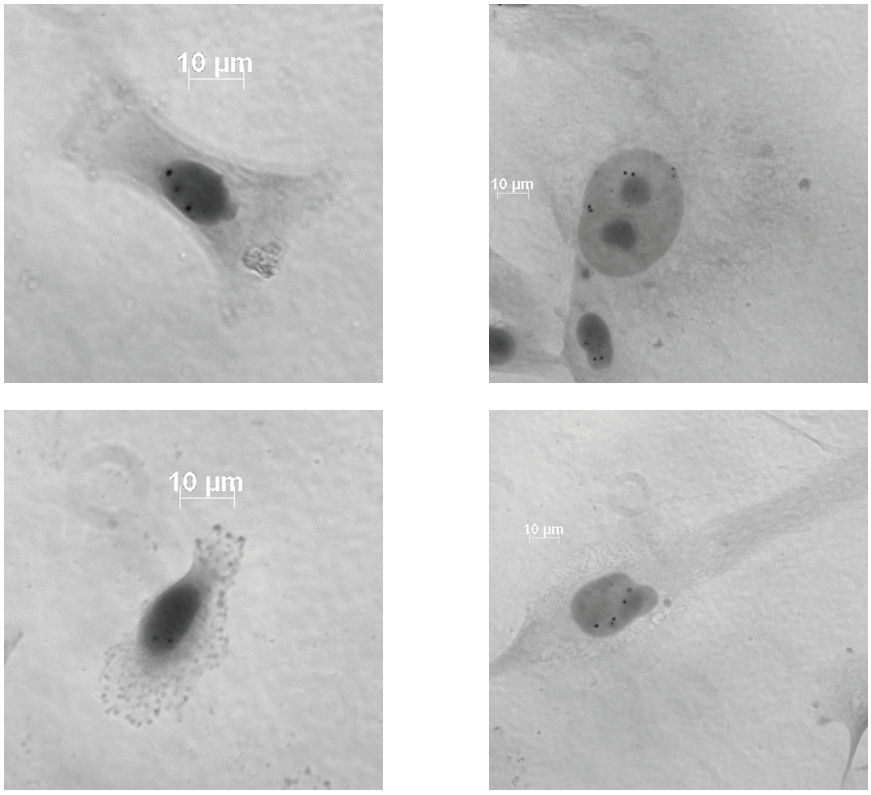

Normal U87

Senescent U87
(1/2 scale)

B.

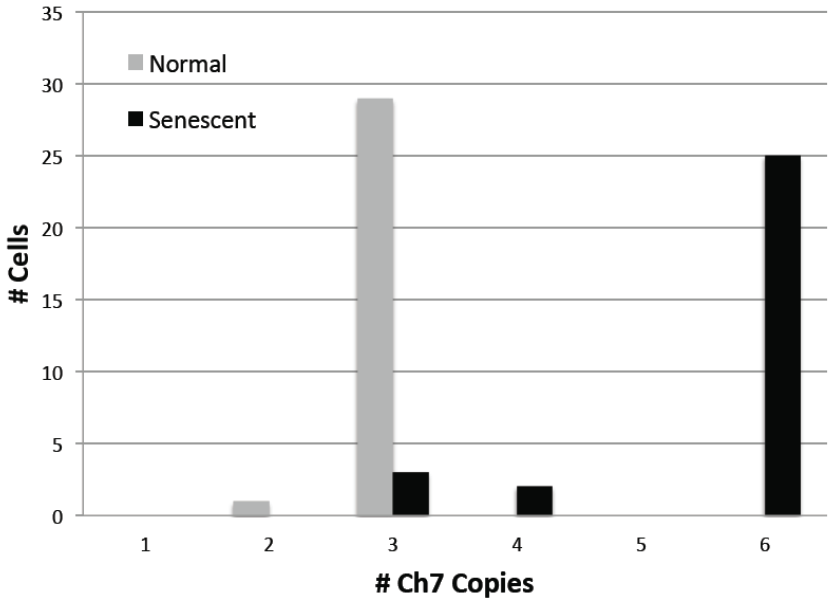

Figure 4. Cyclin expression in senescent glioblastoma cells. A. Representative images of untreated normal and senescent (by morphology) U87MG cells. Immunofluorescence staining of Cyclin B1 (red) and nuclei are stained with DAPI (blue). Senescent cell of interest is shown using an arrow and the normal cell of interest is shown using an asterisk **B.** Immunofluorescence staining of Cyclin E (red) and Ki-67 (green) in an untreated U87MG normal and senescent cell. Nuclei are stained with DAPI (blue) and a brightfield grayscale image of SAβGal is on the far right.

A.

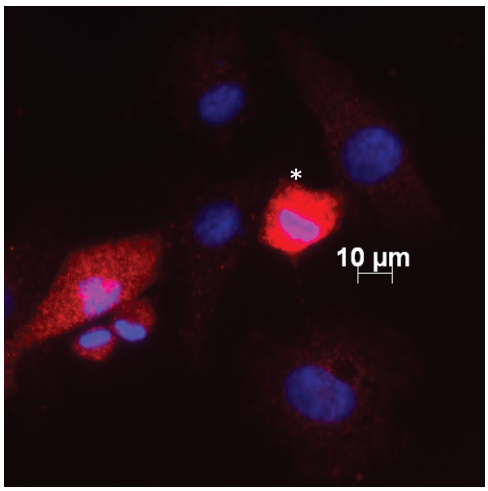

Cyclin B1/DAPI

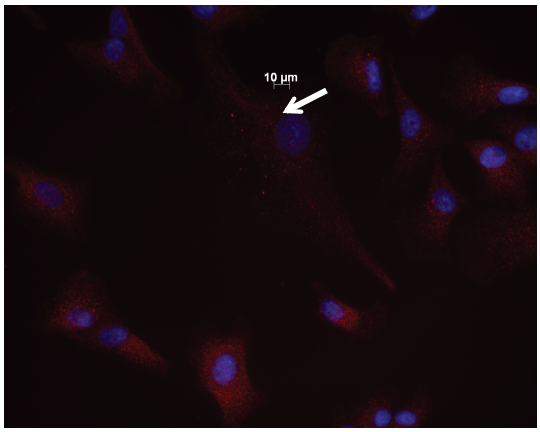

Cyclin B1/DAPI

B.

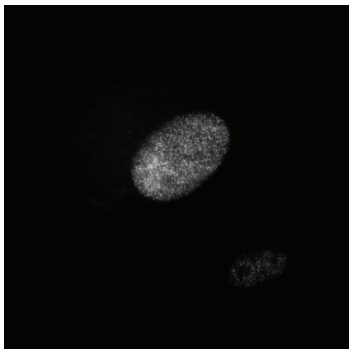

Cyclin E

Ki-67

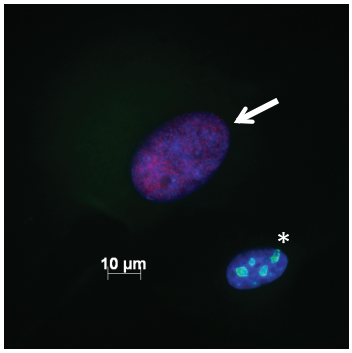

Cyclin E/Ki-67/DAPI

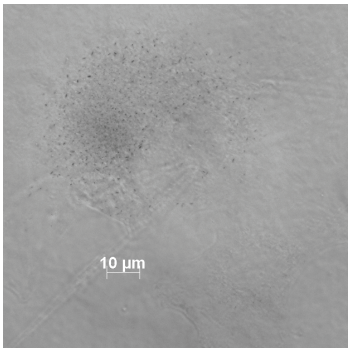

SABGal

PKCι depletion-induced senescence shows markers of mitotic slippage

As previously shown, siRNA targeting PKCι increases cellular senescence in glioblastoma cell lines (Paget et al., 2011). This was replicated in the cell populations used in this experiment to assess markers of mitotic slippage in U87MG cells following PKCι knockdown (Figure 5A). Counting senescent U87MG cells, by morphology and SAβGal positive staining, there is an increased incidence of centrosome aberrations when compared to cells with a normal phenotype. Aberrant centrosomes are observed in senescent cells at a similar frequency in PKCι depleted and control cells (Figure 5B). This demonstrates that the basal level of senescence in culture and PKCι depletion-induced senescence both involve centrosome aberrations, similar to p21-induced senescence. Both control and PKCι depleted senescent cells are also positive for cyclin E (Figure 5C) and negative for Ki-67 (Figure 5D). Following siRNA knockdown of PKCι, counting the whole population of U87MG cells showed an increase in ploidy, shown by CISH staining of chromosome 7 centromeres (Figure 5E). After PKCι depletion, the percent of cells with an increase in ploidy (Figure 5E) was similar to percent of cells that were SAβGal positive in Figure 5A. Similar properties between the basal senescence in the control RNA cells and the PKCι knockdown cells suggest that senescence is occurring by a similar mechanism. Representative immunofluorescence images of senescent U87MG cells, following PKCι depletion by siRNA iota A, have markers of mitotic slippage (Figure 6). A senescent U87MG cell, by morphology and SAβGal positivity, with supernumerary centrosomes is shown near U87MG cells with a normal phenotype and normal centrosome number (Figure 6A). Senescent U87MG cells are also positive for cyclin E and negative for cyclin B1, demonstrating a cell cycle

Figure 5. PKCι depletion-induced senescence shows markers of mitotic slippage. U87MG cells were either mock transfected, transfected with control siRNA (control RNA), or siRNA targeting PKCι (RNA iota A and RNA iota E). After 48hr of siRNA, cells were washed and grown for another 3 days in regular media, followed by fixation and staining. **A.** Quantification of the percent of SAβGal positive staining of all U87MG cells in the two experiments used for counting. A minimum of 100 cells in 3 fields were counted in 2 separate experiments. **B.** Quantification of senescent (same criteria as Figure 1) U87MG cells showing aberrant or normal centrosome morphology. Minimum of 30 cells counted for each condition. **C.** Quantification of senescent U87MG cells that are positive or negative for Cyclin E. Minimum of 30 cells counted for each condition. **D.** Quantification of senescent U87MG cells that are positive or negative for Ki-67. Minimum of 40 cells counted for each condition. **E.** CISH staining using a probe for the centromere of chromosome 7 of all U87MG cells 5 days after siRNA targeting PKCι. Minimum of 100 cells counted for each condition in 3 separate experiments. *P<0.05 using two tailed t-test compared to control RNA.

A.

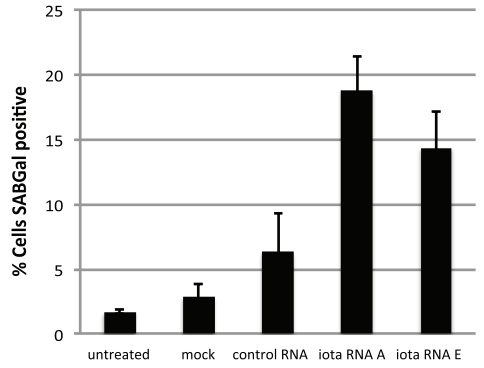
% Cells SABGal positive
25
20
15
10
5
0
untreated
mock
control RNA
iota RNA A
iota RNA E

B.

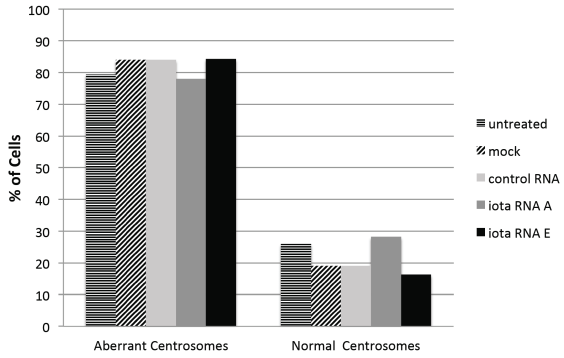
% of Cells
100
90
80
70
60
50
40
30
20
10
0
Aberrant Centrosomes
Normal Centrosomes
untreated
mock
control RNA
iota RNA A
iota RNA E

C.

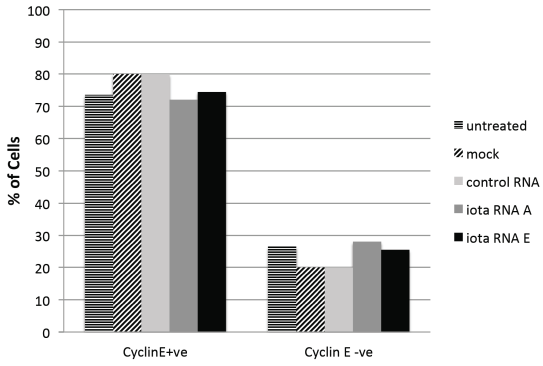
% of Cells
100
90
80
70
60
50
40
30
20
10
0
CyclinE+ve
Cyclin E -ve
untreated
mock
control RNA
iota RNA A
iota RNA E

D.

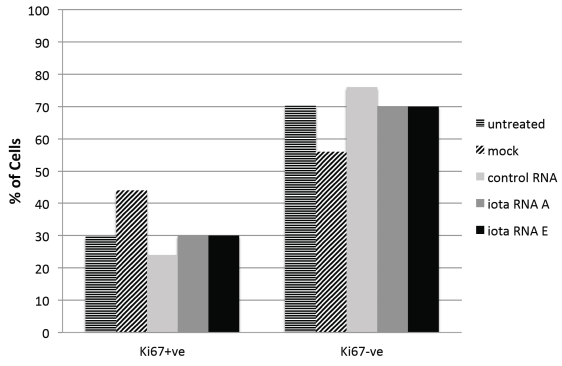
% of Cells
100
90
80
70
60
50
40
30
20
10
0
Ki67+ve
Ki67-ve
untreated
mock
control RNA
iota RNA A
iota RNA E

E.

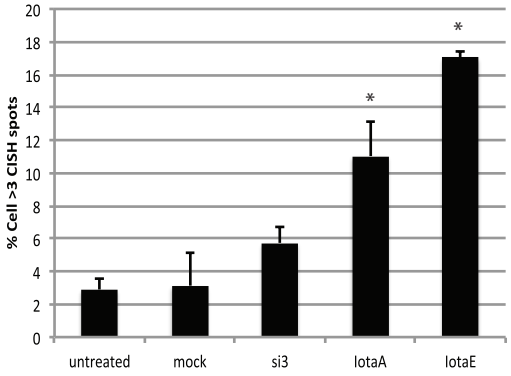
% Cell >3 CISH spots
20
18
16
14
12
10
8
6
4
2
0
*
*
untreated
mock
si3
IotaA
IotaE

Figure 6. Markers of mitotic slippage in senescent U87MG cells after PKCι depletion. Representative immunofluorescence images of senescent U87MG cells 5 days after siRNA iota A treatment. **A.** Top left, phase contrast; top right, SAβGal staining (grayscale); bottom left, DAPI; bottom right, γ-tubulin staining centrosomes. Inset is a magnification of the centrosomes. **B.** Top left, phase contrast; top right, SAβGal staining (grayscale); bottom left, DAPI; bottom right, cyclin E. **C.** Top left, phase contrast; top right, SAβGal staining (grayscale); bottom left, DAPI; bottom right, cyclin B1. **D.** Top left, phase contrast; top right, SAβGal staining (grayscale); bottom left, DAPI; bottom right, Ki67.

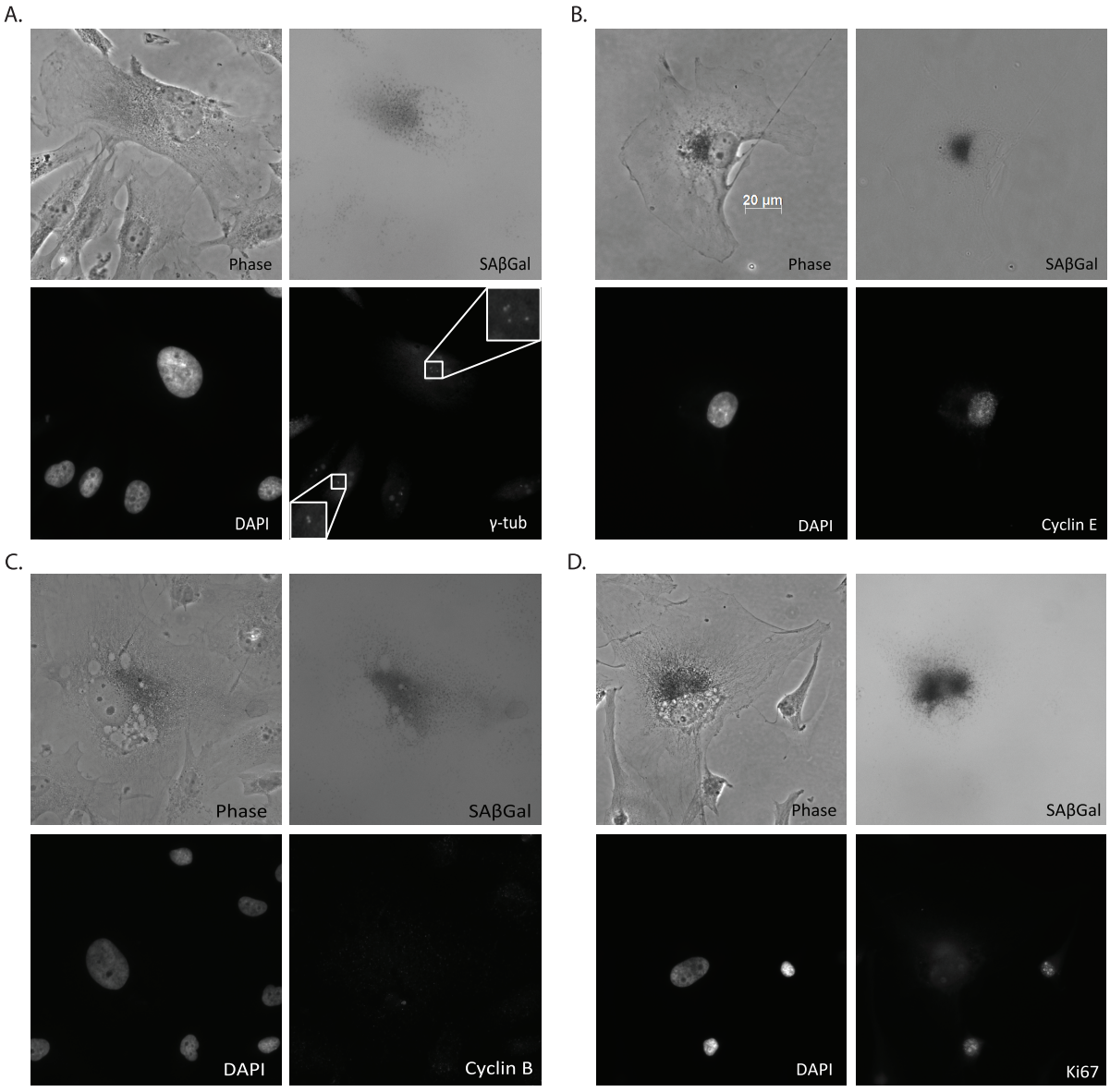
A.
Phase
SAβGal
DAPI
γ-tub
B.
20 µm
Phase
SAβGal
DAPI
Cyclin E
C.
Phase
SAβGal
DAPI
Cyclin B
D.
Phase
SAβGal
DAPI
Ki67

arrest in the G1 phase of the cell cycle (Figure 6B,C). After PKCι depletion, senescent U87MG cells are also Ki-67 negative, whereas U87MG cells with a normal cell phenotype are frequently Ki-67 positive (Figure 6D). Glioblastoma cells that are senescent either at a basal level or due to the knockdown of PKCι have aberrant centrosomes, are Ki-67 negative, are polyploid and arrest at the G1/S checkpoint.

PKCι depletion in vivo in established glioblastoma xenografts

To test the effect of knocking down PKCι in established tumors, a stably selected glioblastoma cell population containing a doxycycline inducible shRNA targeting PKCι was developed (described in Materials and Methods) and injected subcutaneously into nude mice. Two million U87MG cells containing an shRNA sequence matching the siRNA iota E sequence (U87MG-shPKCιE cells) were injected subcutaneously into nude mice. At day 27, with the majority of mice having established tumors of similar sizes, half the mice were switched to a diet containing doxycycline. Mice remaining in the study at day 41 were euthanized and tissue was collected for western blot analysis and tissue staining (Figure 7A). Three mice were excluded from the initiation of the study due to either rapid growth (two mice) or a complete lack of tumor growth (one mouse). On day 27, the remaining 12 mice were divided into two groups (6 mice each), there was no significant difference in tumor volume between the regular diet group and the doxycycline diet group (Figure 7B). Protein lysates from 9 tumors were examined by western blot analysis for the levels of PKCι (Figure 7C). Mice fed with a doxycycline diet for 12-14 days showed a marked decrease in PKCι protein levels. This demonstrates that a doxycycline inducible shRNA targeting PKCι can decrease protein levels in established mouse xenografts of glioblastoma.

Figure 7. PKCι depletion *in vivo* in established glioblastoma xenografts*.* A. A schematic timeline of the *in vivo* depletion of PKCι using a Doxycycline inducible shRNA targeting PKCι. Using the pLKO-Tet-On system from Clontech, U87MG cells were stably infected with an inducible shRNA system targeting PKCι. 2x10^6 U87MG-shPKCιE cells were injected subcutaneously into nude mice until tumors were established, then half the mice were fed Dox chow for 14 days. **B.** Tumor volume of mice at day 27 before separation into two groups (n=6), one fed with regular chow and the other fed with Dox chow. **C.** After reaching the tumor burden endpoint, tumors were collected and frozen in liquid nitrogen, then analyzed by western blot for the presence of PKCι.

A.

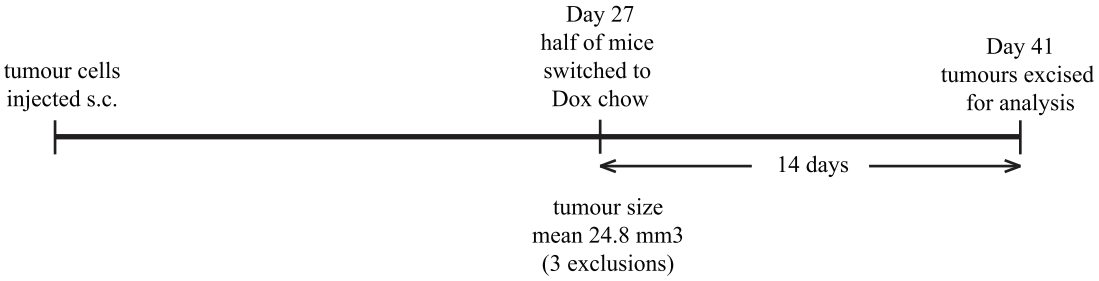

B.

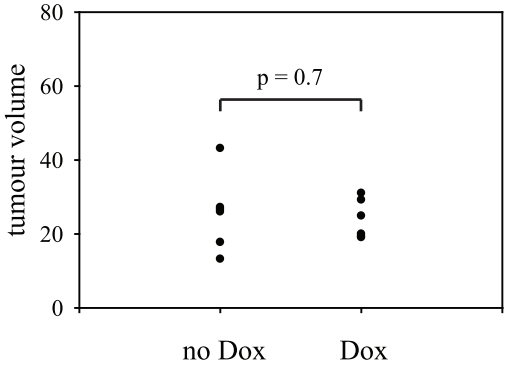

C.

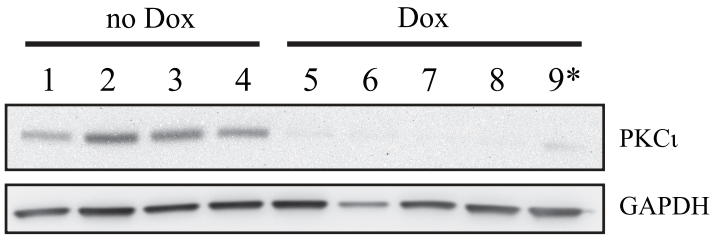

*12 days only (rest were 14 days)

PKCι depletion in vivo decreases cellular proliferation

To analyze a marker of cell proliferation in glioblastoma xenografts after knocking down PKCι protein levels, immunohistochemical staining for Ki-67 was performed (Figure 8A, top). Representative images of positive staining and an isotype-matched negative control are shown above, below that is a representation of Ki-67 staining using positive-pixel count analysis (Figure 8A, middle). This analysis allows for the scoring of the entire tumor section. Quantification of the Ki-67 pixel counts shows a significant decrease in the PKCι depleted mice compared to control mice (Figure 8A, bottom). Tumor tissue was also frozen in liquid nitrogen to be used for SAβGal staining and analysis by positive-pixel counting. The SAβGal score had a trend towards higher staining in the PKCι depleted mice, however this did not reach statistical significance (Figure 8B). The presence of apoptotic cells was also assessed by immunohistochemical staining for cleaved caspase 3 (Figure 8C). There was no significant increase in cleaved caspase 3 staining and the overall staining for apoptotic cells was low in comparison to a positive control. The positive control tissue was kindly provided by Dr. John Bell's laboratory. It is tissue from a U87MG-EGFRvIII xenograft, developed by our lab in 2003, in the same background of nude mice and treated with an oncolytic vaccinia virus (Lavictoire et al., 2003). The endpoint for all mice that were euthanized before day 41 was the overall tumor burden using pre-established wellness criteria. To assess the effect of PKCι knockdown on tumor burden, mouse survival is shown on a Kaplan-Meier plot. Survival of the mice was extended in the PKCι depleted group, however this did not meet statistical significance (Figure 8D). The decrease in Ki-67 score demonstrates that the knockdown of PKCι in established glioblastoma xenografts

Figure 8. PKCι depletion *in vivo* decreases cellular proliferation. A. Immunohistochemical staining of U87MG-shPKCιE nude mouse xenografts using an antibody against the Ki67 antigen. Upper images, representative positive staining of Ki67 next to a negative control (Scale bars are 51.2μm on the left image and 50.2μm on the right image). Lower images, positive pixel count analysis of the representative images. Positive pixel counts of the no Dox and Dox tumors stained using the Ki67 antibody (n=6). **B.** Mouse tumor sections were stained for SAβGal and scored using positive pixel count analysis (n=5). Not statistically significant. **C.** Immunohistochemical staining of U87MG-shPKCιE nude mouse xenografts using an antibody against cleaved caspase 3. Cleaved caspase 3 score was done using positive pixel count analysis. No significant difference between no Dox and Dox groups (n=6). Positive control sample was kindly provided by Dr. John Bell's laboratory. It is tissue from a U87MG-EGFRvIII xenograft grown in the same background (CD1 nude mouse) and treated with an oncolytic vaccinia virus. **D.** A Kaplan-Meier plot of mouse survival during the 14 day dox treatment. Mice were euthanized when they reached the wellness endpoint for tumor burden (n=6). Not statistically significant.

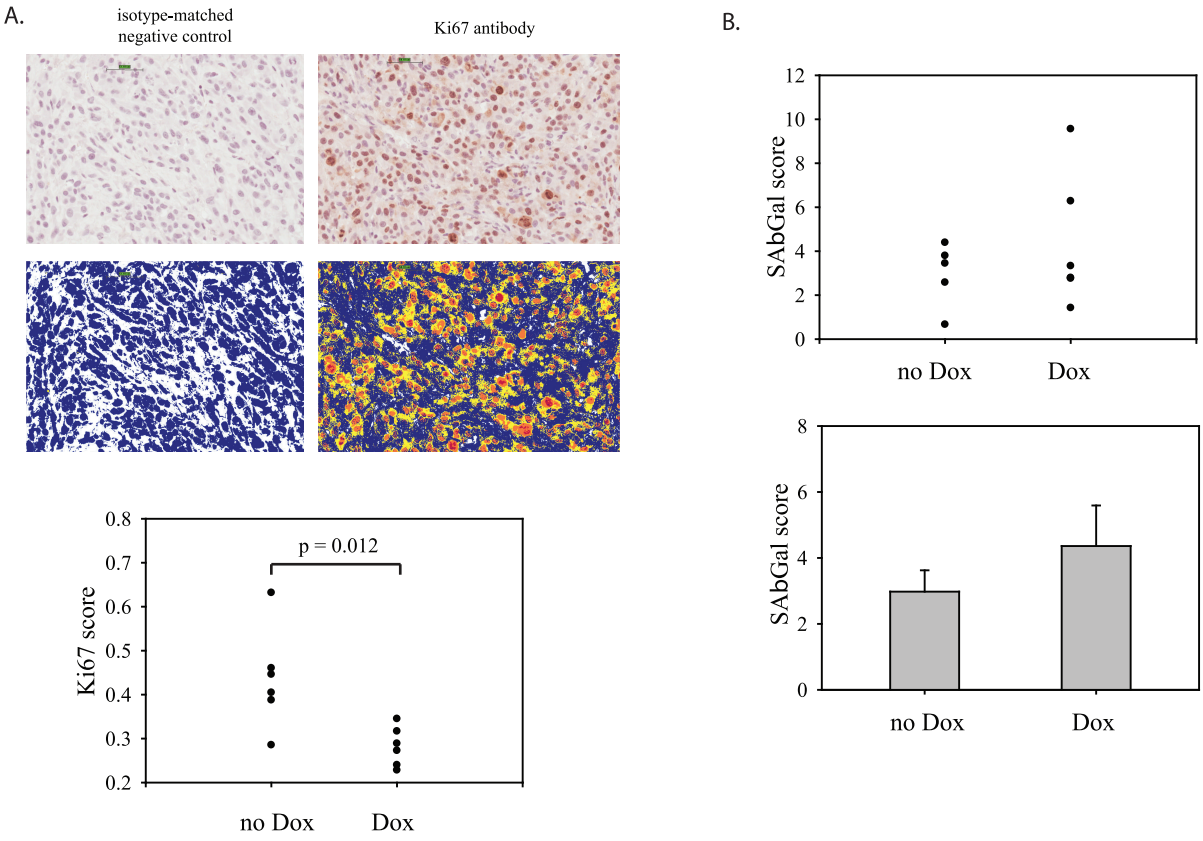
A.
isotype-matched
negative control
Ki67 antibody
Ki67 score
p = 0.012
no Dox
Dox
B.
SAbGal score
no Dox
Dox
SAbGal score
no Dox
Dox
C.
Cleaved caspase 3 score
No Dox
Dox
Pos. Control
D.
Survivors
no Dox
plus Dox
Days after injection

decreases tumor cell proliferation. There is also a trend towards an increase in SAβGal staining without a significant increase in apoptosis and a trend towards an improvement in survival.

PKCι depletion in vivo decreases tumor growth

To observe the effect of PKCι depletion of tumor growth over a longer period of time, depletion of PKCι was started once tumors were established and continued until the tumor burden endpoint. Two million U87MG-shPKCιE cells were injected subcutaneously into nude mice. On day 14, mice with established tumors were separated into two groups, one being fed a regular diet and the other fed a doxycycline diet to deplete PKCι (Figure 9A). Originally, 15 mice were injected with U87MG-shPKCιE cells, however for an unknown reason 8 mice failed to develop tumors in this experiment, never having surpassed $50mm^3$. Tumor tissue was collected as mice reached a pre-determined endpoint for tumor size, occurring from days 37 to 56 (23 to 42 days after the start of the doxycycline diet). Mice were separated into two groups with similar tumor volumes at the start of the doxycycline diet (Figure 9B). Protein lysates were collected as mice from the regular diet and doxycycline groups reached tumor burden endpoint. There was a trend towards a decrease in PKCι protein levels that did not reach significance when quantified (Figure 9C). The lack of PKCι depletion in these samples is likely due to the longer-term exposure to the doxycycline diet. Senescent cells are likely outgrown by neighboring dividing cells or cleared by the innate immune system, which is further addressed in the discussion. The lack of a significant decrease in PKCι levels made the interpretation of other molecular tests, such as the analysis done in Figures 8A-C, questionable after the longer-term

Figure 9. PKCι depletion *in vivo* decreases tumor growth. A. A schematic timeline of the *in vivo* depletion of PKCι using a Doxycycline inducible shRNA targeting PKCι. 2x10^6 U87MG-shPKCιE cells were injected subcutaneously into nude mice until tumors were established. On day 14 half the mice were fed Dox chow until they reached endpoint for tumor size. **B.** Tumor volume of mice at day 14 when separated into two groups at the start of the doxycycline diet (no Dox n=4, Dox n=3). **C.** As mice reached endpoint, tumors were excised and protein lysates were collected. Analysis by western blot was used to detect the presence of PKCι (no Dox n=4, Dox n=3). **D.** Tumor volume of mice following the separation into regular diet (black) and doxycycline diet (red) groups (no Dox n=4, Dox n=3). *P<0.05 using two tailed t-test. **E.** A Kaplan-Meier plot of mouse survival after separation into regular diet (black) and doxycycline diet (red) groups (no Dox n=4, Dox n=3). Mice were euthanized when they reached the wellness endpoint for tumor burden. Statistical significance assessed using Log Rank test.

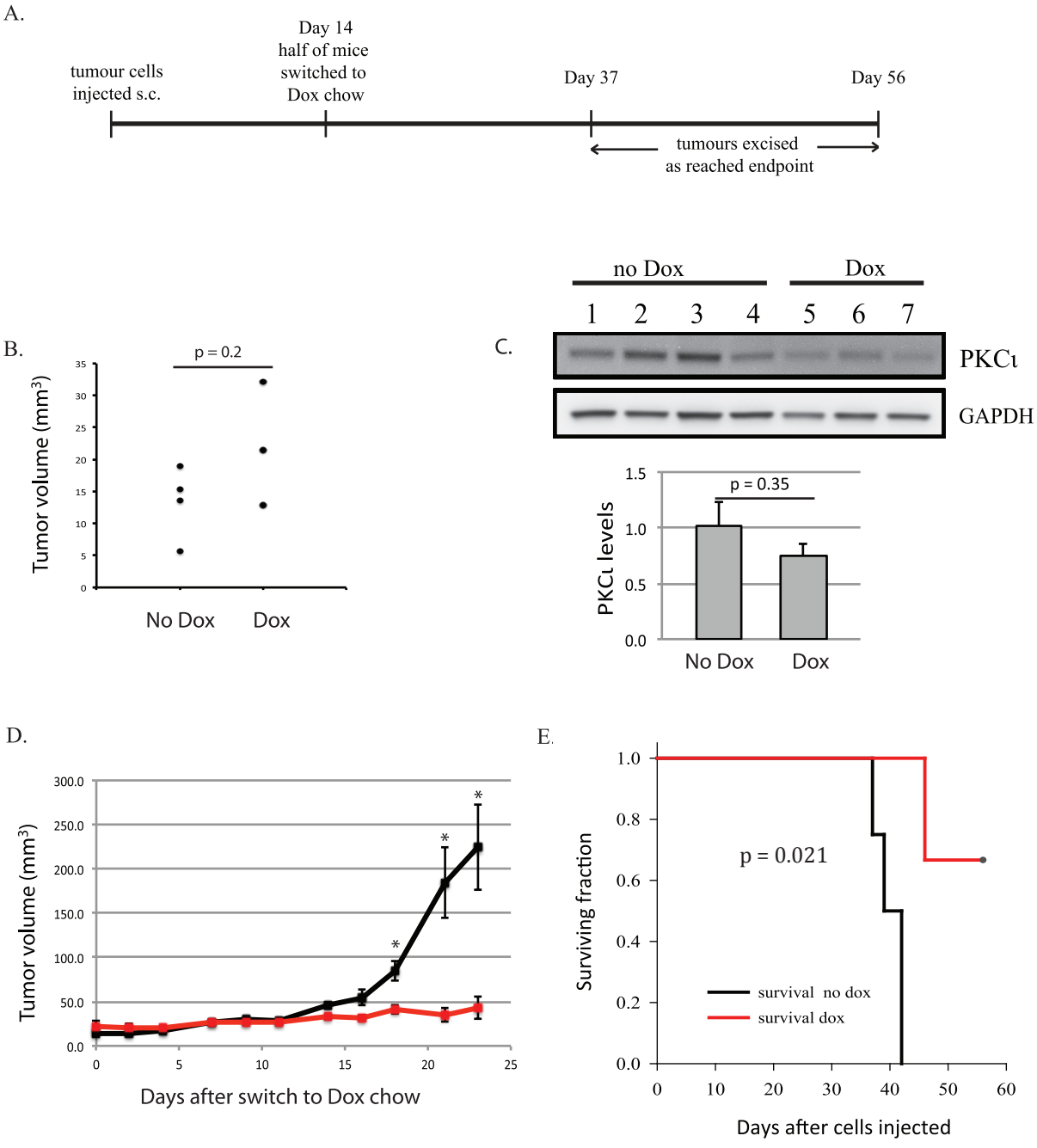
A.
tumour cells injected s.c.
Day 14 half of mice switched to Dox chow
Day 37
Day 56
tumours excised as reached endpoint
B.
p = 0.2
Tumor volume (mm3)
No Dox
Dox
C.
no Dox
Dox
1 2 3 4 5 6 7
PKCι
GAPDH
p = 0.35
PKCι levels
No Dox
Dox
D.
Tumor volume (mm3)
Days after switch to Dox chow
E.
p = 0.021
survival no dox
survival dox
Surviving fraction
Days after cells injected

doxycycline treatment. The average tumor volume following the separation of mice into regular diet and doxycycline diet groups was measured. The average tumor volume is shown up to day 37, when the first mouse in the experiment was euthanized after reaching the tumor burden endpoint (Figure 9D). Depletion of PKCι in the doxycycline diet mice had significantly lower tumor volume once tumors in mice fed the regular diet began growing. The effect of PKCι knockdown on survival was assessed and PKCι depleted mice showed a significant improvement in survival (Figure 9E). Therefore, depletion of PKCι in established glioblastoma xenografts decreased tumor growth and improved survival.

Discussion

The suggestion that centrosome abnormalities played an important role in tumorigenesis was first described in work published in 1915 by Theodore Boveri (Boveri, 2008). Since the more recent reappraisal of Boveri's work, centrosome aberrations have been shown to have a role in aneuploidy, genomic instability, and tumorigenesis (Nigg, 2006). Previously, there has been some evidence linking centrosome aberrations to senescence. Two groups demonstrated that depleting centrosomal proteins induces premature senescence. The knockdown of the centrosomal protein TACC3 in immortalized breast epithelial cells or PCM-1 in human fetal lung fibroblasts induced premature senescence with an increase in p21 (Schmidt et al., 2010b; Srsen et al., 2006). Another group showed that as mouse embryonic fibroblasts (MEFs) reach the same passage number where cells become senescent, there is also an increase in cells with supernumerary centrosomes (Manning and Kumar, 2010). However, there have been well described differences between the mechanisms of senescence between mouse and human cells (Itahana et al., 2004). Altogether, much of the data linking centrosome aberrations to senescence has been correlative, comparing centrosomes and senescent cells in two different populations under similar conditions. In this study, we are among the first groups to show immunofluorescent staining of centrosomes in cells that have already been stained for SAβGal. We observed that the majority of senescent glioblastoma cells have centrosome aberrations. Senescent cells found at a basal level in three different glioblastoma cell lines all had a marked increase in centrosome aberrations. Importantly, centrosome aberrations were not limited to basal levels of senescence as a similar increase in

centrosome aberrations was observed in U87MG and A172 glioblastoma cells that have undergone p21-induced senescence. Basal senescence and p21-induced senescence involves a similar mechanism involving aberrant centrosomes. Therefore, centrosome aberrations in senescent cells are part of a more general premature senescent phenotype in glioblastoma cells. This suggests that centrosome aberrations could be used as a possible marker of senescence in other cancer cells and possibly normal cells; however, this remains to be evaluated.

A relationship between polyploidy and senescence was first described by Saksela and Moorhead in 1963. By analyzing the WI-26 and WI-38 cell strains derived from fetal lung tissue they were able to show that at passages 50±10, where these cell strains enter replicative senescence, there is a 3-4 fold increase in the percent of tetraploid cells (Saksela and Moorhead, 1963). Additionally, Ohshima *et al* observed an association between an increase in supernumerary centrosomes in polyploid late passage human diploid fibroblasts, however senescence wasn't directly assayed (Ohshima and Seyama, 2010). We assessed the ploidy of normal and senescent U87MG cells using CISH to label the centromere of chromosome 7. Consistent with cells having undergone mitotic slippage, U87MG cells with a senescent morphology had twice the chromosome content as U87MG cells with a normal cellular morphology. Furthermore, senescent U87MG cells arrest at the G1/S checkpoint, as they are negative for cyclin B1 and positive for cyclin E. Together with the increase in aberrant centrosomes, this demonstrates a direct link between mitotic slippage and the induction of senescence in glioblastoma cells.

Mitotic slippage is underscored by an inability to successfully progress through mitosis, followed by a mitotic exit into the G1 phase of the cell cycle. The result is a G1 cell that has the 4N DNA content and the centrosome morphology of a cell that has already progressed through the S and G2 phases of the cell cycle and attempted to divide. Publications describe the induction of a G1 arrest and senescence as the cell fate of mitotic slippage without a reference to specific work (Rieder and Maiato, 2004; Vitale et al., 2011). It is very difficult to find published direct evidence that mitotic slippage leads to senescence. This is partly due to mitotic slippage being used in the place of or instead of incongruent terms, such as mitotic catastrophe, mitotic cell death, or failure of cytokinesis. The best evidence to demonstrate that senescence is the cell fate following mitotic slippage is that depleting proteins necessary to satisfy the SAC leads to senescence (Schmidt et al., 2010a). Depleting Mad2 using siRNA induces senescence *in vitro*, and a reduction of BubR1 in mice causes an early onset of senescence *in vivo* (Baker et al., 2004; Prencipe et al., 2009).

Previously, we have shown that PKCι depletion in glioblastoma cells induces p21-dependent senescence *in vitro* (Paget et al., 2011). In this study, we quantitatively analyzed PKCι depletion-induced senescent glioblastoma cells for markers of mitotic slippage. Senescent cells induced by PKCι depletion have the same number of cells with centrosome aberrations, cyclin E positivity, and Ki-67 negativity, when compared to the basal senescence in senescent control cells. Similarly, the percentage of polyploid cells increase after PKCι knockdown to a similar degree that SAβGal positive cells increase. The basal senescence and PKCι depletion-induced senescence in glioblastoma cells

therefore occur through a similar mechanism. Altogether, this demonstrates that PKCι depletion-induced senescence is mediated by mitotic slippage.

To date, the analysis of PKCι depletion *in vivo* has been done using xenograft tumors in mice where the knockdown of PKCι is performed prior to the injection of cells. We have previously shown that PKCι knockdown induces senescence and decreases cell proliferation *in vitro* (Baldwin et al., 2010; Paget et al., 2011). Due to this effect on cell proliferation, it is not clear how the effects of PKCι depletion on tumor initiation have influenced the decrease in tumor burden described in the literature using constitutive PKCι knockdown (Scotti et al., 2010). To address the role of PKCι depletion in established tumors, we developed a U87MG glioblastoma cell population stably selected with a doxycycline inducible shRNA targeting PKCι using the siRNA iota E sequence (U87MG-shPKCιE). PKCι is the only atypical PKC depleted in U87MG-shPKCιE cells since we have previously shown that U87MG cells express PKCι mRNA and no detectable PKCζ mRNA (Baldwin et al., 2006). After glioblastoma xenografts in nude mice were established, mice were separated into a doxycycline diet group, to induce PKCι depletion, and a regular diet group. After 9-14 days of doxycycline diet, PKCι levels in established tumors were markedly decreased. We have therefore developed a system to analyze the effects of PKCι depletion *in vivo* in established glioblastoma xenografts, more closely resembling the clinical process of treating tumors after diagnosis.

Markers of cell proliferation and senescence have not been previously analyzed following PKCι depletion in established tumors. We were able to show a significant decrease of the proliferation marker Ki-67 in glioblastoma xenografts following PKCι

knockdown, similar to the *in vitro* data using siRNA targeting PKCι. Ki-67 staining is used in combination with other markers of senescence to confirm the senescent phenotype. Frozen tissue slices from glioblastoma xenografts were also stained for SAβGal and there was a trend towards an increase in SAβGal staining following PKCι knockdown. However, variation between samples contributed to a lack of statistical significance. Cleaved caspase 3 IHC staining did not show a significant increase in apoptosis in the PKCι depleted mice. Similarly, Scotti *et al* have shown that orthotopically injected pancreatic tumor cells stably expressing shRNA targeting PKCι had decreased tumor growth without apoptosis (Scotti et al., 2010). The survival of mice following 9-14 days of PKCι depletion in established glioblastoma xenografts was improved, although without reaching statistical significance. PKCι depletion in established glioblastoma xenografts decreases tumor cell proliferation with a trend towards increased SAβGal staining and no significant increase in apoptosis.

Following a 14-day exposure to doxycycline diet we observed a decrease in tumor cell proliferation. We therefore wanted to assess the effect of a longer-term exposure to a doxycycline diet and depletion of PKCι. Once palpable glioblastoma xenograft tumors were established in nude mice, one group was fed a regular diet and the other was fed a doxycycline diet. Mice were euthanized as they reached the endpoint for tumor burden on days 37 to 56. Tissue that was collected as mice reached endpoint showed only a moderate decrease in PKCι levels. Due to the increased doxycycline exposure time, the moderate decrease in PKCι protein likely reflects the outgrowth of cells that still express low levels of PKCι and eventually outgrow neighboring cells. Moreover, the clearance of senescent cells by the innate immune

system has been previously demonstrated in nude mice. Xue *et al* were able to demonstrate that the reactivation of p53 in liver tumors triggered OIS in the absence of apoptosis and tumors regressed due to tumor clearance by the innate immune system (Xue et al., 2007). This also highlights the difficulty of detecting SAβGal positive cells in mice, where the optimal experimental timing for tissue collection in order to detect the presence of SAβGal positive cells needs to be determined. Over a longer-term exposure of mice to doxycycline and PKCι depletion, we observed a significant decrease in tumor growth that was reflected in overall survival. We suggest that the decrease in tumor growth seen in PKCι depleted tumors is mediated by senescence and not apoptosis. Overall, this further demonstrates the potential therapeutic benefit of targeting PKCι in established tumors.

Our work has shown a direct link between mitotic slippage and the induction of senescence in glioblastoma cells. Mitotic slippage leads to polyploid, G1 arrested cells with supernumerary centrosomes, resulting in premature senescence. The exact mechanistic details for the signaling checkpoint involved following mitotic slippage remains to be elucidated (Ganem and Pellman, 2007). It is clear however, that mitotic slippage results in cellular stress that does not permit progression from G1 to S-phase and to date the literature implicates a role for p21. The exact signaling pathways are likely to involve multiple factors that arise from a G1 phase cell with all the molecular components of a cell that has entered mitosis without dividing.

If mitotic slippage-induced senescence is part of a more general mechanism of premature senescence then there are some important implications. One potential issue involves the cell cycle analysis of senescent cells. If cell cycle analysis is performed

solely based on flow cytometric analysis using propidium iodide or other DNA stains to assess ploidy, there may be an exaggerated G2 component. Cells that have undergone mitotic slippage and have a 4N DNA content that are arrested at the G1/S checkpoint will appear as though they are arrested at the G2/M checkpoint. This is very important when making conclusions on the phase of the cell cycle arrest in cellular senescence. Another interesting implication is the potential role of mitotic slippage in a more general mechanism of premature senescence. Many inducers of premature senescence have been described and multiple signaling pathways are involved in the induction of premature senescence, without a common root cause. A large physical disruption in the cell, such as an inability to progress through mitosis followed by an exit back into interphase, could be a central source of the stress at the root of premature senescence. A common method of inducing premature senescence is the expression of oncogenic Ras in normal cells, first described by Serrano *et al* (Serrano et al., 1997). Interestingly, expression of oncogenic Ras in normal rat thyroid cells has been shown to promote the bypass of the SAC, resulting in G1 cells with a 4N DNA content (Knauf et al., 2006). This suggests that mitotic slippage may play a role in OIS induced by oncogenic Ras expression. We hypothesize that mitotic slippage may be involved in a more general premature senescence mechanism.

In summary, we have demonstrated that senescent glioblastoma cells in culture have aberrant centrosomes. PKCι depletion-induced senescent cells are arrested at the G1/S checkpoint, are negative for Ki-67 and are polyploid. PKCι depletion by siRNA therefore initiates mitotic slippage-induced senescence. An inducible shRNA knockdown of PKCι in established glioblastoma tumor xenografts depleted PKCι

protein levels, significantly decreased cell proliferation and had a trend towards an increase in SAβGal staining, without a significant increase in apoptosis. Over a longer-term depletion of PKCι, tumor volume was decreased and survival was improved.

Materials and Methods:

Antibodies: PKCι mouse monoclonal antibody (#610176) was from BD Transduction Laboratories (Mississauga, ON, Canada). Ki-67 mouse monoclonal antibody (ab8191) used for immunohistochemistry, Ki-67 rabbit polyclonal antibody (ab15580) used for immunofluorescence, and GAPDH (ab8245) mouse monoclonal antibody were from Abcam (Cambridge, MA, USA). Cleaved caspase-3 rabbit monoclonal antibody (#9664) and cyclin B1 rabbit polyclonal antibody (#4138) were from Cell Signaling Technology (Danvers, MA, USA). Cyclin E mouse monoclonal antibody (sc-247) was from Santa Cruz Biotechnology (Santa Cruz, CA, USA). γ-tubulin mouse monoclonal antibody (T6557) was from Sigma-Aldrich (St. Louis, MO, USA). Secondary antibodies used for western blots were purchased from Jackson Immunoresearch Laboratories (West Grove, PA, USA). Secondary antibodies used for immunofluorescence were conjugated Alexa Fluor goat anti-rabbit 555, goat anti-mouse 555 and chicken anti-rabbit 488 from Life Technologies – Invitrogen (Burlington, ON, Canada).

Cell Culture: A172 and DBTRG cell lines were purchased from ATCC (Manassas, VA, USA). The human U87MG glioblastoma cell line was obtained from Dr. W. Cavenee (Ludwig Institute for Cancer Research, La Jolla, CA, USA). U87MG-shPKCιE cells were established as described below. All cell lines were passaged in Dulbecco's modified Eagle's medium (DMEM) from Thermo Scientific Hyclone (Rockford, IL, USA) with 10% fetal bovine serum and 100 units/ml penicillin, 100 µg/ml streptomycin from Life Technologies – Invitrogen (Burlington, ON, Canada). Cell lines were in culture for less than six months continuously and were routinely checked for mycoplasma contamination.

Lentiviral transduction: The p21 lentiviral vector was created using p21 cDNA from the A172 cell line with the two primers: 5'-GGATCCAGGCACCGAGGCACTCAGAG-3' and 5'-GTCGACGGACTGCAGGCTTCCTGTGG-3'. The cDNA was then cloned into the pLenti vector and sequenced. Cells were transduced with 100µl lentiviral vector, 900µl media and 10mg/ml polybrene.

Establishing and inducible shRNA stable cell line: The inducible shRNA stable cell line was created using the manufacturer's protocol for the pLKO-Tet-On system from Novartis (Cambridge, MA, USA). The shRNA targeting PKCι E cassette sequences used were E1 5'-CCGGGCCTGGATACAATTAACCATTCAAGAGATGGTTAATTGTATCCAGGCTTTTT-3' and E2 5'-AATTAAAAAGCCTGGATACAATTAACCATCTCTTGAATGGTTAATTGTATCCAGGC-3'. The shRNA sequences were annealed by heating to 90°C for 2 minutes and gradual cooling to room temperature. The cassette was then cloned into the pLKO-Tet-On vector using the AgeI and EcoRI sites in the cassette. Clones were verified by sequencing. The lentivirus was packaged in 293T cells using the Gene Juice transfection reagent from EMD Millipore (Merck, Mississauga, ON, Canada) and OptiMEM I from Life Technologies – Invitrogen (Burlington, ON, Canada). The four plasmids transfected together were: pLKO-Tet-On, pLP1, pLP2, and pLP/VSVG. Media was changed on the 293T cells 24 hours later, after 48 hours of fresh media the supernatant was collected, spun down and filtered through a 0.45µM filter. U87MG cells were transduced as described above. The U87MGshPKCιE cell line was a transduced population of U87MG cells that were selected with 1µg/mL puromycin.

Immunofluorescent staining: Cells were plated on gelatin-coated coverslips and following the SAβGal staining procedure (except for cyclin B1 staining), cells were fixed with ice-cold 95% methanol for 10 minutes. Note: the SAβGal procedure involves a 10 minute fixation using 4% paraformaldehyde and the cyclin B1 staining was done after a 30 min 4% paraformaldehyde fixation. Cells were blocked in 5% serum in PBS (goat or chicken) then incubated with the primary antibody for 1 hour in 5% serum at the following concentrations: γ-tubulin 1:800, cyclin B1 1:50, cyclin E 1:50, and Ki-67 1:1500. The relevant secondary antibody was incubated in 5% serum at 2μg/ml for 1 hour. Slides were analyzed using a Zeiss Axioskop 2 microscope from Carl Zeiss Inc (Toronto, ON, Canada).

Immunohistochemistry: Formalin-fixed and paraffin-embedded tissue from glioblastoma xenografts was cut in sections 4 microns thick. Antigen retrieval was completed using the antigen unmasking solution (H3300) from Vector Laboratories (Burlington, ON, Canada) and a microwave treatment. Endogenous peroxidase activity was quenched by incubation in 3% H_2O_2 in PBS. Primary antibodies were used at 0.15mg/ml for Ki-67 and 1:800 for cleaved caspase 3. Antibody detection was performed using the manufacturer's instructions for the Envision Polymer Detection System from Dako (Mississauga, Canada). The slides were then scanned using the Aperio ScanScope console from Aperio ePathology solutions (Vista, CA, USA). Positive pixel counting analysis was performed using the Aperio ImageScope software. The signal for the pixel counting analysis was always assessed manually to confirm it matched the true staining of the tissue.

Western Blot Analysis: Snap frozen mouse tissue was boiled at 95°C for 5 minutes in lysis buffer containing 100mM Tris pH 6.8, 5% glycerol, and 4% SDS. Tissue was mechanically dissociated using an epindorf mortar and pestle and then briefly sonicated. Protein lysates were run on a 4-12% gradient bis-tris polyacrylamide gel Life Technologies – Invitrogen (Burlington, ON, Canada) and transferred to a PVDF nylon membrane GE Healthcare Life Sciences (Baie d'Urfe, QC, Canada). Secondary HRP conjugated antibodies were detected with SuperSignal West Pico Chemiluminescent Substrate reagents Thermo Scientific Pierce (Nepean, ON, Canada). Western blots were visualized and quantified using the Alpha Innotech Fluorchem FC2 system and Alphaview software from ProteinSimple (Santa Clara, CA, USA).

RNA interference: All duplexes were purchased from Dharmacon (Lafayette, CO, USA). RNA duplexes with the following sense strand sequences were used to target PKCι: duplex A, 5'-GTGCATCAACTGCAAACTC-3' (Baldwin et al., 2006); duplex E, 5'-GCCTGGATACAATTAACCATT-3' (Scotti et al., 2010). siGENOME Non-Targeting siRNA #3 from Dharmacon was used as a non-targeting duplex control. RNA transfections were done as described previously but with a final concentration of 10nM (Baldwin et al, 2006). For senescence analysis cells were assayed 5 days after transfection with siRNA washed off after 48hr. Initial plating of cells was 15,000 to 20,000 in a 6-well dish on gelatin-coated cover slips.

SAβGal Staining: Cells were plated in a 6-well dish on gelatin-coated cover slips. 24 hours after plating, transfection of RNA duplexes was performed as described above. Media was refreshed every 48 hours and five days after transfection, cells were fixed in 4% paraformaldehyde for 10 minutes and assayed for SAβGal activity as described by Debacq-Chainiaux *et al* (Debacq-Chainiaux et al., 2009). Slides were analyzed using a Zeiss Axioskop 2 microscope or continued

on to immunofluorescent staining as described above. Total and SAβGal-positive cells were counted in a minimum of three separate fields and a minimum of 100 cells overall for each condition.

Statistical analysis: Unless otherwise indicated, statistical significance was determined by a two tailed t-test. Statistical significance for a Kaplan-Meier plot was determined using the Log Rank test. Values were considered significant when $P<0.05$.

References

Baker, D.J., Jeganathan, K.B., Cameron, J.D., Thompson, M., Juneja, S., Kopecka, A., Kumar, R., Jenkins, R.B., de Groen, P.C., Roche, P.*, et al.* (2004). BubR1 insufficiency causes early onset of aging-associated phenotypes and infertility in mice. Nat Genet *36*, 744-749.

Baldwin, R.M., Barrett, G.M., Parolin, D.A., Gillies, J.K., Paget, J.A., Lavictoire, S.J., Gray, D.A., and Lorimer, I.A. (2010). Coordination of glioblastoma cell motility by PKCiota. Mol Cancer *9*, 233.

Baldwin, R.M., Garratt-Lalonde, M., Parolin, D.A., Krzyzanowski, P.M., Andrade, M.A., and Lorimer, I.A. (2006). Protection of glioblastoma cells from cisplatin cytotoxicity via protein kinase Ciota-mediated attenuation of p38 MAP kinase signaling. Oncogene *25*, 2909-2919.

Baldwin, R.M., Parolin, D.A., and Lorimer, I.A. (2008). Regulation of glioblastoma cell invasion by PKC iota and RhoB. Oncogene *27*, 3587-3595.

Boveri, T. (2008). Concerning the origin of malignant tumours by Theodor Boveri. Translated and annotated by Henry Harris. J Cell Sci *121 Suppl 1*, 1-84.

Brito, D.A., and Rieder, C.L. (2006). Mitotic checkpoint slippage in humans occurs via cyclin B destruction in the presence of an active checkpoint. Curr Biol *16*, 1194-1200.

Cancer Genome Atlas Research, N. (2008). Comprehensive genomic characterization defines human glioblastoma genes and core pathways. Nature *455*, 1061-1068.

Chou, M.M., Hou, W., Johnson, J., Graham, L.K., Lee, M.H., Chen, C.S., Newton, A.C., Schaffhausen, B.S., and Toker, A. (1998). Regulation of protein kinase C zeta by PI 3-kinase and PDK-1. Curr Biol *8*, 1069-1077.

Collado, M., Gil, J., Efeyan, A., Guerra, C., Schuhmacher, A.J., Barradas, M., Benguria, A., Zaballos, A., Flores, J.M., Barbacid, M.*, et al.* (2005). Tumour biology: senescence in premalignant tumours. Nature *436*, 642.

Courtois-Cox, S., Genther Williams, S.M., Reczek, E.E., Johnson, B.W., McGillicuddy, L.T., Johannessen, C.M., Hollstein, P.E., MacCollin, M., and Cichowski, K. (2006). A negative feedback signaling network underlies oncogene-induced senescence. Cancer Cell *10*, 459-472.

Dankort, D., Filenova, E., Collado, M., Serrano, M., Jones, K., and McMahon, M. (2007). A new mouse model to explore the initiation, progression, and therapy of BRAFV600E-induced lung tumors. Genes Dev *21*, 379-384.

Debacq-Chainiaux, F., Erusalimsky, J.D., Campisi, J., and Toussaint, O. (2009). Protocols to detect senescence-associated beta-galactosidase (SA-betagal) activity, a biomarker of senescent cells in culture and in vivo. Nat Protoc *4*, 1798-1806.

Dhomen, N., Reis-Filho, J.S., da Rocha Dias, S., Hayward, R., Savage, K., Delmas, V., Larue, L., Pritchard, C., and Marais, R. (2009). Oncogenic Braf induces melanocyte senescence and melanoma in mice. Cancer Cell *15*, 294-303.

Foley, E.A., and Kapoor, T.M. (2012). Microtubule attachment and spindle assembly checkpoint signalling at the kinetochore. Nat Rev Mol Cell Biol *14*, 25-37.

Ganem, N.J., and Pellman, D. (2007). Limiting the proliferation of polyploid cells. Cell *131*, 437-440.

Gewirtz, D.A., Holt, S.E., and Elmore, L.W. (2008). Accelerated senescence: an emerging role in tumor cell response to chemotherapy and radiation. Biochem Pharmacol *76*, 947-957.

Hanahan, D., and Weinberg, R.A. (2011). Hallmarks of cancer: the next generation. Cell *144*, 646-674.

Harley, C.B., Futcher, A.B., and Greider, C.W. (1990). Telomeres shorten during ageing of human fibroblasts. Nature *345*, 458-460.

Hayflick, L., and Moorhead, P.S. (1961). The serial cultivation of human diploid cell strains. Exp Cell Res *25*, 585-621.

Itahana, K., Campisi, J., and Dimri, G.P. (2004). Mechanisms of cellular senescence in human and mouse cells. Biogerontology *5*, 1-10.

Kanu, O.O., Mehta, A., Di, C., Lin, N., Bortoff, K., Bigner, D.D., Yan, H., and Adamson, D.C. (2009). Glioblastoma multiforme: a review of therapeutic targets. Expert Opin Ther Targets *13*, 701-718.

Knauf, J.A., Ouyang, B., Knudsen, E.S., Fukasawa, K., Babcock, G., and Fagin, J.A. (2006). Oncogenic RAS induces accelerated transition through G2/M and promotes defects in the G2 DNA damage and mitotic spindle checkpoints. J Biol Chem *281*, 3800-3809.

Lavictoire, S.J., Parolin, D.A., Klimowicz, A.C., Kelly, J.F., and Lorimer, I.A. (2003). Interaction of Hsp90 with the nascent form of the mutant epidermal growth factor receptor EGFRvIII. J Biol Chem *278*, 5292-5299.

Le Good, J.A., Ziegler, W.H., Parekh, D.B., Alessi, D.R., Cohen, P., and Parker, P.J. (1998). Protein kinase C isotypes controlled by phosphoinositide 3-kinase through the protein kinase PDK1. Science *281*, 2042-2045.

Lee, J., Kim, J.A., Margolis, R.L., and Fotedar, R. (2010). Substrate degradation by the anaphase promoting complex occurs during mitotic slippage. Cell Cycle *9*, 1792-1801.

Manning, J.A., and Kumar, S. (2010). A potential role for NEDD1 and the centrosome in senescence of mouse embryonic fibroblasts. Cell Death Dis *1*, e35.

Michaloglou, C., Vredeveld, L.C., Soengas, M.S., Denoyelle, C., Kuilman, T., van der Horst, C.M., Majoor, D.M., Shay, J.W., Mooi, W.J., and Peeper, D.S. (2005). BRAFE600-associated senescence-like cell cycle arrest of human naevi. Nature *436*, 720-724.

Murray, N.R., Kalari, K.R., and Fields, A.P. (2011). Protein kinase Ciota expression and oncogenic signaling mechanisms in cancer. J Cell Physiol *226*, 879-887.

Nigg, E.A. (2006). Origins and consequences of centrosome aberrations in human cancers. Int J Cancer *119*, 2717-2723.

Ohshima, S., and Seyama, A. (2010). Cellular aging and centrosome aberrations. Ann N Y Acad Sci *1197*, 108-117.

Paget, J.A., Restall, I.J., Daneshmand, M., Mersereau, J.A., Simard, M.A., Parolin, D.A., Lavictoire, S.J., Amin, M.S., Islam, S., and Lorimer, I.A. (2011). Repression of cancer cell senescence by PKCiota. Oncogene.

Prencipe, M., Fitzpatrick, P., Gorman, S., Tosetto, M., Klinger, R., Furlong, F., Harrison, M., O'Connor, D., Roninson, I.B., O'Sullivan, J.*, et al.* (2009). Cellular senescence induced by aberrant MAD2 levels impacts on paclitaxel responsiveness in vitro. Br J Cancer *101*, 1900-1908.

Regala, R.P., Weems, C., Jamieson, L., Khoor, A., Edell, E.S., Lohse, C.M., and Fields, A.P. (2005). Atypical protein kinase C iota is an oncogene in human non-small cell lung cancer. Cancer Res *65*, 8905-8911.

Rieder, C.L., and Maiato, H. (2004). Stuck in division or passing through: what happens when cells cannot satisfy the spindle assembly checkpoint. Dev Cell *7*, 637-651.

Roberson, R.S., Kussick, S.J., Vallieres, E., Chen, S.Y., and Wu, D.Y. (2005). Escape from therapy-induced accelerated cellular senescence in p53-null lung cancer cells and in human lung cancers. Cancer Res *65*, 2795-2803.

Saksela, E., and Moorhead, P.S. (1963). Aneuploidy in the Degenerative Phase of Serial Cultivation of Human Cell Strains. Proc Natl Acad Sci U S A *50*, 390-395.

Schmidt, S., Essmann, F., Cirtea, I.C., Kuck, F., Thakur, H.C., Singh, M., Kletke, A., Janicke, R.U., Wiek, C., Hanenberg, H.*, et al.* (2010a). The centrosome and mitotic spindle apparatus in cancer and senescence. Cell Cycle *9*, 4469-4473.

Schmidt, S., Schneider, L., Essmann, F., Cirstea, I.C., Kuck, F., Kletke, A., Janicke, R.U., Wiek, C., Hanenberg, H., Ahmadian, M.R.*, et al.* (2010b). The centrosomal protein TACC3 controls paclitaxel sensitivity by modulating a premature senescence program. Oncogene *29*, 6184-6192.

Schneider, L., Essmann, F., Kletke, A., Rio, P., Hanenberg, H., Wetzel, W., Schulze-Osthoff, K., Nurnberg, B., and Piekorz, R.P. (2007). The transforming acidic coiled coil 3 protein

is essential for spindle-dependent chromosome alignment and mitotic survival. J Biol Chem *282*, 29273-29283.

Scotti, M.L., Bamlet, W.R., Smyrk, T.C., Fields, A.P., and Murray, N.R. (2010). Protein kinase Ciota is required for pancreatic cancer cell transformed growth and tumorigenesis. Cancer Res *70*, 2064-2074.

Serrano, M., Lin, A.W., McCurrach, M.E., Beach, D., and Lowe, S.W. (1997). Oncogenic ras provokes premature cell senescence associated with accumulation of p53 and p16INK4a. Cell *88*, 593-602.

Srsen, V., Gnadt, N., Dammermann, A., and Merdes, A. (2006). Inhibition of centrosome protein assembly leads to p53-dependent exit from the cell cycle. J Cell Biol *174*, 625-630.

Stupp, R., Mason, W.P., van den Bent, M.J., Weller, M., Fisher, B., Taphoorn, M.J., Belanger, K., Brandes, A.A., Marosi, C., Bogdahn, U*., et al.* (2005). Radiotherapy plus concomitant and adjuvant temozolomide for glioblastoma. N Engl J Med *352*, 987-996.

te Poele, R.H., Okorokov, A.L., Jardine, L., Cummings, J., and Joel, S.P. (2002). DNA damage is able to induce senescence in tumor cells in vitro and in vivo. Cancer Res *62*, 1876-1883.

Ventura, A., Kirsch, D.G., McLaughlin, M.E., Tuveson, D.A., Grimm, J., Lintault, L., Newman, J., Reczek, E.E., Weissleder, R., and Jacks, T. (2007). Restoration of p53 function leads to tumour regression in vivo. Nature *445*, 661-665.

Vitale, I., Galluzzi, L., Castedo, M., and Kroemer, G. (2011). Mitotic catastrophe: a mechanism for avoiding genomic instability. Nat Rev Mol Cell Biol *12*, 385-392.

Xue, W., Zender, L., Miething, C., Dickins, R.A., Hernando, E., Krizhanovsky, V., Cordon-Cardo, C., and Lowe, S.W. (2007). Senescence and tumour clearance is triggered by p53 restoration in murine liver carcinomas. Nature *445*, 656-660.

Figure S1. p21-induced senescence in glioblastoma cells. A. Western blot analysis of U87MG and A172 cells 24 hours after transduction with GFP or p21 lentivirus. **B.** SAβGal staining of U87MG and A172 cells transduced with a mock, GFP, or p21 lentivirus overnight, washed and fixed for staining four days later (five days after transduction).

A.

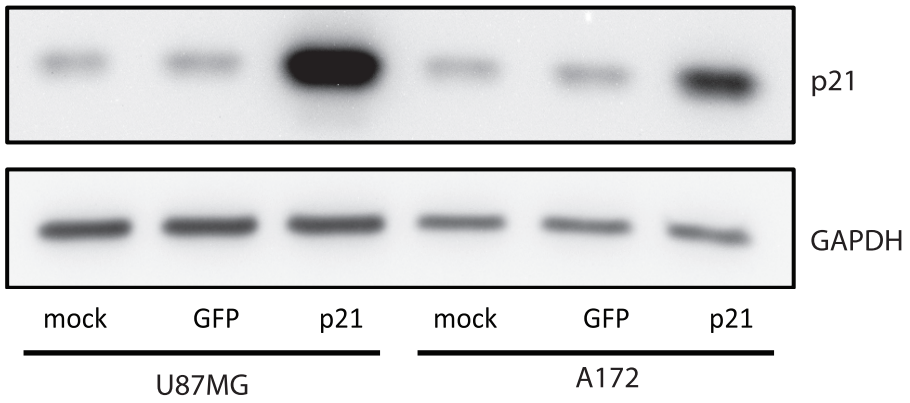
p21
GAPDH
mock
GFP
p21
mock
GFP
p21
U87MG
A172

B.

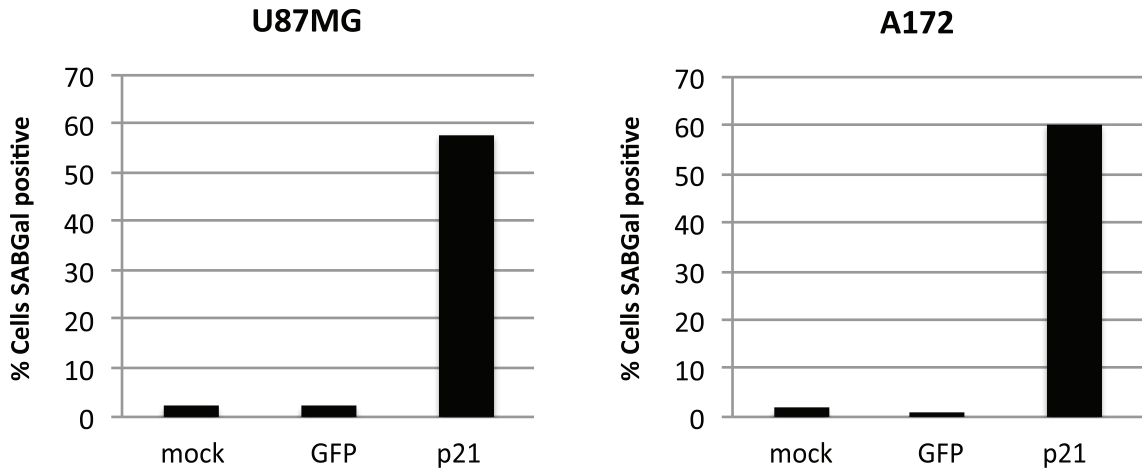
U87MG
A172
% Cells SABGal positive
70
60
50
40
30
20
10
0
mock
GFP
p21

5. Discussion

Research on cellular senescence has now entered its sixth decade. Since the observation of oncogene-induced senescence, the field has seen a steady increase in the amount of publications involving cellular senescence in the cancer field. Replicative senescence is a tumor-suppressor mechanism that limits the proliferative capacity of cells by telomere erosion. OIS is a tumor-suppressor mechanism that limits the transformation of normal cells following the expression of an oncogene. We, and others, are pursuing the area of research that involves targeting proteins to induce senescence in cancer cells that have already bypassed replicative and oncogene-induced senescence.

Previous work in the Hsp90 community focused on apoptosis and transient growth arrest as the outcome following Hsp90 inhibition. The growth arrest was assumed to be transient, even though this assessment was not analyzed in detail. Our work using Hsp90 inhibitors in SCLC cells demonstrated for the first time that Hsp90 inhibition alone induced premature senescence. There has been a link between replicative senescence and Hsp90 since it was shown to chaperone hTERT, a catalytic subunit of telomerase (Holt et al., 1999). However, the induction of senescence was not fully described. Apoptosis was previously reported following treatment of SCLC cells with Hsp90 inhibitors (Rodina et al., 2007). We have shown that at concentrations of Hsp90 inhibitors that induce degradation of Hsp90 client proteins the primary outcome is senescence. Higher concentrations of Hsp90 inhibitors did induce cell death, however this is likely due to the inhibition of Hsp90 paralogs in the cell. The degree of senescence we observed in SCLC cells was markedly high. Generally, in an entire cancer

cell population the induction of senescence is limited to a portion of the population and the percentage of senescent cells is measured. In this study we originally observed the induction of senescence as a complete lack of proliferation that was reproducibly observed for more than 30 days in culture. Senescence induced by Hsp90 inhibition involved the DNA damage response and was dependent on p21. In a few instances a cell population eventually grew out of the senescent population. The protein levels of p21 were undetectable in the outgrown population, which no longer senesced after Hsp90 inhibition. We hypothesize that the outgrowth of cells represents a very small number of cells already present in the population that no longer expresses p21. One of the Hsp90 inhibitors we used to induce senescence in SCLC cells was 17-AAG. Recently, it has been shown that inhibition of Hsp90 using 17-AAG was able to sensitize neuroblastoma cells to doxorubicin (adriamycin) induced senescence (Sarangi et al., 2012). The contribution of Hsp90 inhibition to p21-dependent senescence is shown in the context of the molecular pathways of senescence in Figure 5.1. The precise mechanism of Hsp90 inhibition-induced p21-dependent senescence was not fully elucidated. One possibility involves the previously described feedback loop involving reactive oxygen species (ROS) and p21 in the induction of senescence (Passos et al., 2010). Additionally, a reciprocal relationship between p21 expression and ROS accumulation has been previously described. An increase in cellular ROS can increase p21 expression in a p53-indendent mechanism and overexpression of p21 has been shown to increase ROS (Macip et al., 2002; Russo et al., 1995). Furthermore, inhibition of Hsp90 using geldanamycin or its derivative 17-DMAG has been shown to increase cellular levels of ROS (Clark et al., 2009; Fukuyo et al., 2008). This suggests a role for

Figure 5.1. Revised molecular pathways of senescence induction

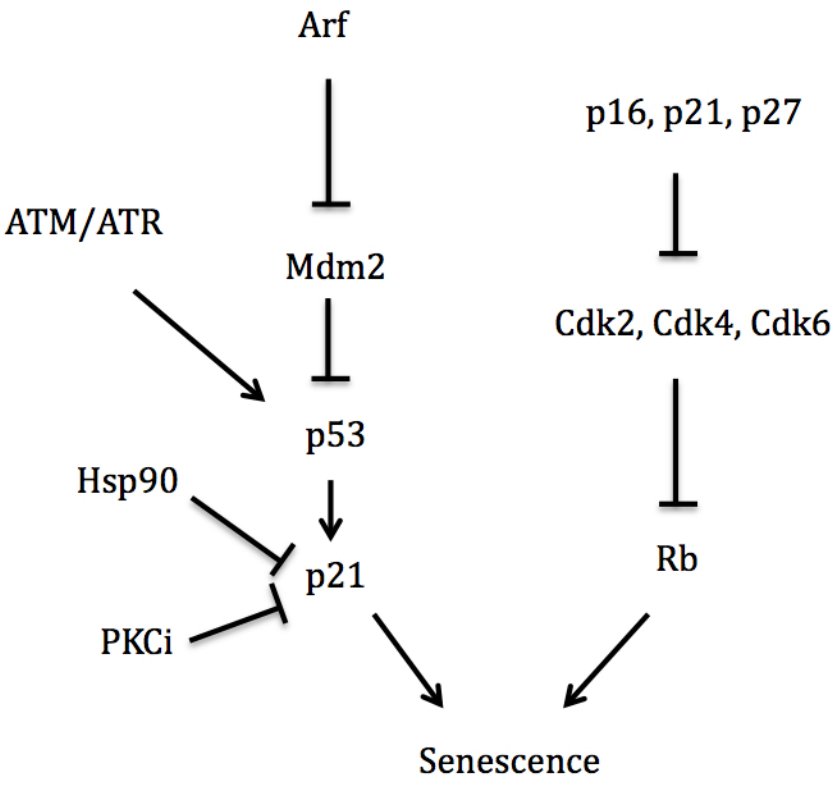
Arf
p16, p21, p27
ATM/ATR
Mdm2
Cdk2, Cdk4, Cdk6
p53
Hsp90
p21
Rb
PKCi
Senescence

Hsp90 inhibition in inducing the ROS-p21 feedback loop resulting in cellular senescence. With 20 different Hsp90 inhibitors now in the clinic there is a lot of excitement to determine the full potential of Hsp90 inhibition as a cancer therapeutic. We hope our work has provided sufficient evidence for senescence to be assessed as an outcome of Hsp90 inhibition in the clinic.

We were also able to describe a novel role for PKCι in the repression of senescence. PKCι depletion-induced senescence was dependent on p21 protein expression. Importantly, it was not dependent on the DNA damage response, p53 or p16 expression but was enhanced by further perturbation of mitosis. There is previous evidence describing the induction of premature senescence that neither involves the DNA damage response pathway nor depends on p53. Two examples involve the depletion of Hsp72 in colon cancer cells and the loss of Skp2 in mice in oncogenic conditions (combined with Arf-/- or PTEN +/-) (Lin et al., 2010; Yaglom et al., 2007). Furthermore, both of these studies showed a dependence on p21, which suggests a role for p21 in premature senescence that is independent of its regulation by p53 following DNA damage. Interestingly, a novel mechanism has been described for the degradation of p21 in mitosis that involves the spindle assembly checkpoint. Cdc20 is an activator of the ubiquitin ligase APC/C and is inhibited by an active spindle assembly checkpoint (SAC). An elegant paper by Amador *et al* demonstrated that Cdc20 is necessary for APC/C mediated ubiquitylation of p21 in mitosis and that silencing Cdc20 results in p21 protein accumulation (Amador et al., 2007). It is not yet known if the inability to degrade p21 in mitotically arrested cells by the SAC could act in combination with or independently from the mechanism originally described by Scott *et al* and referenced

in Chapter 3. Their work identified p21 as a phosphorylation substrate of aPKCs, where phosphorylation of p21 at Ser146 leads to p21 inactivation and degradation. The relationship between PKCι depletion and p21-dependent senescence is shown in the context of the molecular pathways of senescence in Figure 5.1. Altogether, we described a novel outcome of PKCι depletion in cancer cells. The induction of senescence is p21 dependent, DNA-damage independent, and involves defects in mitosis.

We were then able to show that senescent glioblastoma cells have aberrant centrosomes. This is observed in basal senescence, p21-induced senescence and PKCι depletion-induced senescence. Severe defects in mitosis such as mitotic slippage, can result in centrosome aberrations. Mitotic slippage occurs when the SAC is activated for an extended period of time and eventually the cell can exit into the G1 phase of the cell cycle. We were able to show that senescent cells, both basal and induced after PKCι depletion, had undergone mitotic slippage. PKCι was also depleted in established glioblastoma xenografts. *In vivo*, PKCι depletion decreased cell proliferation, delayed tumor growth, and improved survival.

In summary, we have identified two possible targets for the induction of premature senescence in cancer cells. We were able to describe a novel role for Hsp90 inhibition in the induction of premature senescence in SCLC cells. We suggest that SCLC be considered as a candidate for one of the many Hsp90 inhibitors entering clinical trials. We also described a novel mechanism for PKCι depletion-induced senescence that involves defects in mitotic progression. A more detailed analysis revealed that PKCι depletion-induced senescence is mediated by mitotic slippage and results in

centrosome aberrations. We then demonstrated that established tumors in mice are responsive to PKCι depletion, which more closely reflects the timing of therapy following diagnosis in the clinic. This emphasizes the potential of PKCι as a therapeutic target for the treatment of cancer. Overall, there are multiple methods of inducing senescence in cancer and we strongly advocate that the analysis of senescence be performed as frequently as the analysis of apoptosis following cancer therapy.

6. References

Abbas, T., and Dutta, A. (2009). p21 in cancer: intricate networks and multiple activities. Nat Rev Cancer *9*, 400-414.

Akimoto, K., Mizuno, K., Osada, S., Hirai, S., Tanuma, S., Suzuki, K., and Ohno, S. (1994). A new member of the third class in the protein kinase C family, PKC lambda, expressed dominantly in an undifferentiated mouse embryonal carcinoma cell line and also in many tissues and cells. J Biol Chem *269*, 12677-12683.

Amador, V., Ge, S., Santamaria, P.G., Guardavaccaro, D., and Pagano, M. (2007). APC/C(Cdc20) controls the ubiquitin-mediated degradation of p21 in prometaphase. Mol Cell *27*, 462-473.

Baldwin, R.M., Barrett, G.M., Parolin, D.A., Gillies, J.K., Paget, J.A., Lavictoire, S.J., Gray, D.A., and Lorimer, I.A. (2010). Coordination of glioblastoma cell motility by PKCiota. Mol Cancer *9*, 233.

Baldwin, R.M., Garratt-Lalonde, M., Parolin, D.A., Krzyzanowski, P.M., Andrade, M.A., and Lorimer, I.A. (2006). Protection of glioblastoma cells from cisplatin cytotoxicity via protein kinase Ciota-mediated attenuation of p38 MAP kinase signaling. Oncogene *25*, 2909-2919.

Baldwin, R.M., Parolin, D.A., and Lorimer, I.A. (2008). Regulation of glioblastoma cell invasion by PKC iota and RhoB. Oncogene *27*, 3587-3595.

Balendran, A., Biondi, R.M., Cheung, P.C., Casamayor, A., Deak, M., and Alessi, D.R. (2000). A 3-phosphoinositide-dependent protein kinase-1 (PDK1) docking site is required for the phosphorylation of protein kinase Czeta (PKCzeta) and PKC-related kinase 2 by PDK1. J Biol Chem *275*, 20806-20813.

Bandyopadhyay, G., Standaert, M.L., Sajan, M.P., Kanoh, Y., Miura, A., Braun, U., Kruse, F., Leitges, M., and Farese, R.V. (2004). Protein kinase C-lambda knockout in embryonic stem cells and adipocytes impairs insulin-stimulated glucose transport. Mol Endocrinol *18*, 373-383.

Bartkova, J., Rezaei, N., Liontos, M., Karakaidos, P., Kletsas, D., Issaeva, N., Vassiliou, L.V., Kolettas, E., Niforou, K., Zoumpourlis, V.C., *et al.* (2006). Oncogene-induced senescence is part of the tumorigenesis barrier imposed by DNA damage checkpoints. Nature *444*, 633-637.

Basso, A.D., Solit, D.B., Munster, P.N., and Rosen, N. (2002). Ansamycin antibiotics inhibit Akt activation and cyclin D expression in breast cancer cells that overexpress HER2. Oncogene *21*, 1159-1166.

Beckmann, R.P., Mizzen, L.E., and Welch, W.J. (1990). Interaction of Hsp 70 with newly synthesized proteins: implications for protein folding and assembly. Science *248*, 850-854.

Bodnar, A.G., Ouellette, M., Frolkis, M., Holt, S.E., Chiu, C.P., Morin, G.B., Harley, C.B., Shay, J.W., Lichtsteiner, S., and Wright, W.E. (1998). Extension of life-span by introduction of telomerase into normal human cells. Science *279*, 349-352.

Brugge, J., Yonemoto, W., and Darrow, D. (1983). Interaction between the Rous sarcoma virus transforming protein and two cellular phosphoproteins: analysis of the turnover and distribution of this complex. Mol Cell Biol *3*, 9-19.

Bullwinkel, J., Baron-Luhr, B., Ludemann, A., Wohlenberg, C., Gerdes, J., and Scholzen, T. (2006). Ki-67 protein is associated with ribosomal RNA transcription in quiescent and proliferating cells. J Cell Physiol *206*, 624-635.

Cesare, A.J., and Reddel, R.R. (2010). Alternative lengthening of telomeres: models, mechanisms and implications. Nat Rev Genet *11*, 319-330.

Chehab, N.H., Malikzay, A., Stavridi, E.S., and Halazonetis, T.D. (1999). Phosphorylation of Ser-20 mediates stabilization of human p53 in response to DNA damage. Proc Natl Acad Sci U S A *96*, 13777-13782.

Chen, Z., Trotman, L.C., Shaffer, D., Lin, H.K., Dotan, Z.A., Niki, M., Koutcher, J.A., Scher, H.I., Ludwig, T., Gerald, W.*, et al.* (2005). Crucial role of p53-dependent cellular senescence in suppression of Pten-deficient tumorigenesis. Nature *436*, 725-730.

Chou, M.M., Hou, W., Johnson, J., Graham, L.K., Lee, M.H., Chen, C.S., Newton, A.C., Schaffhausen, B.S., and Toker, A. (1998). Regulation of protein kinase C zeta by PI 3-kinase and PDK-1. Curr Biol *8*, 1069-1077.

Clark, C.B., Rane, M.J., El Mehdi, D., Miller, C.J., Sachleben, L.R., Jr., and Gozal, E. (2009). Role of oxidative stress in geldanamycin-induced cytotoxicity and disruption of Hsp90 signaling complex. Free Radic Biol Med *47*, 1440-1449.

Collado, M., Gil, J., Efeyan, A., Guerra, C., Schuhmacher, A.J., Barradas, M., Benguria, A., Zaballos, A., Flores, J.M., Barbacid, M.*, et al.* (2005). Tumour biology: senescence in premalignant tumours. Nature *436*, 642.

Courtois-Cox, S., Genther Williams, S.M., Reczek, E.E., Johnson, B.W., McGillicuddy, L.T., Johannessen, C.M., Hollstein, P.E., MacCollin, M., and Cichowski, K. (2006). A negative feedback signaling network underlies oncogene-induced senescence. Cancer Cell *10*, 459-472.

Csermely, P., Schnaider, T., Soti, C., Prohaszka, Z., and Nardai, G. (1998). The 90-kDa molecular chaperone family: structure, function, and clinical applications. A comprehensive review. Pharmacol Ther *79*, 129-168.

d'Adda di Fagagna, F., Reaper, P.M., Clay-Farrace, L., Fiegler, H., Carr, P., Von Zglinicki, T., Saretzki, G., Carter, N.P., and Jackson, S.P. (2003). A DNA damage checkpoint response in telomere-initiated senescence. Nature *426*, 194-198.

Dankort, D., Filenova, E., Collado, M., Serrano, M., Jones, K., and McMahon, M. (2007). A new mouse model to explore the initiation, progression, and therapy of BRAFV600E-induced lung tumors. Genes Dev *21*, 379-384.

De Maio, A., Santoro, M.G., Tanguay, R.M., and Hightower, L.E. (2012). Ferruccio Ritossa's scientific legacy 50 years after his discovery of the heat shock response: a new view of biology, a new society, and a new journal. Cell Stress Chaperones *17*, 139-143.

Debacq-Chainiaux, F., Erusalimsky, J.D., Campisi, J., and Toussaint, O. (2009). Protocols to detect senescence-associated beta-galactosidase (SA-betagal) activity, a biomarker of senescent cells in culture and in vivo. Nat Protoc *4*, 1798-1806.

Deng, C., Zhang, P., Harper, J.W., Elledge, S.J., and Leder, P. (1995). Mice lacking p21CIP1/WAF1 undergo normal development, but are defective in G1 checkpoint control. Cell *82*, 675-684.

Dhomen, N., Reis-Filho, J.S., da Rocha Dias, S., Hayward, R., Savage, K., Delmas, V., Larue, L., Pritchard, C., and Marais, R. (2009). Oncogenic Braf induces melanocyte senescence and melanoma in mice. Cancer Cell *15*, 294-303.

Dimri, G.P., Lee, X., Basile, G., Acosta, M., Scott, G., Roskelley, C., Medrano, E.E., Linskens, M., Rubelj, I., Pereira-Smith, O.*, et al.* (1995). A biomarker that identifies senescent human cells in culture and in aging skin in vivo. Proc Natl Acad Sci U S A *92*, 9363-9367.

Echeverria, P.C., Bernthaler, A., Dupuis, P., Mayer, B., and Picard, D. (2011). An interaction network predicted from public data as a discovery tool: application to the Hsp90 molecular chaperone machine. PLoS One *6*, e26044.

Eder, A.M., Sui, X., Rosen, D.G., Nolden, L.K., Cheng, K.W., Lahad, J.P., Kango-Singh, M., Lu, K.H., Warneke, C.L., Atkinson, E.N.*, et al.* (2005). Atypical PKCiota contributes to poor prognosis through loss of apical-basal polarity and cyclin E overexpression in ovarian cancer. Proc Natl Acad Sci U S A *102*, 12519-12524.

Eletto, D., Dersh, D., and Argon, Y. (2010). GRP94 in ER quality control and stress responses. Semin Cell Dev Biol *21*, 479-485.

Franza, B.R., Jr., Maruyama, K., Garrels, J.I., and Ruley, H.E. (1986). In vitro establishment is not a sufficient prerequisite for transformation by activated ras oncogenes. Cell *44*, 409-418.

Fukuyo, Y., Inoue, M., Nakajima, T., Higashikubo, R., Horikoshi, N.T., Hunt, C., Usheva, A., Freeman, M.L., and Horikoshi, N. (2008). Oxidative stress plays a critical role in inactivating mutant BRAF by geldanamycin derivatives. Cancer Res *68*, 6324-6330.

Gerdes, J., Schwab, U., Lemke, H., and Stein, H. (1983). Production of a mouse monoclonal antibody reactive with a human nuclear antigen associated with cell proliferation. Int J Cancer *31*, 13-20.

Gewirtz, D.A., Holt, S.E., and Elmore, L.W. (2008). Accelerated senescence: an emerging role in tumor cell response to chemotherapy and radiation. Biochem Pharmacol *76*, 947-957.

Gorgoulis, V.G., and Halazonetis, T.D. (2010). Oncogene-induced senescence: the bright and dark side of the response. Curr Opin Cell Biol *22*, 816-827.

Grbovic, O.M., Basso, A.D., Sawai, A., Ye, Q., Friedlander, P., Solit, D., and Rosen, N. (2006). V600E B-Raf requires the Hsp90 chaperone for stability and is degraded in response to Hsp90 inhibitors. Proc Natl Acad Sci U S A *103*, 57-62.

Greider, C.W., and Blackburn, E.H. (1985). Identification of a specific telomere terminal transferase activity in Tetrahymena extracts. Cell *43*, 405-413.

Greider, C.W., and Blackburn, E.H. (1987). The telomere terminal transferase of Tetrahymena is a ribonucleoprotein enzyme with two kinds of primer specificity. Cell *51*, 887-898.

Guerra, C., Collado, M., Navas, C., Schuhmacher, A.J., Hernandez-Porras, I., Canamero, M., Rodriguez-Justo, M., Serrano, M., and Barbacid, M. (2011). Pancreatitis-induced inflammation contributes to pancreatic cancer by inhibiting oncogene-induced senescence. Cancer Cell *19*, 728-739.

Harley, C.B., Futcher, A.B., and Greider, C.W. (1990). Telomeres shorten during ageing of human fibroblasts. Nature *345*, 458-460.

Hayflick, L. (1965). The Limited in Vitro Lifetime of Human Diploid Cell Strains. Exp Cell Res *37*, 614-636.

Hayflick, L., and Moorhead, P.S. (1961). The serial cultivation of human diploid cell strains. Exp Cell Res *25*, 585-621.

Holt, S.E., Aisner, D.L., Baur, J., Tesmer, V.M., Dy, M., Ouellette, M., Trager, J.B., Morin, G.B., Toft, D.O., Shay, J.W.*, et al.* (1999). Functional requirement of p23 and Hsp90 in telomerase complexes. Genes Dev *13*, 817-826.

Hsu, L.C., Kapali, M., DeLoia, J.A., and Gallion, H.H. (2005). Centrosome abnormalities in ovarian cancer. Int J Cancer *113*, 746-751.

Kamal, A., Thao, L., Sensintaffar, J., Zhang, L., Boehm, M.F., Fritz, L.C., and Burrows, F.J. (2003). A high-affinity conformation of Hsp90 confers tumour selectivity on Hsp90 inhibitors. Nature *425*, 407-410.

Kang, B.H. (2012). TRAP1 regulation of mitochondrial life or death decision in cancer cells and mitochondria-targeted TRAP1 inhibitors. BMB Rep *45*, 1-6.

Kang, G.H., Lee, E.J., Jang, K.T., Kim, K.M., Park, C.K., Lee, C.S., Kang, D.Y., Lee, S.H., Sohn, T.S., and Kim, S. (2010). Expression of HSP90 in gastrointestinal stromal tumours and mesenchymal tumours. Histopathology *56*, 694-701.

Kang, T.W., Yevsa, T., Woller, N., Hoenicke, L., Wuestefeld, T., Dauch, D., Hohmeyer, A., Gereke, M., Rudalska, R., Potapova, A.*, et al.* (2011). Senescence surveillance of pre-malignant hepatocytes limits liver cancer development. Nature *479*, 547-551.

Kayser, G., Gerlach, U., Walch, A., Nitschke, R., Haxelmans, S., Kayser, K., Hopt, U., Werner, M., and Lassmann, S. (2005). Numerical and structural centrosome aberrations are an early and stable event in the adenoma-carcinoma sequence of colorectal carcinomas. Virchows Arch *447*, 61-65.

Kojima, Y., Akimoto, K., Nagashima, Y., Ishiguro, H., Shirai, S., Chishima, T., Ichikawa, Y., Ishikawa, T., Sasaki, T., Kubota, Y.*, et al.* (2008). The overexpression and altered localization of the atypical protein kinase C lambda/iota in breast cancer correlates with the pathologic type of these tumors. Hum Pathol *39*, 824-831.

Kosar, M., Bartkova, J., Hubackova, S., Hodny, Z., Lukas, J., and Bartek, J. (2011). Senescence-associated heterochromatin foci are dispensable for cellular senescence, occur in a cell type- and insult-dependent manner and follow expression of p16(ink4a). Cell Cycle *10*, 457-468.

Kovac, J., Oster, H., and Leitges, M. (2007). Expression of the atypical protein kinase C (aPKC) isoforms iota/lambda and zeta during mouse embryogenesis. Gene Expr Patterns *7*, 187-196.

Kramer, A., Schweizer, S., Neben, K., Giesecke, C., Kalla, J., Katzenberger, T., Benner, A., Muller-Hermelink, H.K., Ho, A.D., and Ott, G. (2003). Centrosome aberrations as a possible mechanism for chromosomal instability in non-Hodgkin's lymphoma. Leukemia *17*, 2207-2213.

Kurz, D.J., Decary, S., Hong, Y., and Erusalimsky, J.D. (2000). Senescence-associated (beta)-galactosidase reflects an increase in lysosomal mass during replicative ageing of human endothelial cells. J Cell Sci *113 (Pt 20)*, 3613-3622.

Lamark, T., Perander, M., Outzen, H., Kristiansen, K., Overvatn, A., Michaelsen, E., Bjorkoy, G., and Johansen, T. (2003). Interaction codes within the family of mammalian Phox and Bem1p domain-containing proteins. J Biol Chem *278*, 34568-34581.

Land, H., Parada, L.F., and Weinberg, R.A. (1983). Tumorigenic conversion of primary embryo fibroblasts requires at least two cooperating oncogenes. Nature *304*, 596-602.

Lawless, C., Wang, C., Jurk, D., Merz, A., Zglinicki, T., and Passos, J.F. (2010). Quantitative assessment of markers for cell senescence. Exp Gerontol *45*, 772-778.

Le Good, J.A., Ziegler, W.H., Parekh, D.B., Alessi, D.R., Cohen, P., and Parker, P.J. (1998). Protein kinase C isotypes controlled by phosphoinositide 3-kinase through the protein kinase PDK1. Science *281*, 2042-2045.

Lee, B.Y., Han, J.A., Im, J.S., Morrone, A., Johung, K., Goodwin, E.C., Kleijer, W.J., DiMaio, D., and Hwang, E.S. (2006). Senescence-associated beta-galactosidase is lysosomal beta-galactosidase. Aging Cell *5*, 187-195.

Leitges, M., Sanz, L., Martin, P., Duran, A., Braun, U., Garcia, J.F., Camacho, F., Diaz-Meco, M.T., Rennert, P.D., and Moscat, J. (2001). Targeted disruption of the zetaPKC gene results in the impairment of the NF-kappaB pathway. Mol Cell *8*, 771-780.

Leppa, S., and Sistonen, L. (1997). Heat shock response--pathophysiological implications. Ann Med *29*, 73-78.

Li, Q., Wang, J.M., Liu, C., Xiao, B.L., Lu, J.X., and Zou, S.Q. (2008). Correlation of aPKC-iota and E-cadherin expression with invasion and prognosis of cholangiocarcinoma. Hepatobiliary Pancreat Dis Int *7*, 70-75.

Lin, H.K., Chen, Z., Wang, G., Nardella, C., Lee, S.W., Chan, C.H., Yang, W.L., Wang, J., Egia, A., Nakayama, K.I.*, et al.* (2010). Skp2 targeting suppresses tumorigenesis by Arf-p53-independent cellular senescence. Nature *464*, 374-379.

Lingle, W.L., Barrett, S.L., Negron, V.C., D'Assoro, A.B., Boeneman, K., Liu, W., Whitehead, C.M., Reynolds, C., and Salisbury, J.L. (2002). Centrosome amplification drives chromosomal instability in breast tumor development. Proc Natl Acad Sci U S A *99*, 1978-1983.

Lopez, F., Belloc, F., Lacombe, F., Dumain, P., Reiffers, J., Bernard, P., and Boisseau, M.R. (1991). Modalities of synthesis of Ki67 antigen during the stimulation of lymphocytes. Cytometry *12*, 42-49.

Lowe, S.W., and Sherr, C.J. (2003). Tumor suppression by Ink4a-Arf: progress and puzzles. Curr Opin Genet Dev *13*, 77-83.

Macip, S., Igarashi, M., Fang, L., Chen, A., Pan, Z.Q., Lee, S.W., and Aaronson, S.A. (2002). Inhibition of p21-mediated ROS accumulation can rescue p21-induced senescence. EMBO J *21*, 2180-2188.

McCarthy, M.M., Pick, E., Kluger, Y., Gould-Rothberg, B., Lazova, R., Camp, R.L., Rimm, D.L., and Kluger, H.M. (2008). HSP90 as a marker of progression in melanoma. Ann Oncol *19*, 590-594.

Michaloglou, C., Vredeveld, L.C., Soengas, M.S., Denoyelle, C., Kuilman, T., van der Horst, C.M., Majoor, D.M., Shay, J.W., Mooi, W.J., and Peeper, D.S. (2005). BRAFE600-associated senescence-like cell cycle arrest of human naevi. Nature *436*, 720-724.

Mikule, K., Delaval, B., Kaldis, P., Jurcyzk, A., Hergert, P., and Doxsey, S. (2007). Loss of centrosome integrity induces p38-p53-p21-dependent G1-S arrest. Nat Cell Biol *9*, 160-170.

Modi, S., Stopeck, A., Linden, H., Solit, D., Chandarlapaty, S., Rosen, N., D'Andrea, G., Dickler, M., Moynahan, M.E., Sugarman, S.*, et al.* (2011). HSP90 inhibition is effective in breast cancer: a phase II trial of tanespimycin (17-AAG) plus trastuzumab in patients with HER2-positive metastatic breast cancer progressing on trastuzumab. Clin Cancer Res *17*, 5132-5139.

Morin, G.B. (1989). The human telomere terminal transferase enzyme is a ribonucleoprotein that synthesizes TTAGGG repeats. Cell *59*, 521-529.

Moulick, K., Ahn, J.H., Zong, H., Rodina, A., Cerchietti, L., Gomes DaGama, E.M., Caldas-Lopes, E., Beebe, K., Perna, F., Hatzi, K.*, et al.* (2011). Affinity-based proteomics reveal cancer-specific networks coordinated by Hsp90. Nat Chem Biol *7*, 818-826.

Murray, N.R., Jamieson, L., Yu, W., Zhang, J., Gokmen-Polar, Y., Sier, D., Anastasiadis, P., Gatalica, Z., Thompson, E.A., and Fields, A.P. (2004). Protein kinase Ciota is required for Ras transformation and colon carcinogenesis in vivo. J Cell Biol *164*, 797-802.

Murray, N.R., Kalari, K.R., and Fields, A.P. (2011). Protein kinase Ciota expression and oncogenic signaling mechanisms in cancer. J Cell Physiol *226*, 879-887.

Narita, M., Nunez, S., Heard, E., Lin, A.W., Hearn, S.A., Spector, D.L., Hannon, G.J., and Lowe, S.W. (2003). Rb-mediated heterochromatin formation and silencing of E2F target genes during cellular senescence. Cell *113*, 703-716.

Neckers, L., and Workman, P. (2012). Hsp90 molecular chaperone inhibitors: are we there yet? Clin Cancer Res *18*, 64-76.

Nigg, E.A. (2002). Centrosome aberrations: cause or consequence of cancer progression? Nat Rev Cancer *2*, 815-825.

Nishizuka, Y. (1995). Protein kinase C and lipid signaling for sustained cellular responses. FASEB J *9*, 484-496.

Olovnikov, A.M. (1971). [Principle of marginotomy in template synthesis of polynucleotides]. Dokl Akad Nauk SSSR *201*, 1496-1499.

Olovnikov, A.M. (1973). A theory of marginotomy. The incomplete copying of template margin in enzymic synthesis of polynucleotides and biological significance of the phenomenon. J Theor Biol *41*, 181-190.

Olovnikov, A.M. (1996). Telomeres, telomerase, and aging: origin of the theory. Exp Gerontol *31*, 443-448.

Ono, Y., Fujii, T., Ogita, K., Kikkawa, U., Igarashi, K., and Nishizuka, Y. (1989). Protein kinase C zeta subspecies from rat brain: its structure, expression, and properties. Proc Natl Acad Sci U S A *86*, 3099-3103.

Oppermann, H., Levinson, W., and Bishop, J.M. (1981). A cellular protein that associates with the transforming protein of Rous sarcoma virus is also a heat-shock protein. Proc Natl Acad Sci U S A *78*, 1067-1071.

Passos, J.F., Nelson, G., Wang, C., Richter, T., Simillion, C., Proctor, C.J., Miwa, S., Olijslagers, S., Hallinan, J., Wipat, A.*, et al.* (2010). Feedback between p21 and reactive oxygen production is necessary for cell senescence. Mol Syst Biol *6*, 347.

Patel, R., Win, H., Desai, S., Patel, K., Matthews, J.A., and Acevedo-Duncan, M. (2008). Involvement of PKC-iota in glioma proliferation. Cell Prolif *41*, 122-135.

Pick, E., Kluger, Y., Giltnane, J.M., Moeder, C., Camp, R.L., Rimm, D.L., and Kluger, H.M. (2007). High HSP90 expression is associated with decreased survival in breast cancer. Cancer Res *67*, 2932-2937.

Pihan, G.A., Purohit, A., Wallace, J., Malhotra, R., Liotta, L., and Doxsey, S.J. (2001). Centrosome defects can account for cellular and genetic changes that characterize prostate cancer progression. Cancer Res *61*, 2212-2219.

Pihan, G.A., Wallace, J., Zhou, Y., and Doxsey, S.J. (2003). Centrosome abnormalities and chromosome instability occur together in pre-invasive carcinomas. Cancer Res *63*, 1398-1404.

Prodromou, C., Roe, S.M., O'Brien, R., Ladbury, J.E., Piper, P.W., and Pearl, L.H. (1997). Identification and structural characterization of the ATP/ADP-binding site in the Hsp90 molecular chaperone. Cell *90*, 65-75.

Rahmanzadeh, R., Huttmann, G., Gerdes, J., and Scholzen, T. (2007). Chromophore-assisted light inactivation of pKi-67 leads to inhibition of ribosomal RNA synthesis. Cell Prolif *40*, 422-430.

Regala, R.P., Weems, C., Jamieson, L., Copland, J.A., Thompson, E.A., and Fields, A.P. (2005a). Atypical protein kinase Ciota plays a critical role in human lung cancer cell growth and tumorigenicity. J Biol Chem *280*, 31109-31115.

Regala, R.P., Weems, C., Jamieson, L., Khoor, A., Edell, E.S., Lohse, C.M., and Fields, A.P. (2005b). Atypical protein kinase C iota is an oncogene in human non-small cell lung cancer. Cancer Res *65*, 8905-8911.

Reiter, R., Gais, P., Steuer-Vogt, M.K., Boulesteix, A.L., Deutschle, T., Hampel, R., Wagenpfeil, S., Rauser, S., Walch, A., Bink, K.*, et al.* (2009). Centrosome abnormalities in head and neck squamous cell carcinoma (HNSCC). Acta Otolaryngol *129*, 205-213.

Ritossa, F. (1962). A New Puffing Pattern Induced by Temperature Shock and DNP in Drosophila. Experientia *18*, 3.

Robbins, E., Levine, E.M., and Eagle, H. (1970). Morphologic changes accompanying senescence of cultured human diploid cells. J Exp Med *131*, 1211-1222.

Roberson, R.S., Kussick, S.J., Vallieres, E., Chen, S.Y., and Wu, D.Y. (2005). Escape from therapy-induced accelerated cellular senescence in p53-null lung cancer cells and in human lung cancers. Cancer Res *65*, 2795-2803.

Rodina, A., Vilenchik, M., Moulick, K., Aguirre, J., Kim, J., Chiang, A., Litz, J., Clement, C.C., Kang, Y., She, Y.*, et al.* (2007). Selective compounds define Hsp90 as a major inhibitor of apoptosis in small-cell lung cancer. Nat Chem Biol *3*, 498-507.

Russo, T., Zambrano, N., Esposito, F., Ammendola, R., Cimino, F., Fiscella, M., Jackman, J., O'Connor, P.M., Anderson, C.W., and Appella, E. (1995). A p53-independent pathway for activation of WAF1/CIP1 expression following oxidative stress. J Biol Chem *270*, 29386-29391.

Sarangi, U., Paithankar, K.R., Kumar, J.U., Subramaniam, V., and Sreedhar, A.S. (2012). 17AAG Treatment Accelerates Doxorubicin Induced Cellular Senescence: Hsp90 Interferes with Enforced Senescence of Tumor Cells. Drug Target Insights *6*, 19-39.

Sarkisian, C.J., Keister, B.A., Stairs, D.B., Boxer, R.B., Moody, S.E., and Chodosh, L.A. (2007). Dose-dependent oncogene-induced senescence in vivo and its evasion during mammary tumorigenesis. Nat Cell Biol *9*, 493-505.

Sato, S., Fujita, N., and Tsuruo, T. (2000). Modulation of Akt kinase activity by binding to Hsp90. Proc Natl Acad Sci U S A *97*, 10832-10837.

Schmidt, S., Schneider, L., Essmann, F., Cirstea, I.C., Kuck, F., Kletke, A., Janicke, R.U., Wiek, C., Hanenberg, H., Ahmadian, M.R.*, et al.* (2010). The centrosomal protein TACC3 controls paclitaxel sensitivity by modulating a premature senescence program. Oncogene *29*, 6184-6192.

Schneider, C., Sepp-Lorenzino, L., Nimmesgern, E., Ouerfelli, O., Danishefsky, S., Rosen, N., and Hartl, F.U. (1996). Pharmacologic shifting of a balance between protein refolding and degradation mediated by Hsp90. Proc Natl Acad Sci U S A *93*, 14536-14541.

Schulte, T.W., Blagosklonny, M.V., Ingui, C., and Neckers, L. (1995). Disruption of the Raf-1-Hsp90 molecular complex results in destabilization of Raf-1 and loss of Raf-1-Ras association. J Biol Chem *270*, 24585-24588.

Scotti, M.L., Bamlet, W.R., Smyrk, T.C., Fields, A.P., and Murray, N.R. (2010). Protein kinase Ciota is required for pancreatic cancer cell transformed growth and tumorigenesis. Cancer Res *70*, 2064-2074.

Sequist, L.V., Gettinger, S., Senzer, N.N., Martins, R.G., Janne, P.A., Lilenbaum, R., Gray, J.E., Iafrate, A.J., Katayama, R., Hafeez, N.*, et al.* (2010). Activity of IPI-504, a novel heat-shock protein 90 inhibitor, in patients with molecularly defined non-small-cell lung cancer. J Clin Oncol *28*, 4953-4960.

Serrano, M., Lin, A.W., McCurrach, M.E., Beach, D., and Lowe, S.W. (1997). Oncogenic ras provokes premature cell senescence associated with accumulation of p53 and p16INK4a. Cell *88*, 593-602.

Shay, J.W., and Bacchetti, S. (1997). A survey of telomerase activity in human cancer. Eur J Cancer *33*, 787-791.

Sherr, C.J. (1996). Cancer cell cycles. Science *274*, 1672-1677.

Sherr, C.J. (2001). The INK4a/ARF network in tumour suppression. Nat Rev Mol Cell Biol *2*, 731-737.

Smith, D.F., Whitesell, L., and Katsanis, E. (1998). Molecular chaperones: biology and prospects for pharmacological intervention. Pharmacol Rev *50*, 493-514.

Srsen, V., Gnadt, N., Dammermann, A., and Merdes, A. (2006). Inhibition of centrosome protein assembly leads to p53-dependent exit from the cell cycle. J Cell Biol *174*, 625-630.

Stepanova, L., Leng, X., Parker, S.B., and Harper, J.W. (1996). Mammalian p50Cdc37 is a protein kinase-targeting subunit of Hsp90 that binds and stabilizes Cdk4. Genes Dev *10*, 1491-1502.

Taipale, M., Jarosz, D.F., and Lindquist, S. (2010). HSP90 at the hub of protein homeostasis: emerging mechanistic insights. Nat Rev Mol Cell Biol *11*, 515-528.

Takai, H., Smogorzewska, A., and de Lange, T. (2003). DNA damage foci at dysfunctional telomeres. Curr Biol *13*, 1549-1556.

te Poele, R.H., Okorokov, A.L., Jardine, L., Cummings, J., and Joel, S.P. (2002). DNA damage is able to induce senescence in tumor cells in vitro and in vivo. Cancer Res *62*, 1876-1883.

Tissieres, A., Mitchell, H.K., and Tracy, U.M. (1974). Protein synthesis in salivary glands of Drosophila melanogaster: relation to chromosome puffs. J Mol Biol *84*, 389-398.

Travers, J., Sharp, S., and Workman, P. (2012). HSP90 inhibition: two-pronged exploitation of cancer dependencies. Drug Discov Today *17*, 242-252.

Ventura, A., Kirsch, D.G., McLaughlin, M.E., Tuveson, D.A., Grimm, J., Lintault, L., Newman, J., Reczek, E.E., Weissleder, R., and Jacks, T. (2007). Restoration of p53 function leads to tumour regression in vivo. Nature *445*, 661-665.

Verheijen, R., Kuijpers, H.J., Schlingemann, R.O., Boehmer, A.L., van Driel, R., Brakenhoff, G.J., and Ramaekers, F.C. (1989a). Ki-67 detects a nuclear matrix-associated proliferation-related antigen. I. Intracellular localization during interphase. J Cell Sci *92 (Pt 1)*, 123-130.

Verheijen, R., Kuijpers, H.J., van Driel, R., Beck, J.L., van Dierendonck, J.H., Brakenhoff, G.J., and Ramaekers, F.C. (1989b). Ki-67 detects a nuclear matrix-associated proliferation-related antigen. II. Localization in mitotic cells and association with chromosomes. J Cell Sci *92 (Pt 4)*, 531-540.

Watson, J.D. (1972). Origin of concatemeric T7 DNA. Nat New Biol *239*, 197-201.

Wegele, H., Muller, L., and Buchner, J. (2004). Hsp70 and Hsp90--a relay team for protein folding. Rev Physiol Biochem Pharmacol *151*, 1-44.

Whitesell, L., and Lindquist, S.L. (2005). HSP90 and the chaperoning of cancer. Nat Rev Cancer *5*, 761-772.

Whitesell, L., Mimnaugh, E.G., De Costa, B., Myers, C.E., and Neckers, L.M. (1994). Inhibition of heat shock protein HSP90-pp60v-src heteroprotein complex formation by benzoquinone ansamycins: essential role for stress proteins in oncogenic transformation. Proc Natl Acad Sci U S A *91*, 8324-8328.

Whitesell, L., Shifrin, S.D., Schwab, G., and Neckers, L.M. (1992). Benzoquinonoid ansamycins possess selective tumoricidal activity unrelated to src kinase inhibition. Cancer Res *52*, 1721-1728.

Whyte, P., Buchkovich, K.J., Horowitz, J.M., Friend, S.H., Raybuck, M., Weinberg, R.A., and Harlow, E. (1988). Association between an oncogene and an anti-oncogene: the adenovirus E1A proteins bind to the retinoblastoma gene product. Nature *334*, 124-129.

Xue, W., Zender, L., Miething, C., Dickins, R.A., Hernando, E., Krizhanovsky, V., Cordon-Cardo, C., and Lowe, S.W. (2007). Senescence and tumour clearance is triggered by p53 restoration in murine liver carcinomas. Nature *445*, 656-660.

Yaglom, J.A., Gabai, V.L., and Sherman, M.Y. (2007). High levels of heat shock protein Hsp72 in cancer cells suppress default senescence pathways. Cancer Res *67*, 2373-2381.

Yamamoto, Y., Matsuyama, H., Furuya, T., Oga, A., Yoshihiro, S., Okuda, M., Kawauchi, S., Sasaki, K., and Naito, K. (2004). Centrosome hyperamplification predicts progression and tumor recurrence in bladder cancer. Clin Cancer Res *10*, 6449-6455.

Yamanaka, T., Horikoshi, Y., Suzuki, A., Sugiyama, Y., Kitamura, K., Maniwa, R., Nagai, Y., Yamashita, A., Hirose, T., Ishikawa, H*., et al.* (2001). PAR-6 regulates aPKC activity in a novel way and mediates cell-cell contact-induced formation of the epithelial junctional complex. Genes Cells *6*, 721-731.

Yang, Y.L., Chu, J.Y., Luo, M.L., Wu, Y.P., Zhang, Y., Feng, Y.B., Shi, Z.Z., Xu, X., Han, Y.L., Cai, Y*., et al.* (2008). Amplification of PRKCI, located in 3q26, is associated with lymph node metastasis in esophageal squamous cell carcinoma. Genes Chromosomes Cancer *47*, 127-136.

Zhang, R., Chen, W., and Adams, P.D. (2007). Molecular dissection of formation of senescence-associated heterochromatin foci. Mol Cell Biol *27*, 2343-2358.

Zhang, Y., and Yang, J.M. (2011). The impact of cellular senescence in cancer therapy: is it true or not? Acta Pharmacol Sin *32*, 1199-1207.